Title

Transient Aerodynamic Effects on a Four-Car Platoon During Passing Maneuvers: Data Summary

Authors

Tsuei, L.
Hedrick, J. K.
Savas, O.

Publication Date

1999-08-01

CALIFORNIA PATH PROGRAM
INSTITUTE OF TRANSPORTATION STUDIES
UNIVERSITY OF CALIFORNIA, BERKELEY

Transient Aerodynamic Effects on a Four-Car Platoon During Passing Maneuvers: Data Summary

L. Tsuei, J.K. Hedrick, 0 . Savas

California PATH Research Report
UCB-ITS-PRR-99-29

This work was performed as part of the California PATH Program of the University of California, in cooperation with the State of California Business, Transportation, and Housing Agency, Department of Transportation; and the United States Department of Transportation, Federal Highway Administration.

Report for MOU 307

August 1999

ISSN 1055-1425

Transient Aerodynamic Effects on a Four-Car Platoon during Passing Maneuvers: Data Summary

L. Tsuei, J. K. Hedrick, and 0 . Savag

Department of Mechanical Engineering
University of California at Berkeley
Berkeley, CA 94720-1740

California PATH Research Report

California PATH Program
Institute of Transportation Studies
University of California, Berkeley

July 1999

Transient Aerodynamic Effects on a Four-Car Platoon during Passing Maneuvers: Data Summary

L. Tsuei, J. K. Hedrick, and 0 . Savag
Department of Mechanical Engineering
University of California at Berkeley
Berkeley, CA 94720-1740

Abstract

In order to provide reliable control algorithms on PATH automated highway system, knowledge of the transient aerodynamic forces is important from the point of the controllability of the platoon and individual vehicles. In a passing maneuver, the platoon members may experience severe aerodynamic forces and yaw moment when another vehicle overtakes. Similar phenomenon can be seen in our daily life as one car passes the other but much more complicated flow field is expected when the interaction involves in a multi-vehicle platoon. It is the purpose of this study to quantify the unsteady aerodynamic forces and moment so as to assure the safety of the system.

Wind tunnel experiments are conducted to study the transient aerodynamic effects experienced by every member of a platoon during passing maneuvers. Four identical 1/20-scale passenger car models are aligned as a platoon with an inter-vehicle separation of 2/5 car length. To simulate a passing maneuver, a fifth identical model is driven longitudinally by a linear motion system which is located parallel to the platoon at various lateral spacings. When the mobile model moves forward, the simulation represents a vehicle passing the platoon. When it moves backward, a vehicle overtaken by a platoon is simulated. The drag force, side force, and yaw moment coefficients on each of the four vehicles in the platoon are determined simultaneously using strain gauge balances during the maneuver to characterize the transient effects.

The results show that each member in the platoon experiences significantly increased drag when the mobile model moves to the proximity of it. When the mobile vehicle is in the neighborhood of the rear half of a platoon member, the side force on it is found to be directed away from the mobile model. The side force reverses its direction and points toward the mobile model when the mobile model is in the proximity of the front half of the platoon member. The lateral spacing between the platoon and the mobile model is found to be an important factor in the passing maneuver. The closer the mobile model to the platoon is, the greater the forces experienced by the platoon members are. The influence of the relative velocity between the platoon and the mobile model is investigated, and it is found that lower relative velocities generate higher force coefficients on each member of the platoon. When a rectangular box is used as the mobile model, the platoon members experience much greater forces. Similar trends in force coefficients are observed in both simulations of a vehicle passing a platoon and a platoon overtaking a vehicle. The measured yaw moments are negligible compared with the magnitudes of drag and side forces. These data are summarized as dimensionless coefficients and the results are presented in graphical forms.

Keywords: platoon aerodynamics, bluff-body aerodynamics, bluff-body flow, transient aerodynamics, vehicle aerodynamics, passing maneuver

Contents

List of Tables

List of Figures

Chapter 1

Introduction

It is a common experience among drivers that one feels a severe aerodynamic side force when his vehicle passes or is passed by a large truck. This phenomenon has been studied, and it is discovered that a passed car experiences a significant change of drag, side force, and yaw moment induced by a larger overtaking vehicle, which may cause the disturbed car's lost of control. These studies, however, focus on the aerodynamic interaction between two cars, and most of the experiments are conducted in the wind tunnel under steady conditions.

On the other hand, in order to increase the capacity of the highway, California PATH proposes a system that many vehicles are "platooning" as a unit and all of them travel at the same speed. By platooning automobiles at small longitudinal inter-vehicle spacings, a great reduction of drag can be achieved, and that contributes directly to fuel economy. However, the mutual interaction between vehicles in close proximity also means any cause that changes the flow field may result in unpredictable aerodynamic effects. In order to provide reliable control algorithms on PATH automated highway system, knowledge of the unsteady aerodynamic forces becomes of paramount importance from the point of controllability of the platoon and individual vehicles. The control algorithms require reasonable estimates of the magnitude and direction of aerodynamic forces and moments which are generated due to changes of flow field during platoon maneuvers. The transient aerodynamic effects experienced by a platoon when a single car passes by is one of these examples. This question is worth studying because of the following reasons: (a) aerodynamic interaction between two cars as one overtakes the other has been studied and proved to be important,

but efforts have not yet been made to the field of platoon aerodynamics during passing maneuvers; (b) by lining up several cars with small longitudinal separations, the flow field around the platoon is almost symmetric, but any change in platoon configuration may result in destroying the symmetry and pose serious controllability and safety problems; (c) most studies of vehicle aerodynamics are conducted with the assumption that the force and moment affecting the cars have reached the equilibrium state, which can only works as a first approximation but not sufficient to characterize its transient nature.

Due to the high desire of understanding the transient aerodynamics experienced by a platoon during passing maneuvers, it is the purpose of this study to quantify the unsteady force so as to assure the safety of the system. This investigation is a continuation of our previous studies in transient aerodynamics under lane change maneuvers. In our previous investigations, various time scales are used to simulate one vehicle merging into and departing from a platoon with varying accelerations and decelerations, and the effect of longitudinal spacings is also investigated [1][2]. We discover that the change of side force is the same order of change of drag during the lane change maneuvers, which means the distorted flow pattern may pose serious controllability problems in a very short period of time and space. The quasi-steady results obtained also confirm data collected at USC [3]. In addition to wind tunnel experiments, a curve fitting model based on data collected in Chen [2] has been developed and implemented in the vehicle control simulation programs [4]. This model can provide the control with an estimate of the aerodynamic forces for which it must compensate, which greatly improves the ability of the control algorithms to handle the aerodynamic forces that a real vehicle experiences on the road.

This report summaries transient aerodynamic data collected in a wind tunnel investigation about a single vehicle passes a four-car platoon, and vice versa. Description of experiments including the definition of each parameter, is presented in Chapter **2.** Details of the data acquisition and data analysis can be found in Tsuei [5]. Four factors are considered to be important in this study. They are mobile vehicle's direction, relative velocities and lateral spacings between the mobile car and the platoon, and shapes of the mobile model. The results regarding to each factor are presented in separate chapters. In Chapter

3, aerodynamic forces experienced by every member of the platoon are compared when the platoon is overtaken by a single car and when it is passing a single car. In Chapter **4,** data collected under the influence of different overtaking velocities are summarized and compared. In Chapter 5, various lateral spacings between the platoon and the mobile model are applied to provide information about their role played in the passing maneuvers. Both a passenger vehicle model and a rectangular box with sharp corners are used as the mobile model. The results are compared in Chapter 6. The position, velocity, and acceleration of the mobile model are determined by motor resolver and this information are provided in Chapter 7. All the data are presented in graphical forms for quick access.

Chapter 2

Description of Experiments

2.1 Overview

In order to understand transient aerodynamic effects on a four-car platoon during passing maneuvers, experiments are performed in a low turbulence, low-speed wind tunnel. Four identical 1/20-scale vehicle models are aligned as a platoon with a fixed inter-vehicle separation of 2/5 car length $(10.2cm)$. To simulate a passing maneuver, a mobile model is driven longitudinally by a linear motion system which is located parallel to the platoon at various lateral spacings. The drag force, side force, and yaw moment on each of the four vehicles in the platoon are measured simultaneously using strain gauge balances during the maneuver to characterize the transient effects.

2.2 Experimental Setup

Four identical 1997 Buick LaSabre vehicle models are employed in the experiments as platoon members. These models are constructed in 1/20-scale and their mold are created by stereolithography with surface data of the full scale vehicle. The longitudinal spacing between each car in the platoon is $10.2cm$, equivalent to $2m$ or 2/5 car length in full scale. Each member of the platoon is connected to a force balance on which 16 strain gauges are mounted. These gauges measure strain on each arm of the force balance resulting from the aerodynamic forces and moment on the vehicle. Four of these strain gauges are used to obtain the strain caused by drag, and another four gauges measure strain by side force. The

rest eight gauges are wired around the center of the balance to measure strain caused by yaw moment. Each force balance generates three voltage outputs based on the measurement of stain gauges. The voltage outputs are corresponding to the drag force, side force and yaw moment which apply to each balance. The force balances are calibrated carefully before the experiments. During the calibration process, three voltage outputs are measured simultaneously when known masses are applied to them, such that the relationship between voltage outputs and known loads are drawn as a calibration curve for each of the four force balances. The calibration curves appear to be very linear for the force measurements, therefore we can use the curves and the voltage outputs obtained during the experiments to calculate the aerodynamic forces and moment experienced by the vehicles. The details about the constructions of the scale models and force balances, and calibration of force balances, can be found in Chen [1].

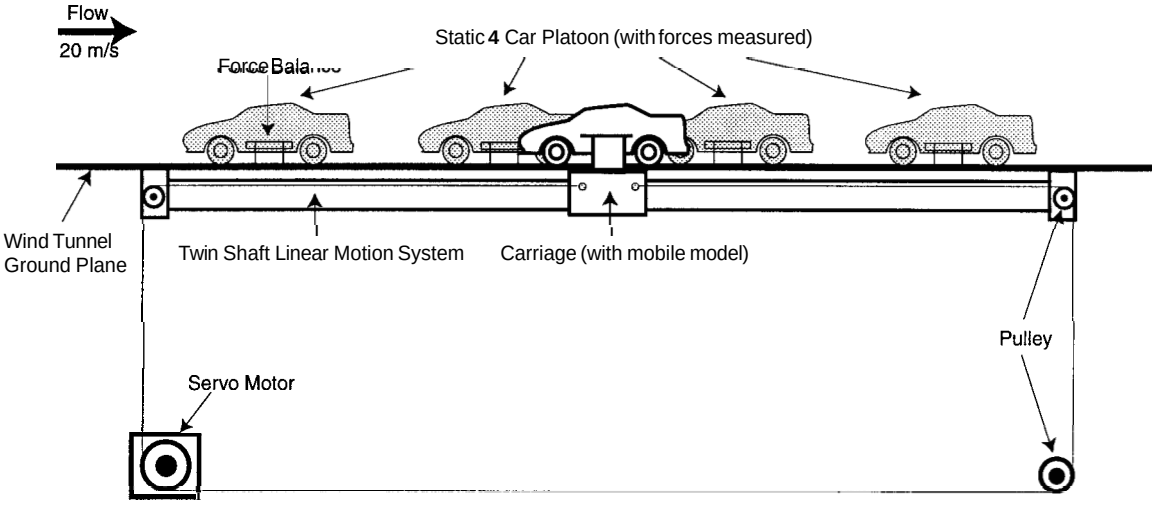

Figure 2.1: Experimental Apparatus

The experimental apparatus is shown in figure 2.1. A servo motor and a pulley system are used to pull the mobile model that is mounted on a carriage longitudinally along a twin shaft linear motion rail. The whole system is located parallel to the platoon with various lateral separation distances. Figure 2.2 shows a two dimensional layout of the experimental setup and the four factors controlled in this experiment. The wind tunnel flow is set to

be $20m/s$, which is equivalent to $60mph$ or $26.7m/s$ highway travelling velocity. When the mobile model is pulled forward (positive u in figure 2.2), the simulation represents a vehicle passing the platoon. When it is mobilized backward (negative u in figure 2.2), **a** vehicle overtaken by a platoon is simulated. The relative velocities between the mobile model and the platoon are ranging from 0 to $6.25m/s$. The zero relative velocity corresponds to the case while a single car moves at the same speed as the platoon. When the passing model moves at $6.25m/s$, it is equivalent to a single car at a speed $78.75mph$ $(35m/s)$ overtakes a platoon that is travelling at $60mph$ $(26.7m/s)$. Four lateral spacings $(1in,\ 2in,\ 4in,$ and $6in)$ between the platoon and the mobile model are applied during the investigations. The separation distances are corresponding to $\frac{1}{4}$, $\frac{1}{2}$, *1*, and $\frac{3}{2}$ of the width of the box model. The travelling distance of the mobile model is $1.2m$, starting from $6.7cm$ behind the front end of the fourth car in the platoon, and ending at $6.7cm$ ahead of the front end of the first platoon member. To determine the influence of the shapes of the mobile model on the platoon, a passenger vehicle model (identical to the platoon members) and a similar sized rectangular box are applied separately. The dimensions of the full scale *1997* Buick LaSabre, the scale vehicle model, and the rectangular box can be found in table *2.1.*

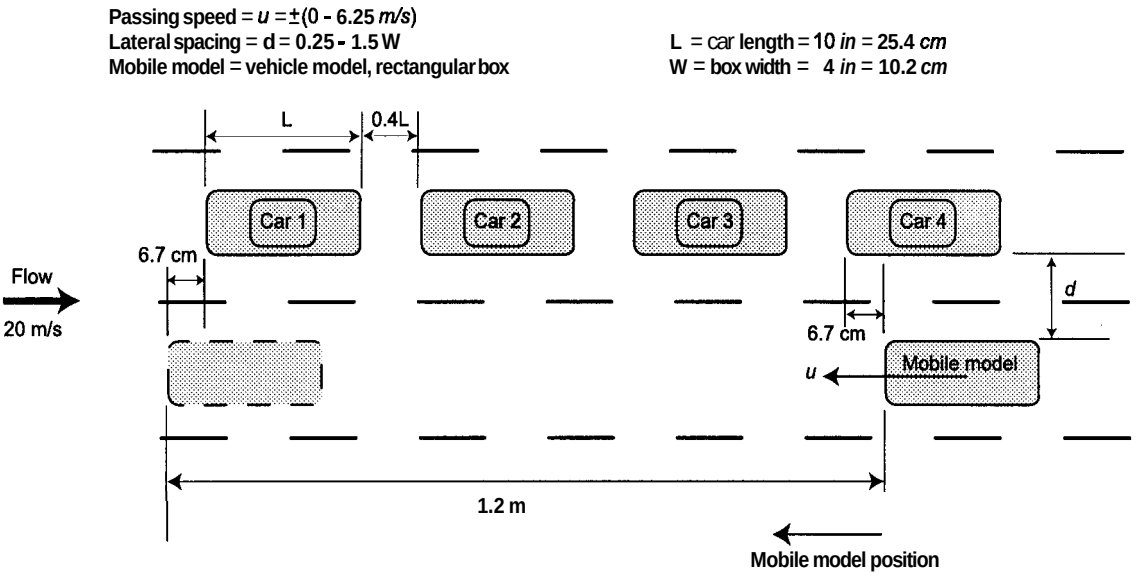

Figure *2.2:* Experimental Layout

Dimensions	1997 Buick LeSabre	Vehicle Model	Box Model
Length(L)	5.1 m	**25.4** cm	**25.4** cm
Width(W)	**1.9** m	**9.4** cm	10.2 cm
Height(H)	**1.4** m	**7.1** cm	**7.6** cm
Ground clearance	**0.26** m	**1.3** cm	**1.3** cm

Table **2.1:** Dimensions of **1997** Buick LeSabre and models used in the experiments

2.3 Scaling of Measured Quantities

To complete the dynamical similarity of two geometrically similar flows, the Reynolds number Re

$$Re = \frac{UL}{\nu} \tag{2.1}$$

where U is the flow velocity, L is the characteristic length scale, and ν is the kinematic viscosity of air, should be the same. In our experiment, the Reynolds number $Re \sim 3.3 \times 10^5$, is lower than the full scale flow, where it is $Re \sim$ **9.1** x 10^6. Despite the mismatch, the experimental flow field can still provide sufficient information about the real flow because the Reynolds number in both cases are high enough that the inertia forces dominate the viscous forces, except in boundary layers.

To compare the force and moment data for different flows, the measured transient aerodynamic data are nondimensionalized by defining force and moment coefficients. By scaling the drag force with the dynamic head, the drag coefficient is defined as

$$C_D = \frac{D}{\frac{1}{2}\rho U^2 A} \tag{2.2}$$

where D is the measured drag force and A is the frontal area of the vehicle exposed to the oncoming flow. In this case, the frontal area is

$$A = wh \tag{2.3}$$

where w is the width and h is the height of the vehicle model. Similarly, a side force coefficient C_S is defined as

$$C_S = \frac{S}{\frac{1}{2}\rho U^2 A} \tag{2.4}$$

where S is the side force. A yaw moment coefficient C_M is defined as

$$C_M = \frac{M}{\frac{1}{2}\rho U^2 V} \tag{2.5}$$

where M is the yaw moment, and the volume V is defined as

$$V = Al \tag{2.6}$$

and l is the length of the model.

These nondimensional coefficients will be used in the following chapters to characterize the transient aerodynamic forces and moment measured in different experimental cases. The coefficients measured in a "clean" four-car platoon, which means no mobile model is presented near the platoon, are provided in table 2.2. Based on the data in table 2.2, we can determine the aerodynamic effects on the platoon brought by a overtaking (overtaken) vehicle.

Coefficients	Drag C_{D_C}	Side Force C_{S_C}	Yaw Moment C_{M_C}
CAR 1	0.230	0.030	-0.002
CAR 2	0.204	-0.002	0.001
CAR 3	0.133	0.000	-0.007
CAR 4	0.202	0.003	-0.001

Table 2.2: Force and moment coefficients measured in a clean platoon

Chapter 3

Effects of Mobile Direction

Aerodynamic forces and yaw moment experienced by every car in the platoon are compared for the cases that the mobile model is in forward and backward motions. As mentioned previously, the two situations represent a single car passes a platoon and a platoon passes a single car, respectively. Forces and moment measured on the four platoon members are recorded simultaneously as the mobile model travels for $1.2m$ at the assigned velocity. The coefficients on each of the four cars are plotted with respect to the position of the front end of the mobile model. The position of each platoon member and its coefficients measured in a clean platoon condition are also plotted for reference. Figure 3.1 to figure 3.12 show the data while a rectangular box is used as the mobile model, and figure 3.13 to figure 3.24 show the measurements while a vehicle model is applied. Four lateral spacings ($d = \frac{1}{4}, \frac{1}{2}, 1,$ and $\frac{3}{2}W$, where $W = 10.2cm =$ box width) and three velocities ($v = 1.25, 2.50,$ and $3.75m/s$) are examined for both mobile models.

Two runs are conducted for each condition, and both data sets are shown in these figures. In most measurements, as expected, the two runs under identical testing conditions agree with each other, but in some cases, they shift upward or downward a little due to electronic drift [5]. By considering the coefficients on each platoon member should be close to the clean platoon measurements when the mobile model is far away, we choose the one whose reading is more reasonable in this sense and apply this set of data later in this report. Yaw moment coefficients are too small to be noticed in all conditions, therefore we skip the moment data hereafter and focus on the changes in drag and side forces.

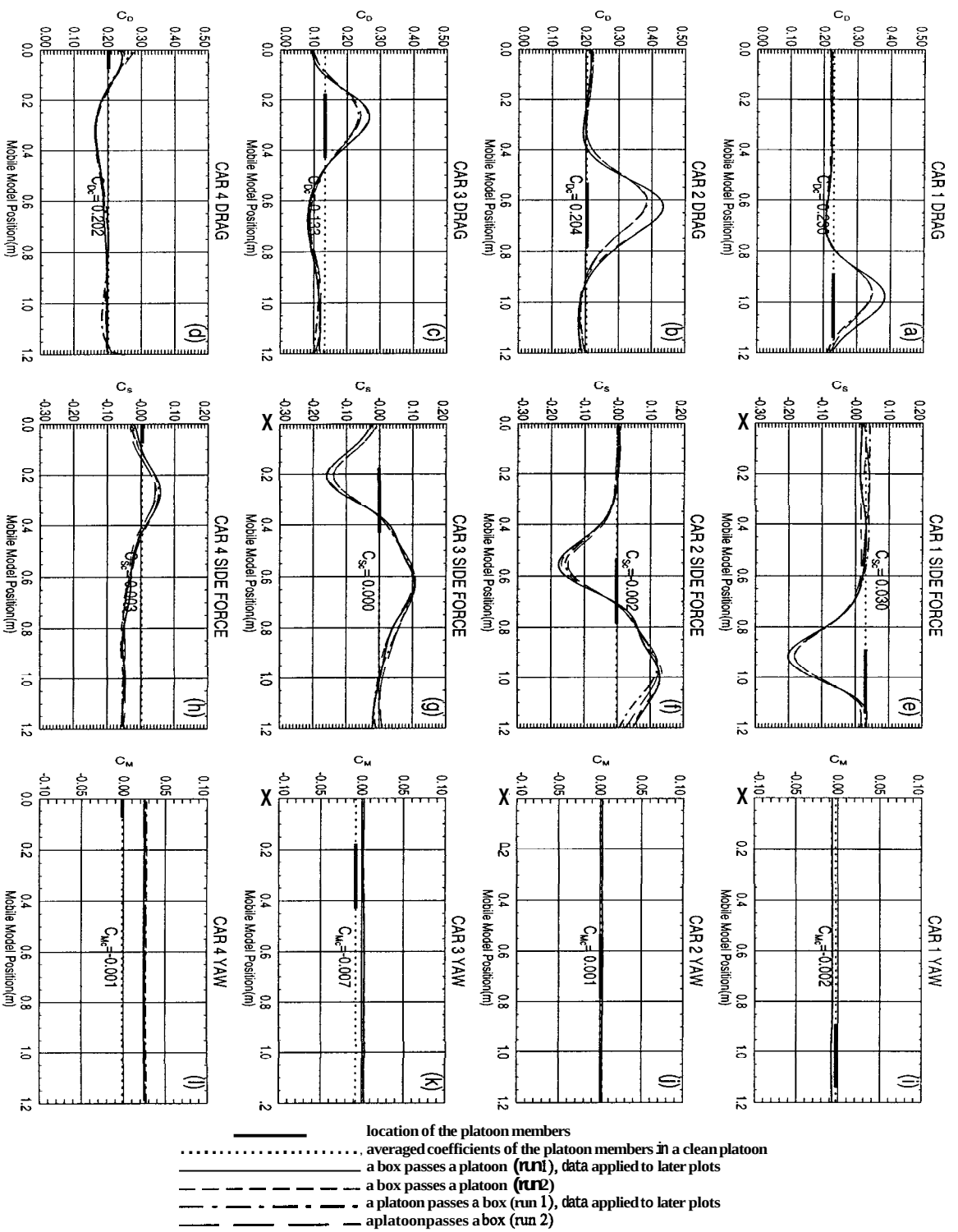

Figure **3.1:** Comparison of passing directions - a box vs. a platoon ($d = \frac{1}{4}W, v = 1.25m/s$). The drag [frames (a)-(d)], side force [frames (e)-(h)],and yaw moment [frames (i)-(l)] coefficients on each car in the platoon are shown with respect to the position of mobile model.

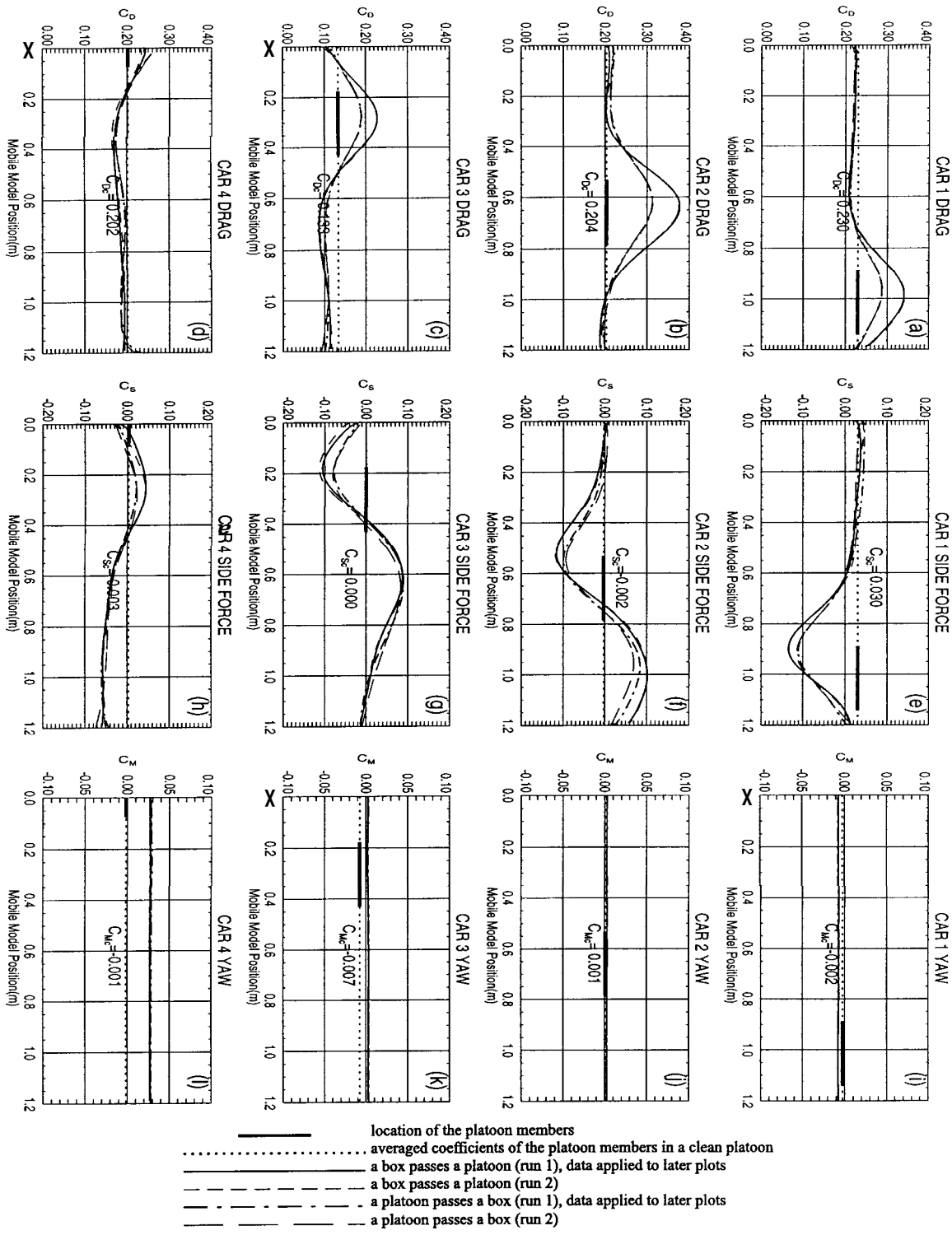

Figure 3.2: Comparison of passing directions - a box vs. a platoon ($d = \frac{1}{4}W, v = 2.50m/s$). The drag [frames (a)-(d)], side force [frames (e)-(h)], and yaw moment [frames (i)-(l)] coefficients on each car in the platoon are shown with respect to the position of mobile model.

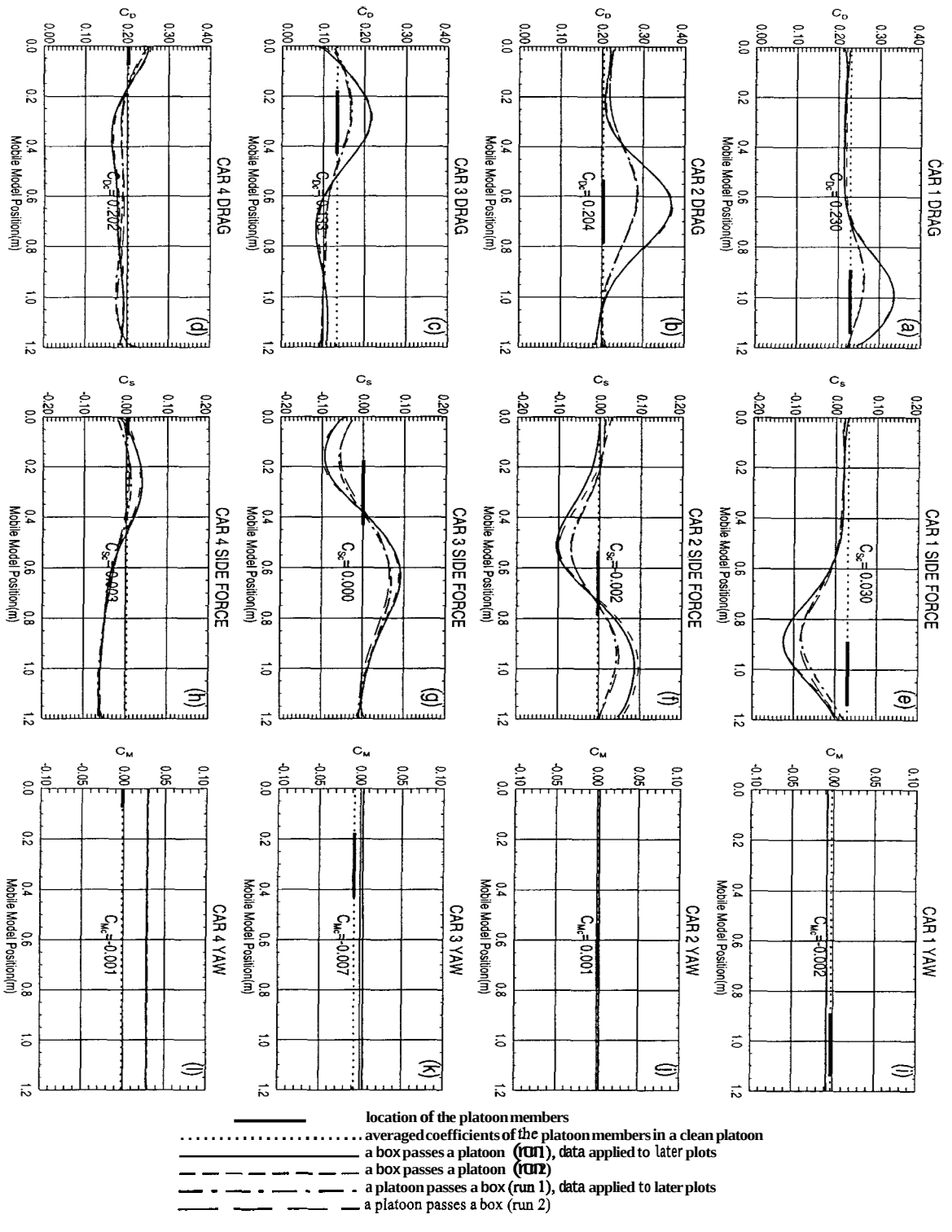

Figure *3.3:* Comparison of passing directions - a box vs. a platoon ($d = \frac{1}{4}W, v = 3.75m/s$). The drag [frames (a)-(d)],side force [frames (e)-(h)],and yaw moment [frames (i)-(l)] coefficients on each car in the platoon are shown with respect to the position of mobile model.

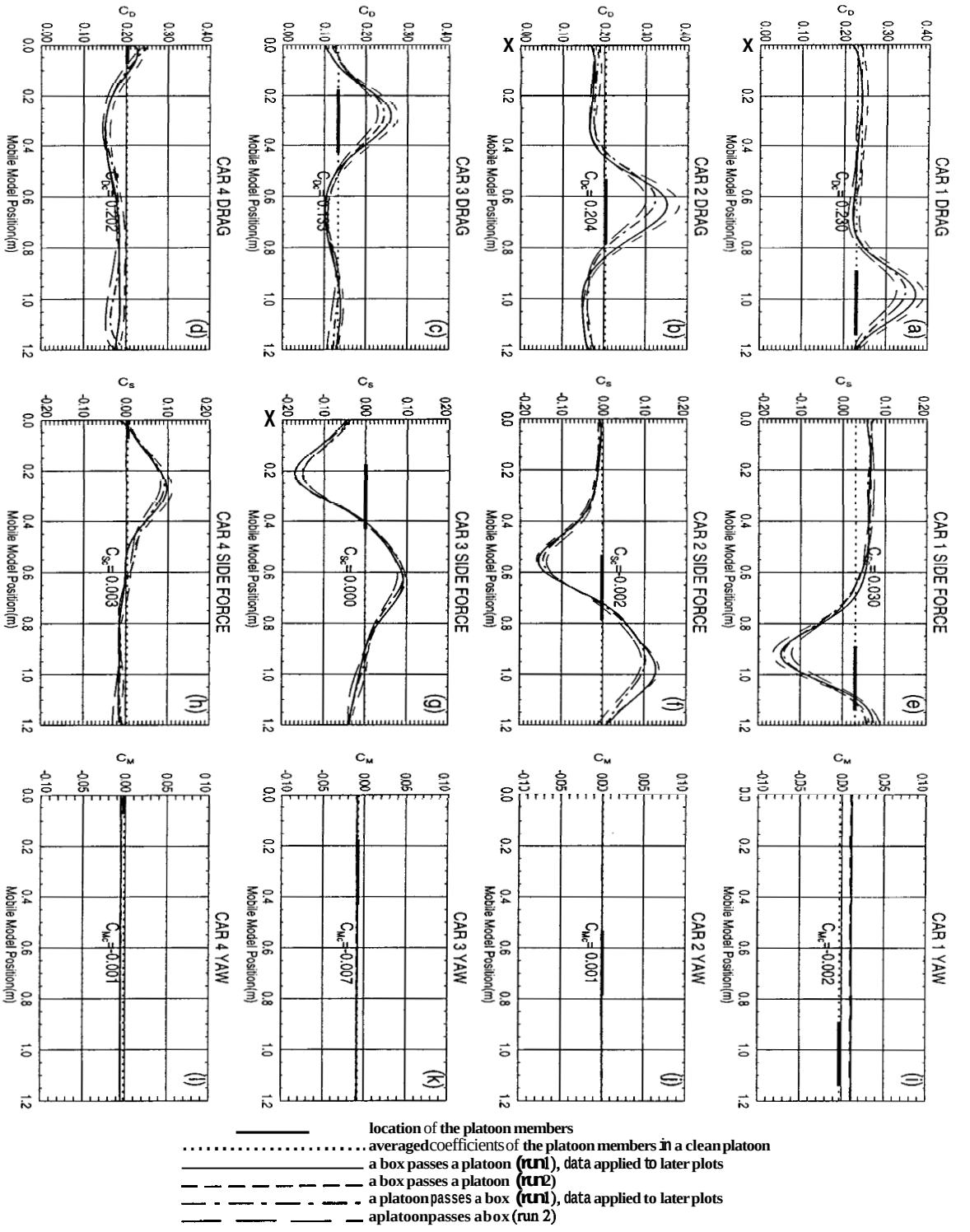

Figure **3.4:** Comparison of passing directions - a box vs. a platoon $(d = \frac{1}{2}W, v = 1.25m/s)$. The drag [frames (a)-(d)],side force [frames (e)-(h)],and yaw moment [frames (i)-(l)] coefficients on each car in the platoon are shown with respect to the position of mobile model.

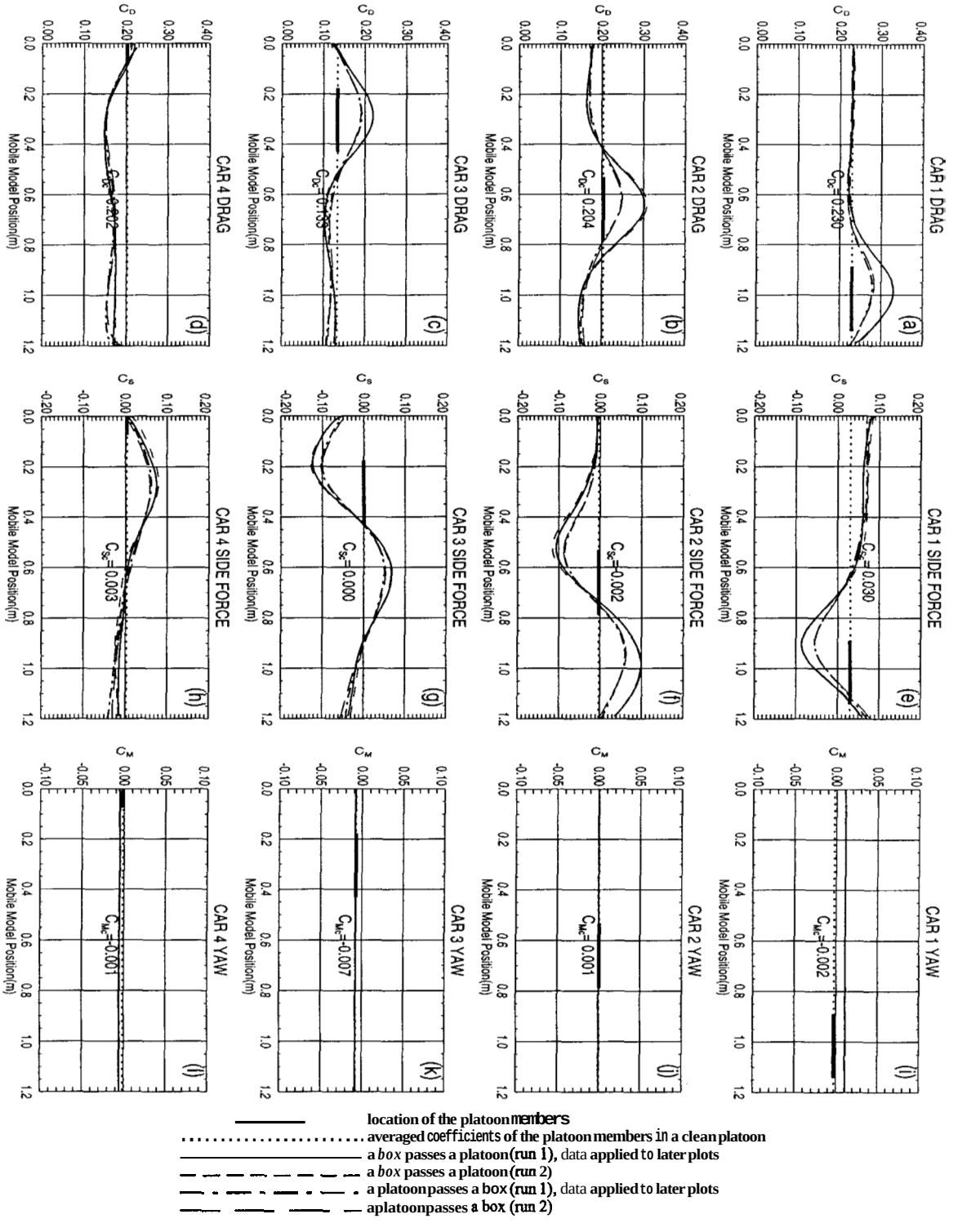

Figure 3.5: Comparison of passing directions - a box vs. a platoon ($d = \frac{1}{2}W, v = 2.50m/s$). The drag [frames (a)-(d)], side force [frames (e)-(h)], and yaw moment [frames (i)-(l)] coefficients on each car in the platoon are shown with respect to the position of mobile model.

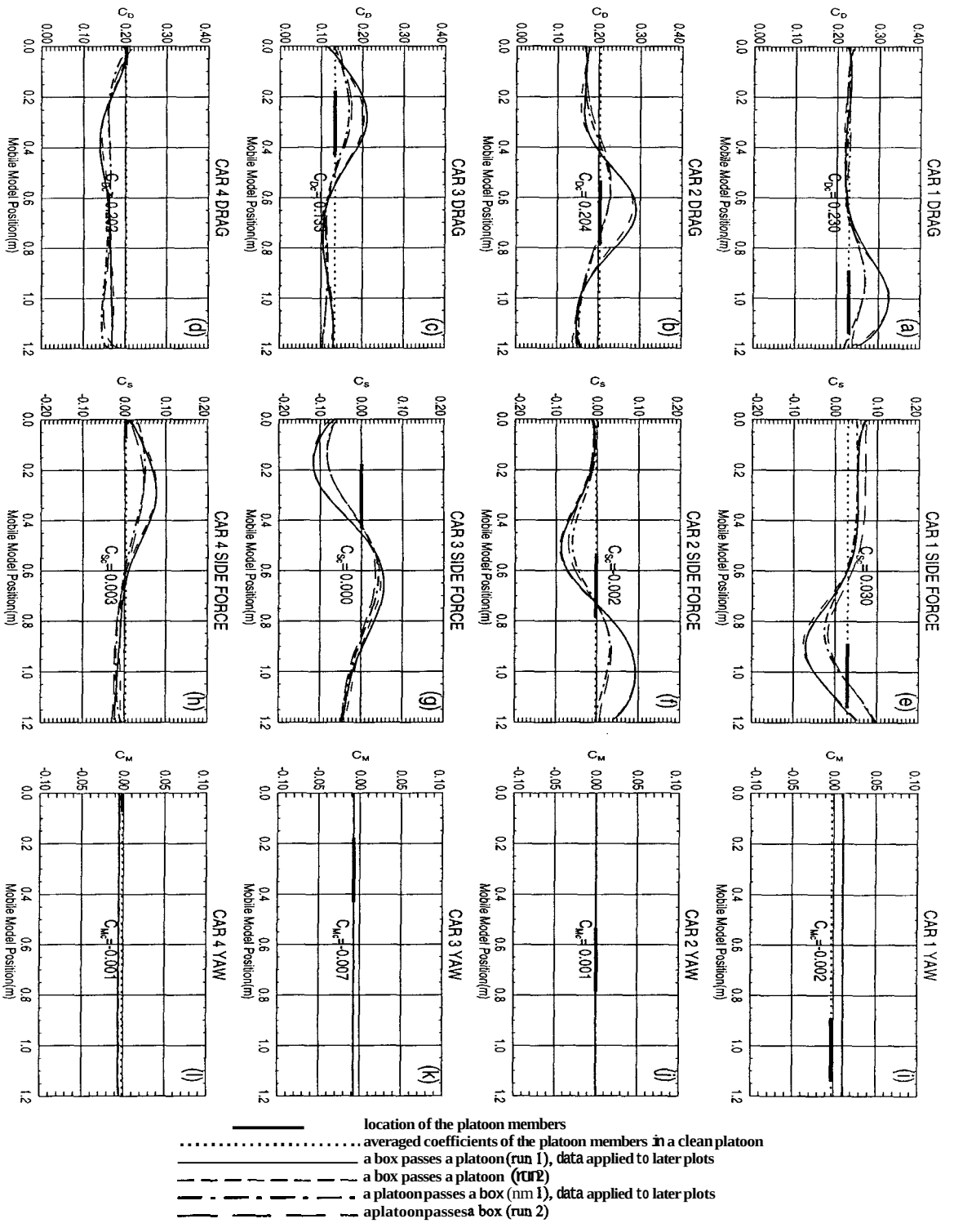

Figure **3.6:** Comparison of passing directions - a box vs. a platoon $(d = \frac{1}{2}W, v = 3.75m/s)$. The drag [frames (a)-(d)], side force [frames (e)-(h)], and yaw moment [frames (i)-(l)] coefficients on each car in the platoon are shown with respect to the position of mobile model.

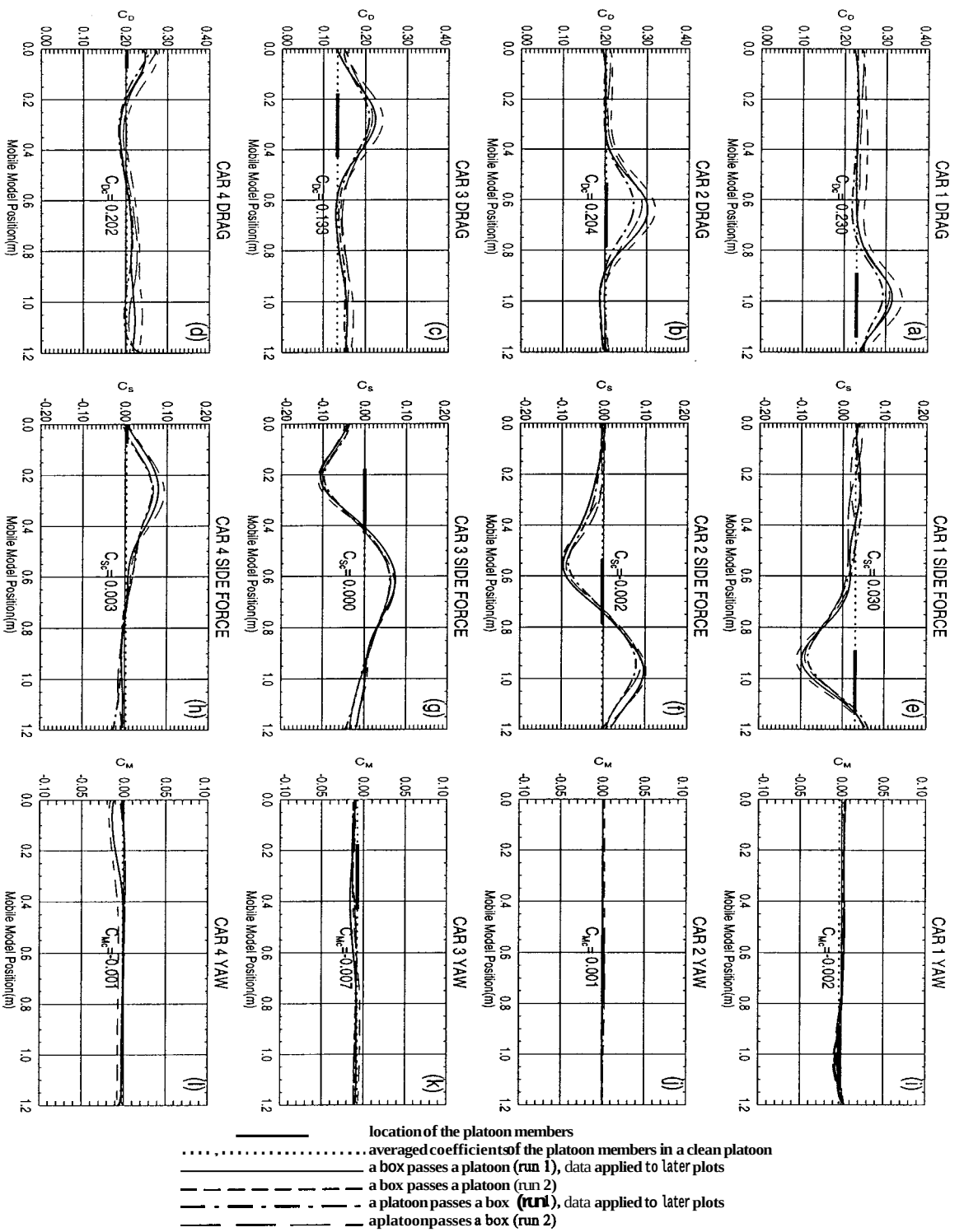

Figure 3.7: Comparison of passing directions - a box vs. a platoon $(d = 1W, v = 1.25m/s)$. The drag [frames (a)-(d)],side force [frames (e)-(h)],and yaw moment [frames (i)-(l)] coefficients on each car in the platoon are shown with respect to the position of mobile model.

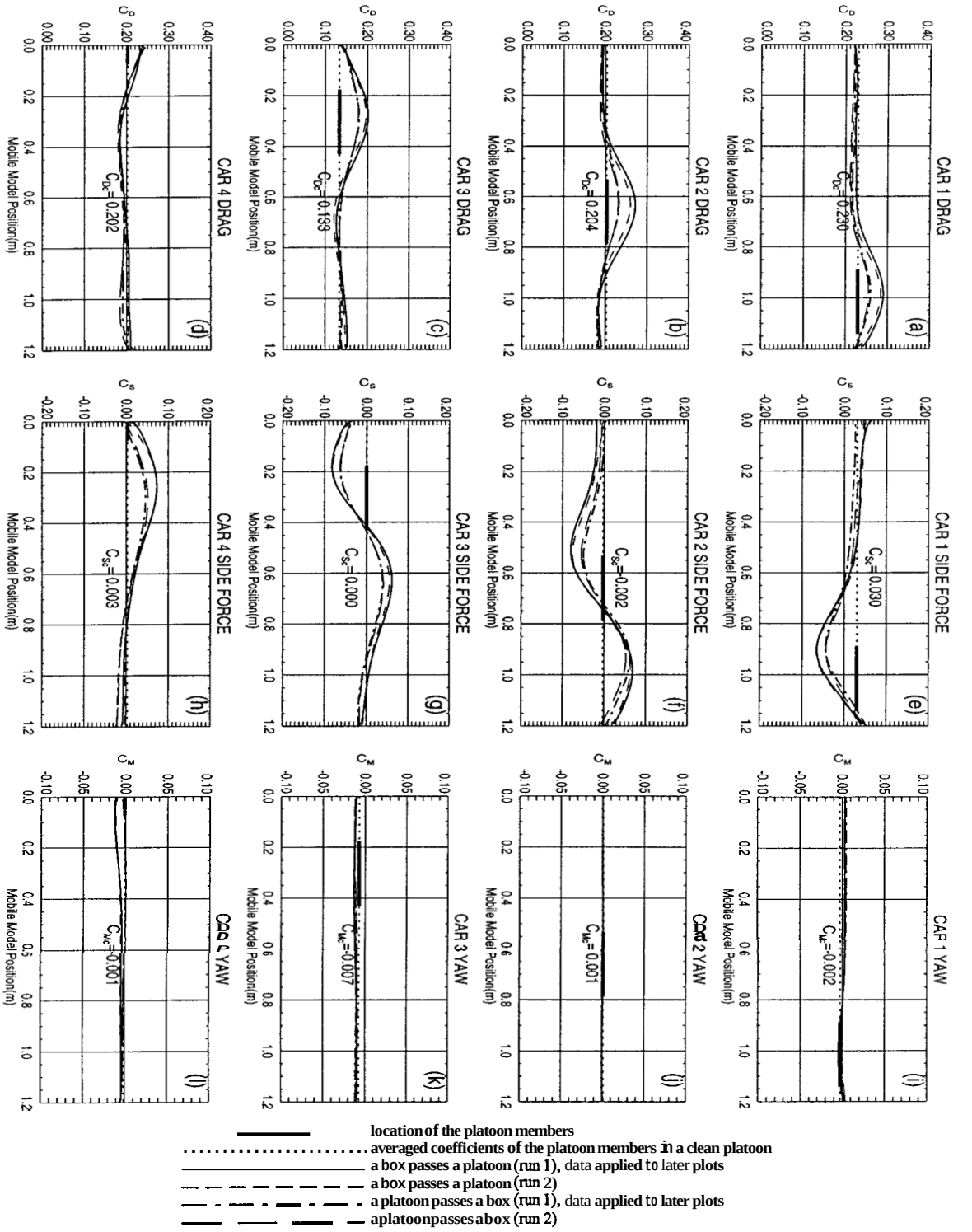

Figure **3.8:** Comparison of passing directions - a box vs. a platoon $(d = 1W, v = 2.50m/s)$. The drag [frames (a)-(d)],side force [frames (e)-(h)],and yaw moment [frames (i)-(l)] coefficients on each car in the platoon are shown with respect to the position of mobile model.

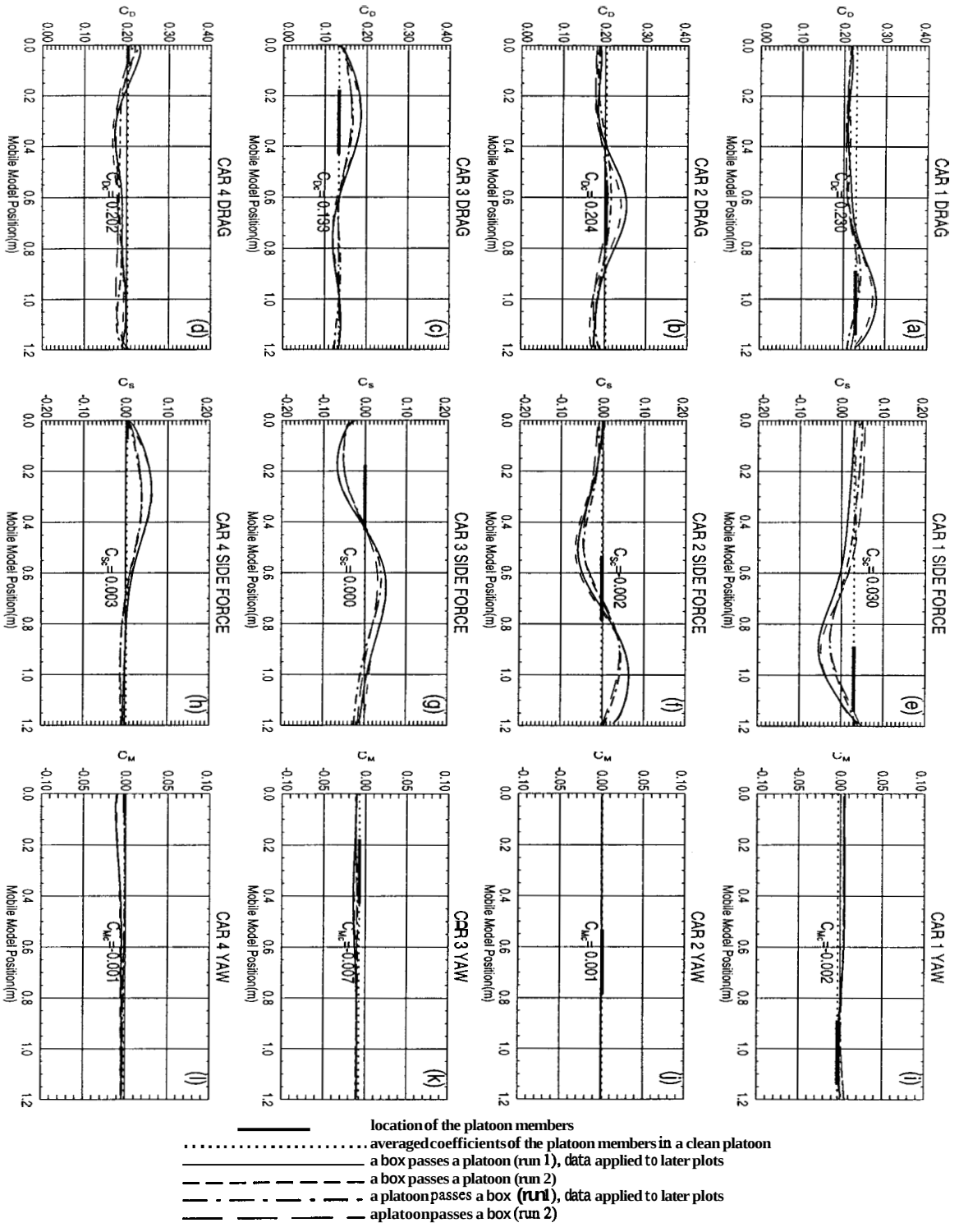

Figure **3.9:** Comparison of passing directions - a box vs. a platoon $(d = 1W, v = 3.75m/s)$. The drag [frames (a)-(d)],side force [frames (e)-(h)],and yaw moment [frames (i)-(l)] coefficients on each car in the platoon are shown with respect to the position of mobile model.

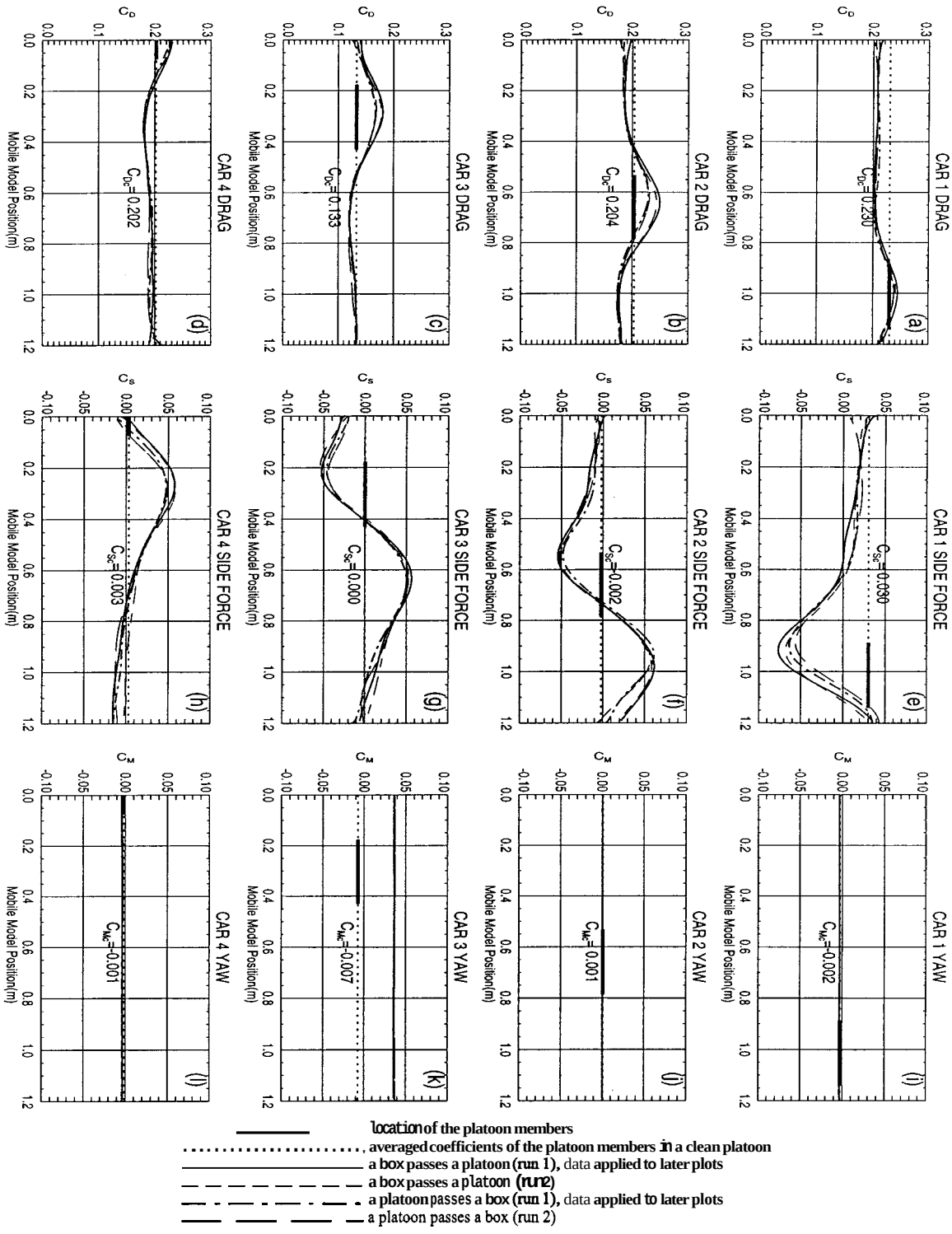

Figure **3.10:** Comparison of passing directions - a **box** vs. a platoon $(d = \frac{3}{2}W, v = 1.25m/s)$. The drag [frames (a)-(d)], side force [frames (e)-(h)], and yaw moment [frames (i)-(l)] coefficients on each car in the platoon are shown with respect to the position of mobile model.

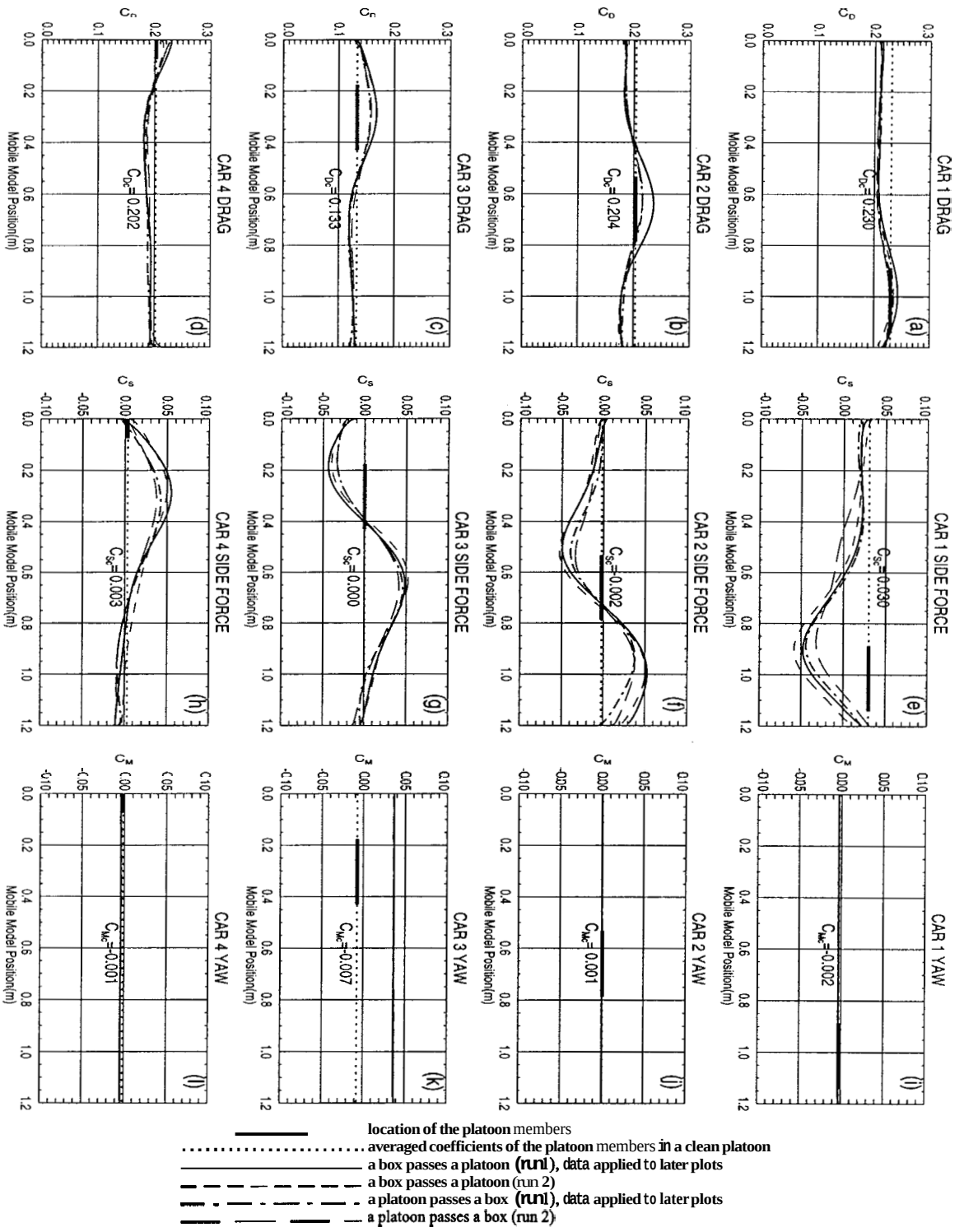

Figure 3.11: Comparison of passing directions - a box vs. a platoon ($d = \frac{3}{2}W, v = 2.50m/s$). The drag [frames (a)-(d)], side force [frames (e)-(h)],and yaw moment [frames (i)-(l)] coefficients on each car in the platoon are shown with respect to the position of mobile model.

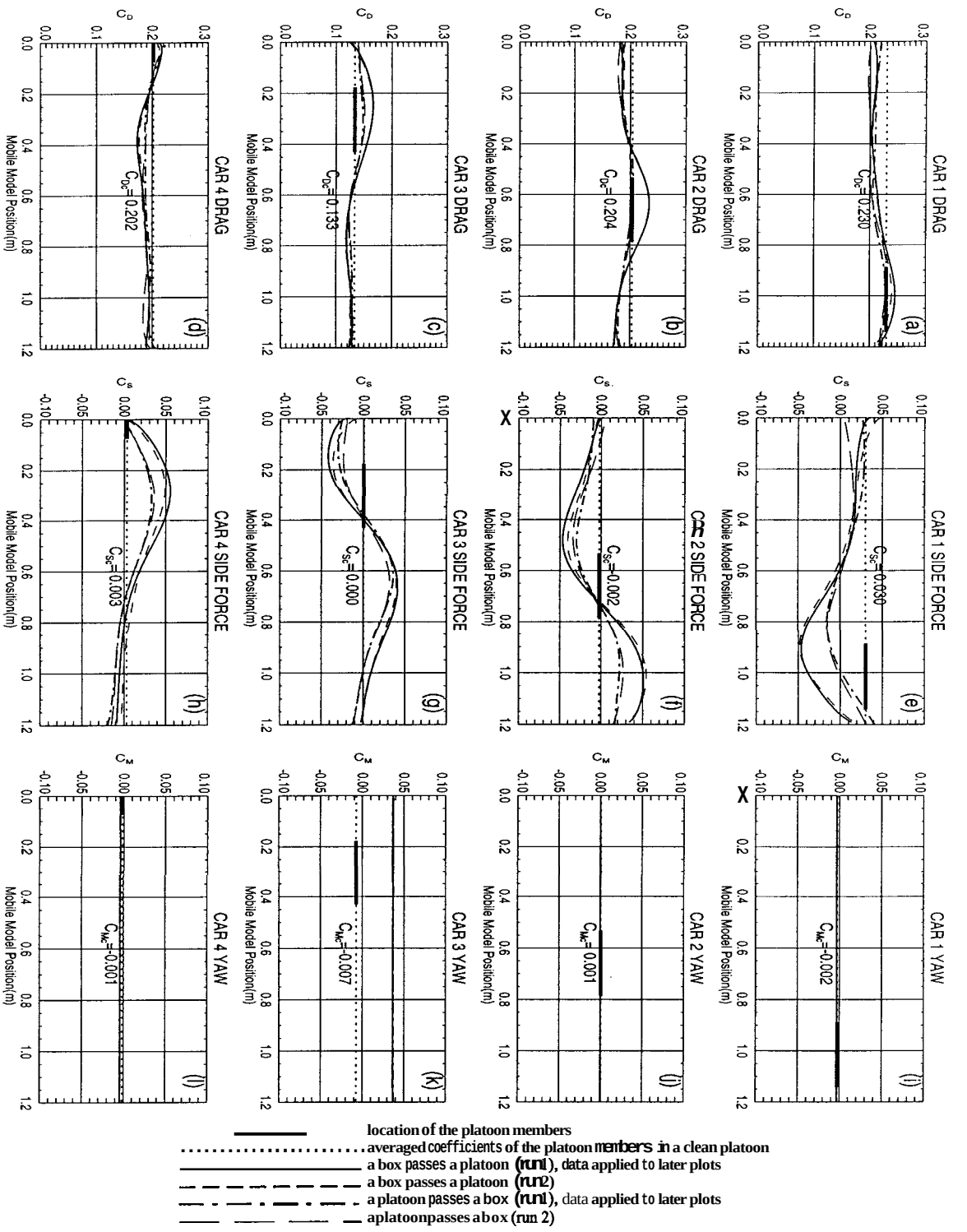

Figure **3.12:** Comparison of passing directions - a box vs. a platoon $(d = \frac{3}{2}W, v = 3.75m/s)$. The drag [frames (a)-(d)],side force [frames (e)-(h)], and yaw moment [frames (i)-(l)] coefficients on each car in the platoon are shown with respect to the position of mobile model.

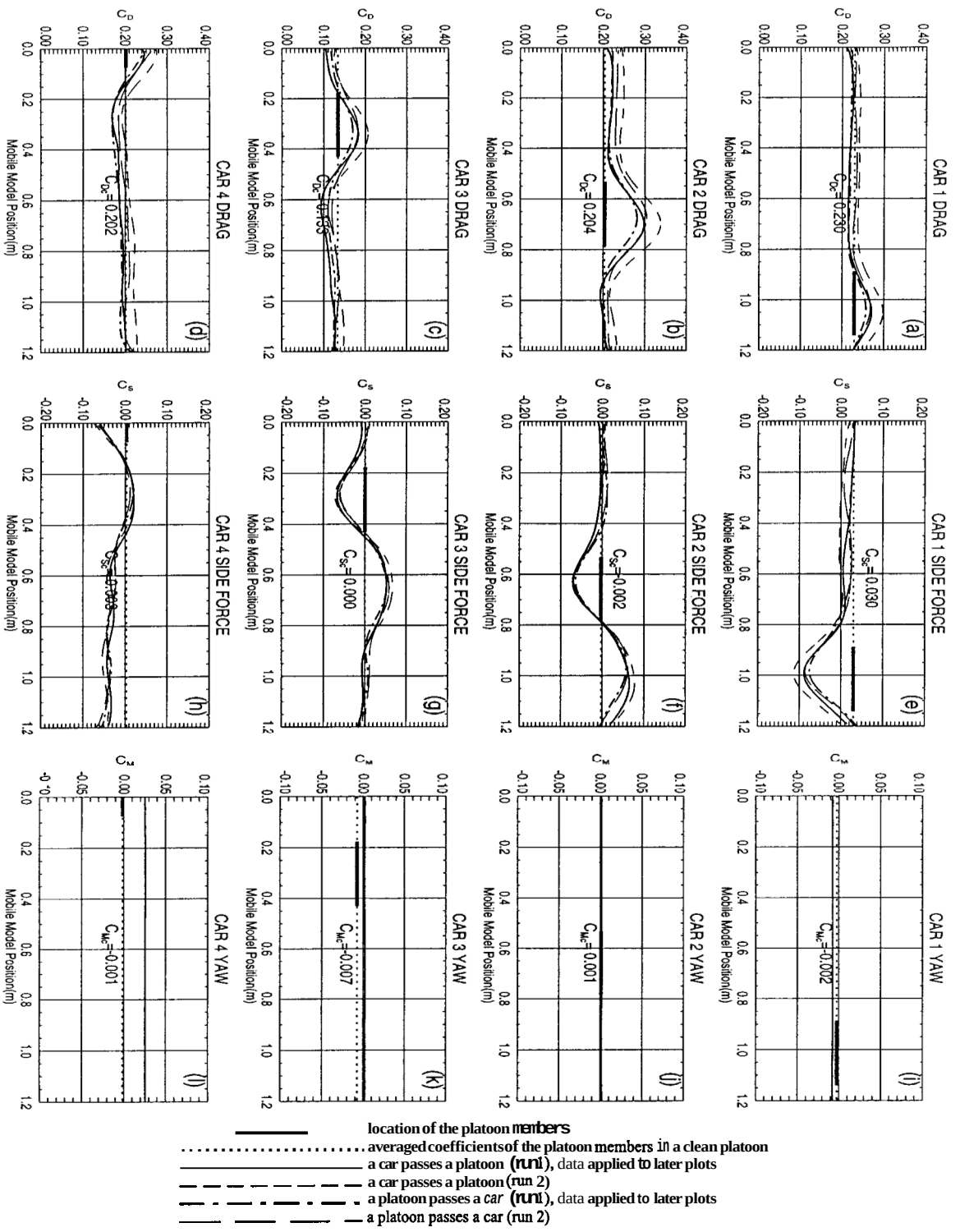

Figure **3.13:** Comparison of passing directions - a car vs. a platoon ($d = \frac{1}{4}W, v = 1.25m/s$). The drag [frames (a)-(d)],side force [frames (e)-(h)],and yaw moment [frames (i)-(l)] coefficients on each car in the platoon are shown with respect to the position of mobile model.

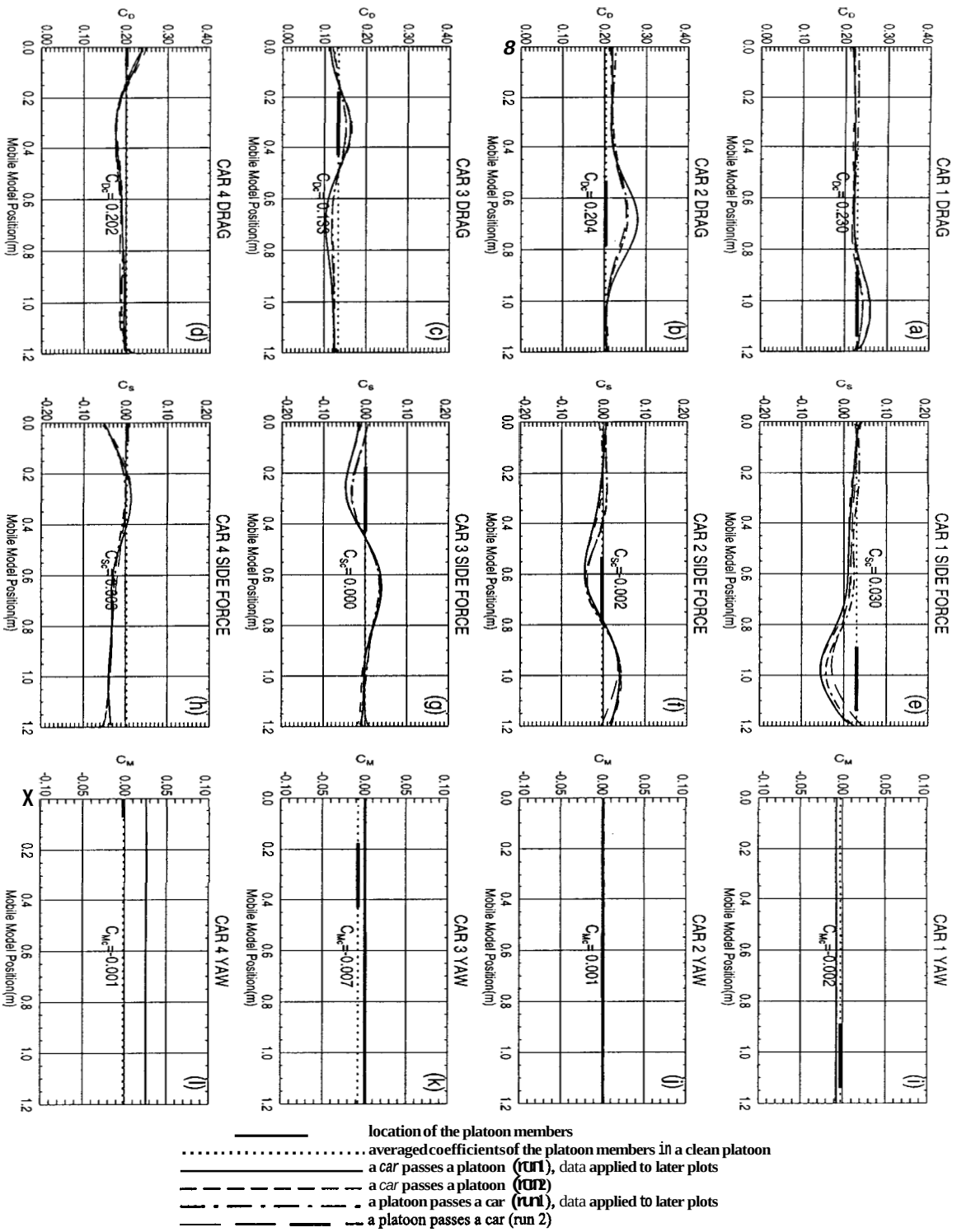

Figure **3.14:** Comparison of passing directions - a car vs. a platoon $(d = \frac{1}{4}W, v = 2.50m/s)$. The drag [frames (a)-(d)],side force [frames (e)-(h)],and yaw moment [frames (i)-(l)] coefficients on each car in the platoon are shown with respect to the position of mobile model.

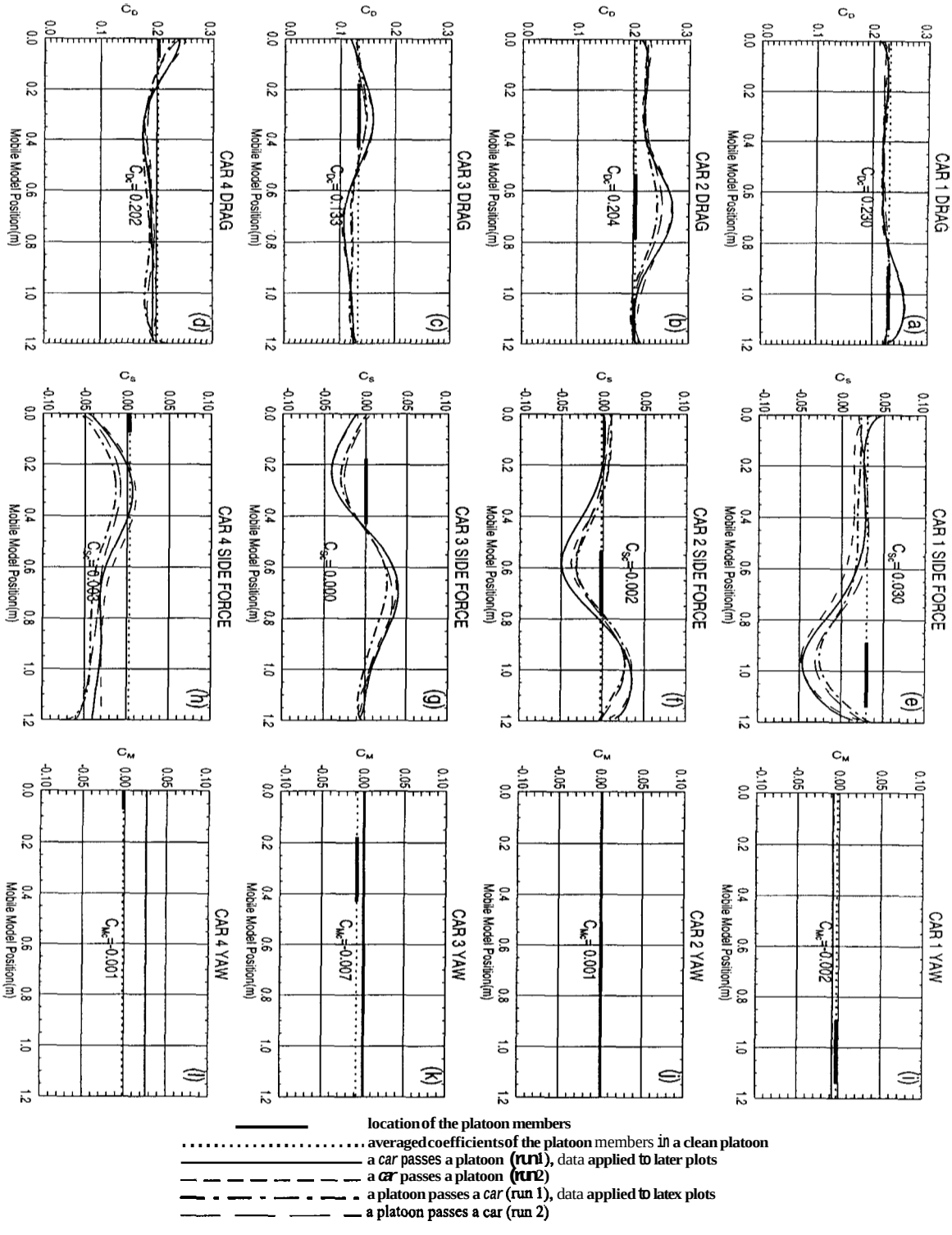

Figure **3.15:** Comparison of passing directions - a car vs. a platoon $(d = \frac{1}{4}W, v = 3.75m/s)$. The drag [frames (a)-(d)], side force [frames (e)-(h)],and yaw moment [frames (i)-(l)] coefficients on each car in the platoon are shown with respect to the position of mobile model.

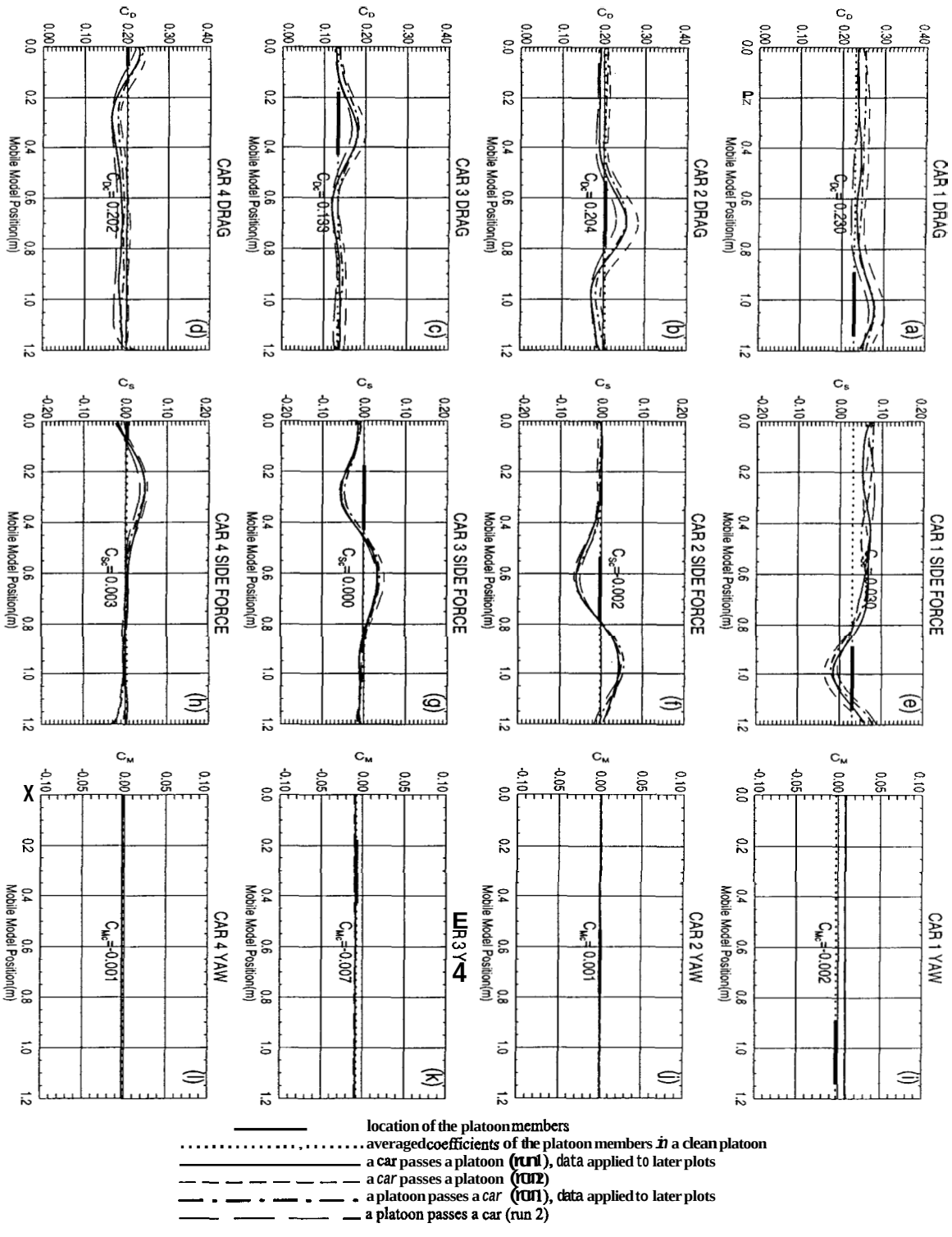

Figure **3.16:** Comparison of passing directions - a car vs. a platoon ($d = \frac{1}{2}W, v = 1.25m/s$). The drag [frames (a)-(d)],side force [frames (e)-(h)],and yaw moment [frames (i)-(l)] coefficients on each car in the platoon are shown with respect to the position of mobile model.

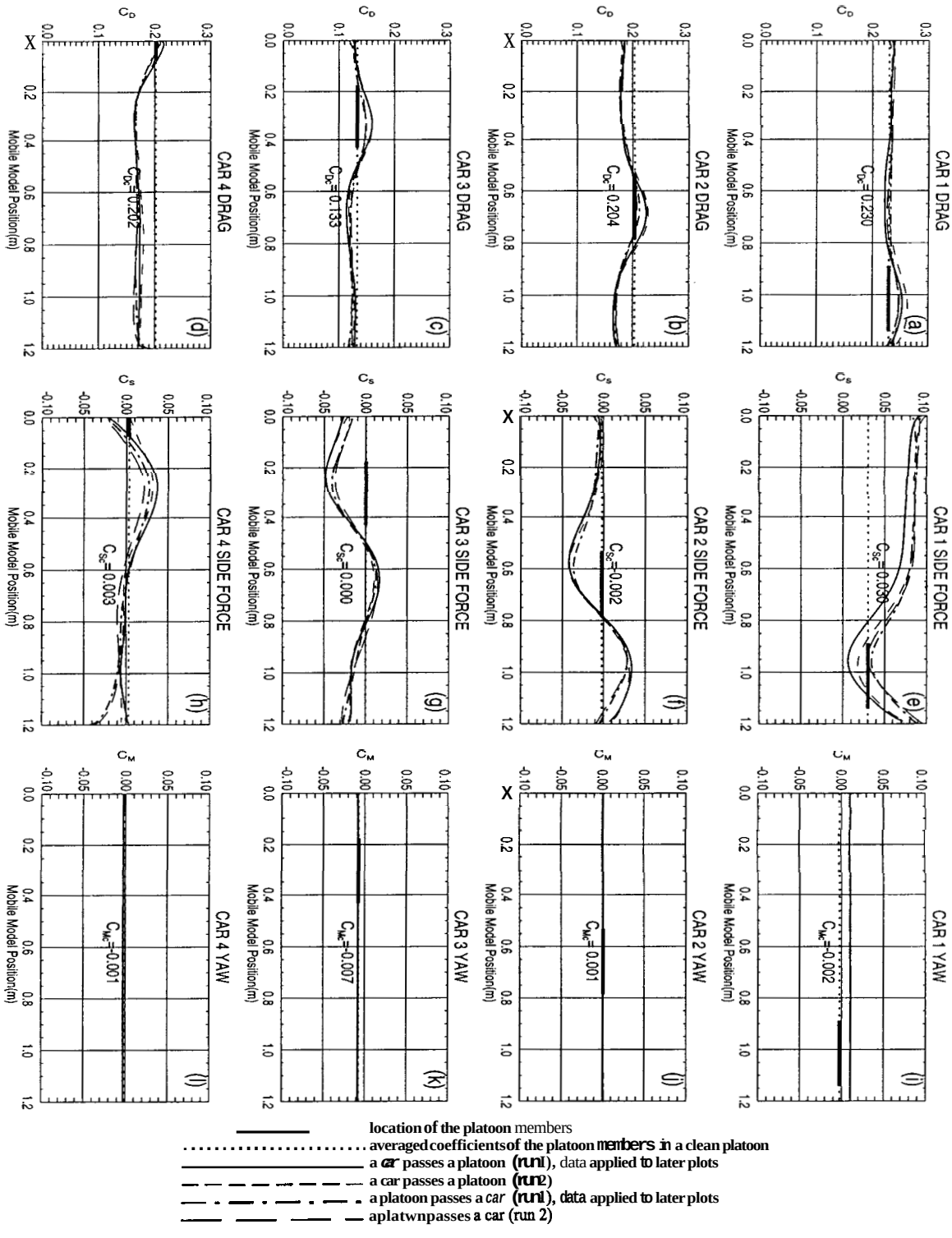

Figure **3.17:** Comparison of passing directions - a car vs. a platoon $(d = \frac{1}{2}W, u = 2.50 m/s)$. The drag [frames (a)-(d)],side force [frames (e)-(h)], and yaw moment [frames (i)-(l)] coefficients on each car in the platoon are shown with respect to the position of mobile model.

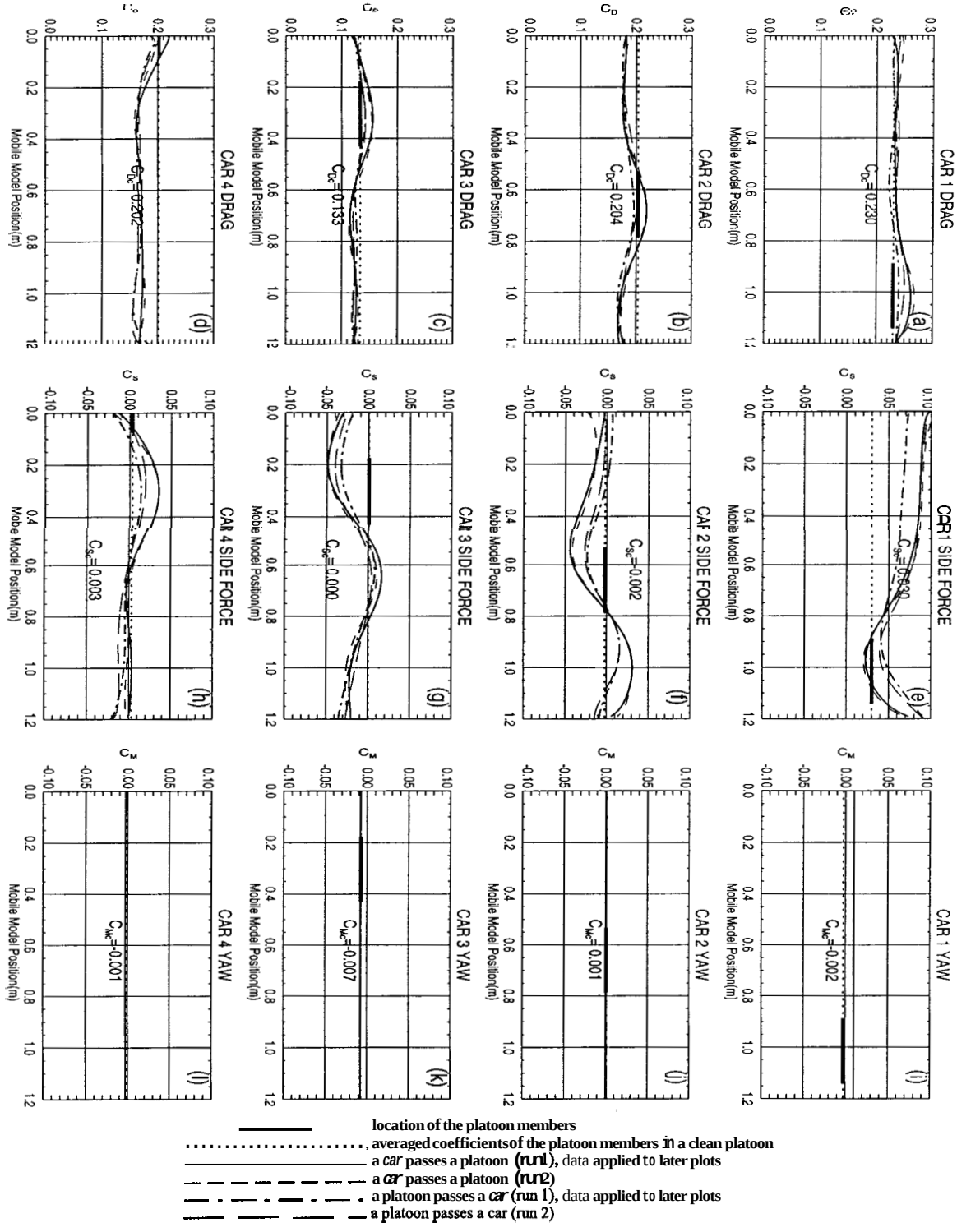

Figure **3.18:** Comparison of passing directions - a car vs. a platoon ($d = \frac{1}{2}W, v = 3.75m/s$). The drag [frames (a)-(d)],side force [frames (e)-(h)], and yaw moment [frames (i)-(l)] coefficients on each car in the platoon are shown with respect to the position of mobile model.

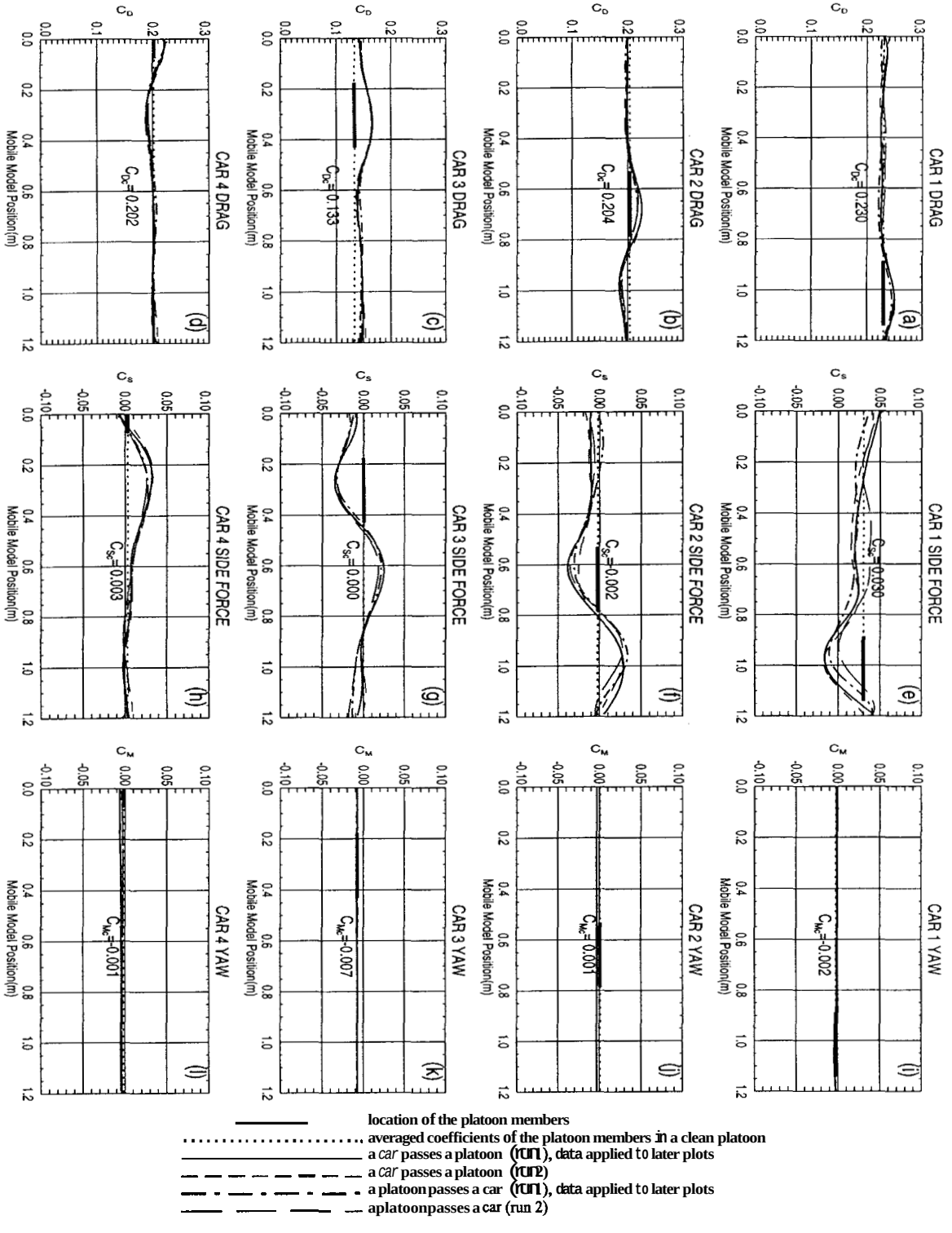

Figure **3.19:** Comparison of passing directions - a car vs. a platoon ($d = 1W, v = 1.25m/s$). The drag [frames (a)-(d)],side force [frames (e)-(h)],and yaw moment [frames (i)-(l)] coefficients on each car in the platoon are shown with respect to the position of mobile model.

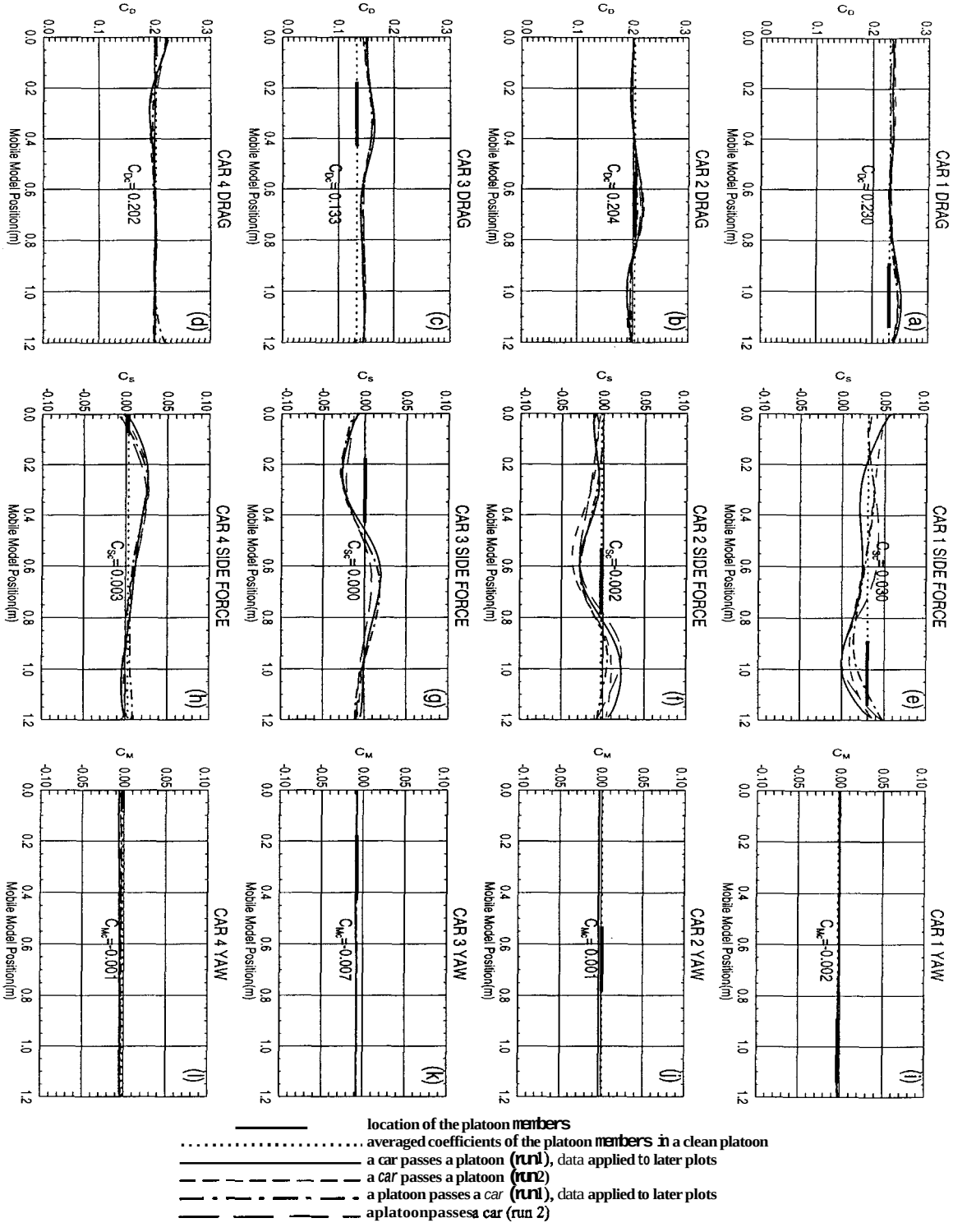

Figure **3.20:** Comparison of passing directions - a car vs. a platoon $(d = 1W, v = 2.50m/s)$. The drag [frames (a)-(d)], side force [frames (e)-(h)], and yaw moment [frames (i)-(l)] coefficients on each car in the platoon are shown with respect to the position of mobile model.

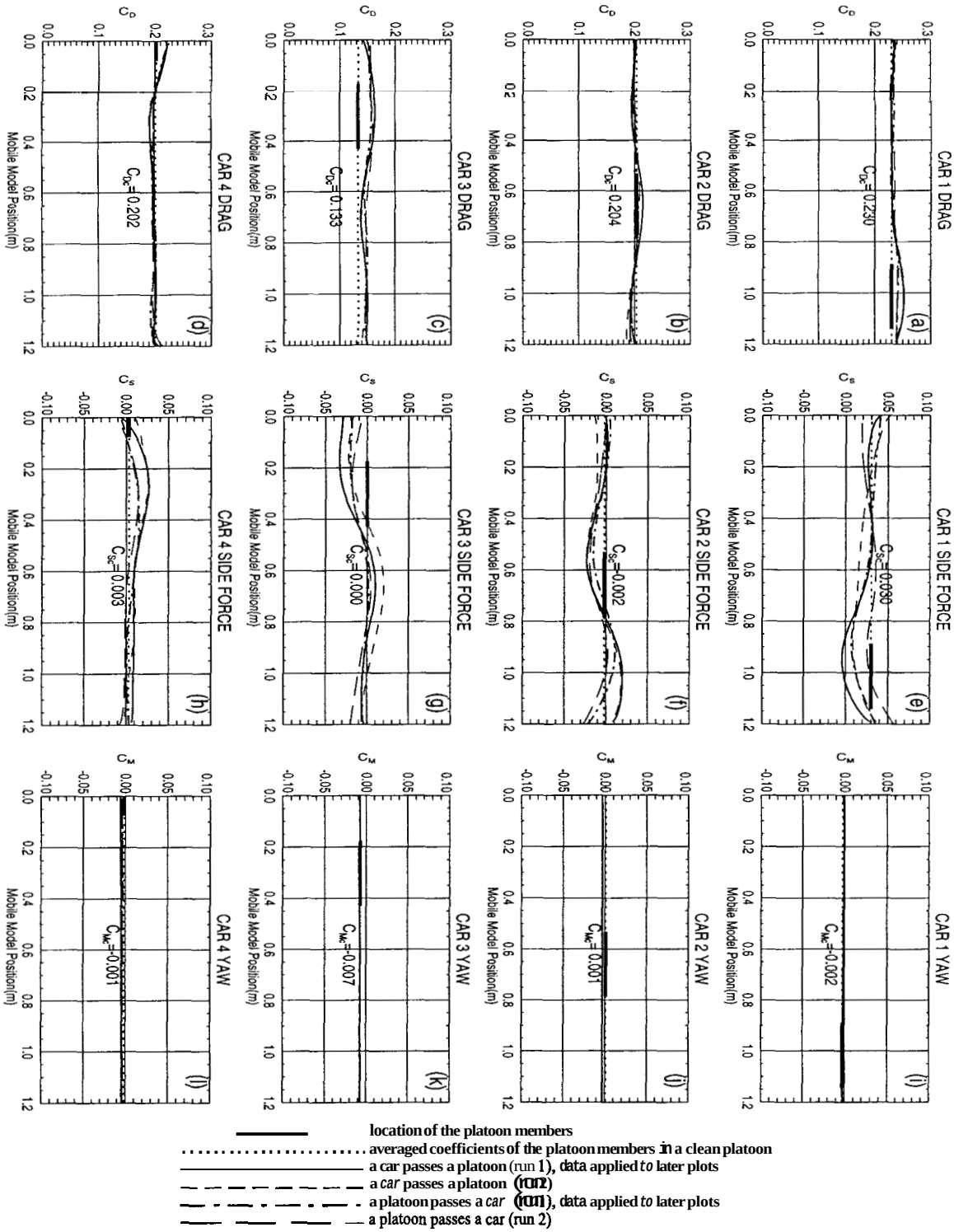

Figure **3.21:** Comparison of passing directions - a car vs. a platoon $(d = 1W, v = 3.75m/s)$. The drag [frames (a)-(d)], side force [frames (e)-(h)], and yaw moment [frames (i)-(l)] coefficients on each car in the platoon are shown with respect to the position of mobile model.

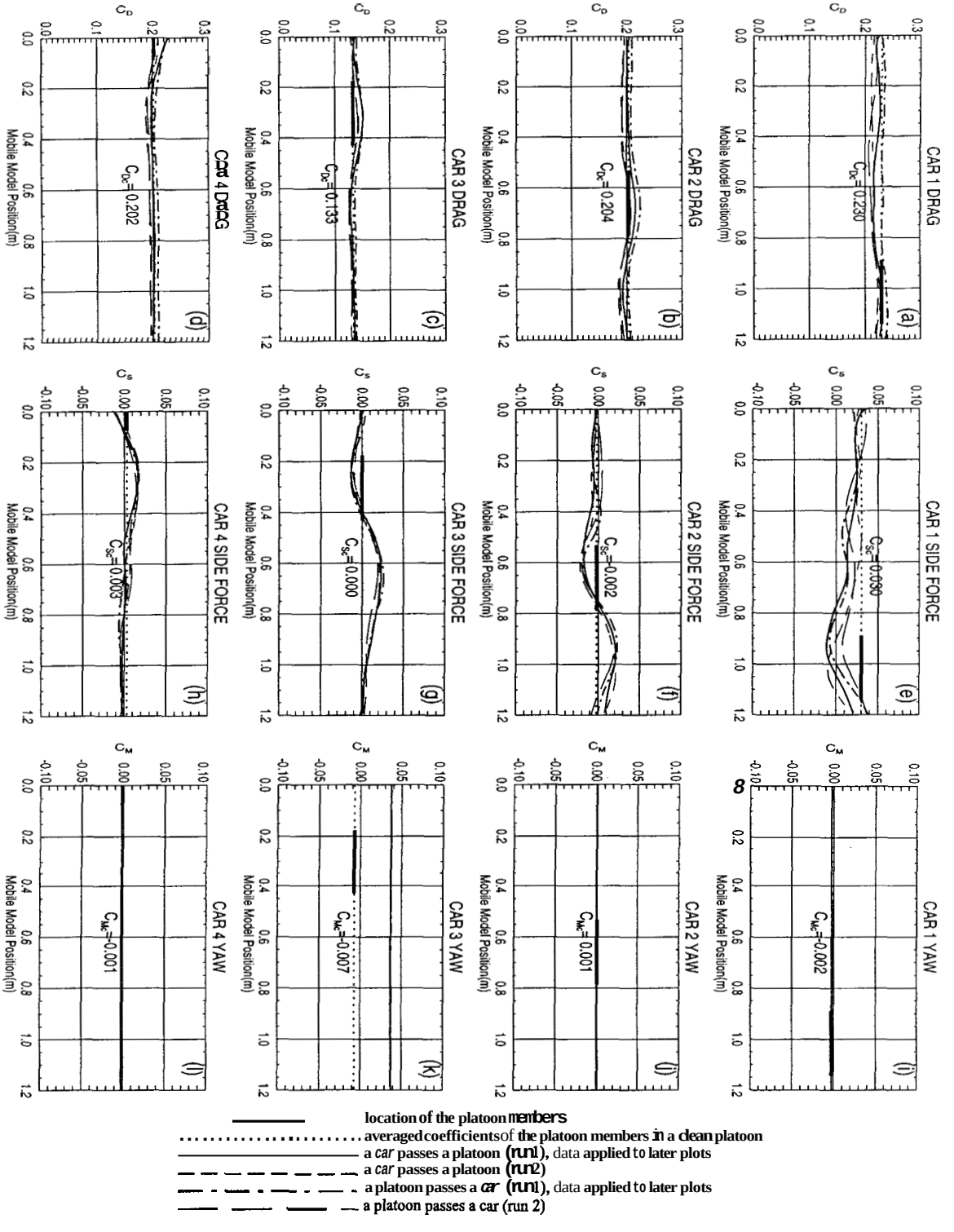

Figure 3.22: Comparison of passing directions - a **car** vs. a platoon $(d = \frac{3}{2}W, v = 1.25m/s)$. The drag [frames (a)-(d)],side force [frames (e)-(h)],and yaw moment [frames (i)-(l)] coefficients on each car in the platoon are shown with respect to the position of mobile model.

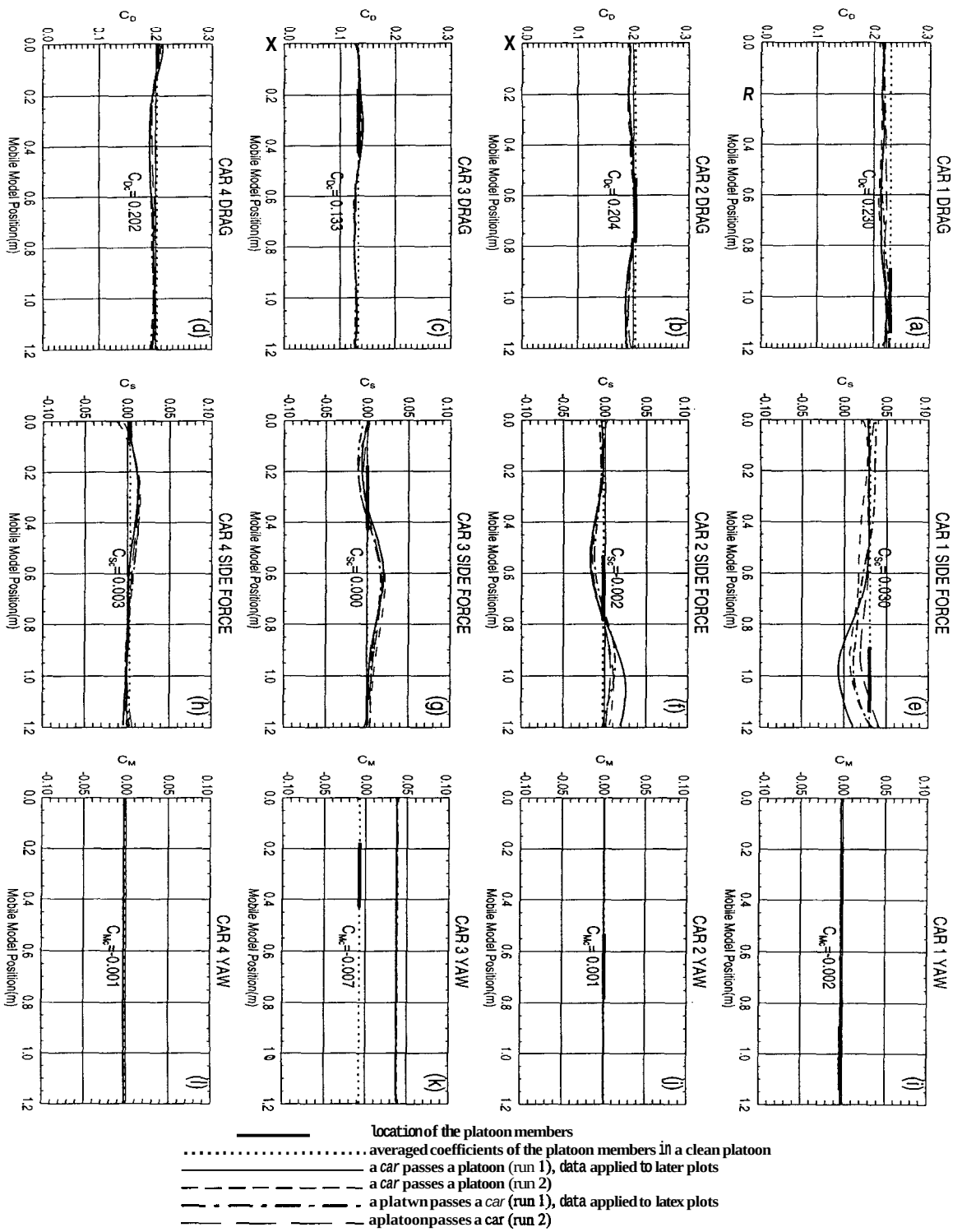

Figure 3.23: Comparison of passing directions - a car vs. a platoon ($d = \frac{3}{2}W, v = 2.50m/s$). The drag [frames (a)-(d)], side force [frames (e)-(h)], and yaw moment [frames (i)-(l)] coefficients on each car in the platoon are shown with respect to the position of mobile model.

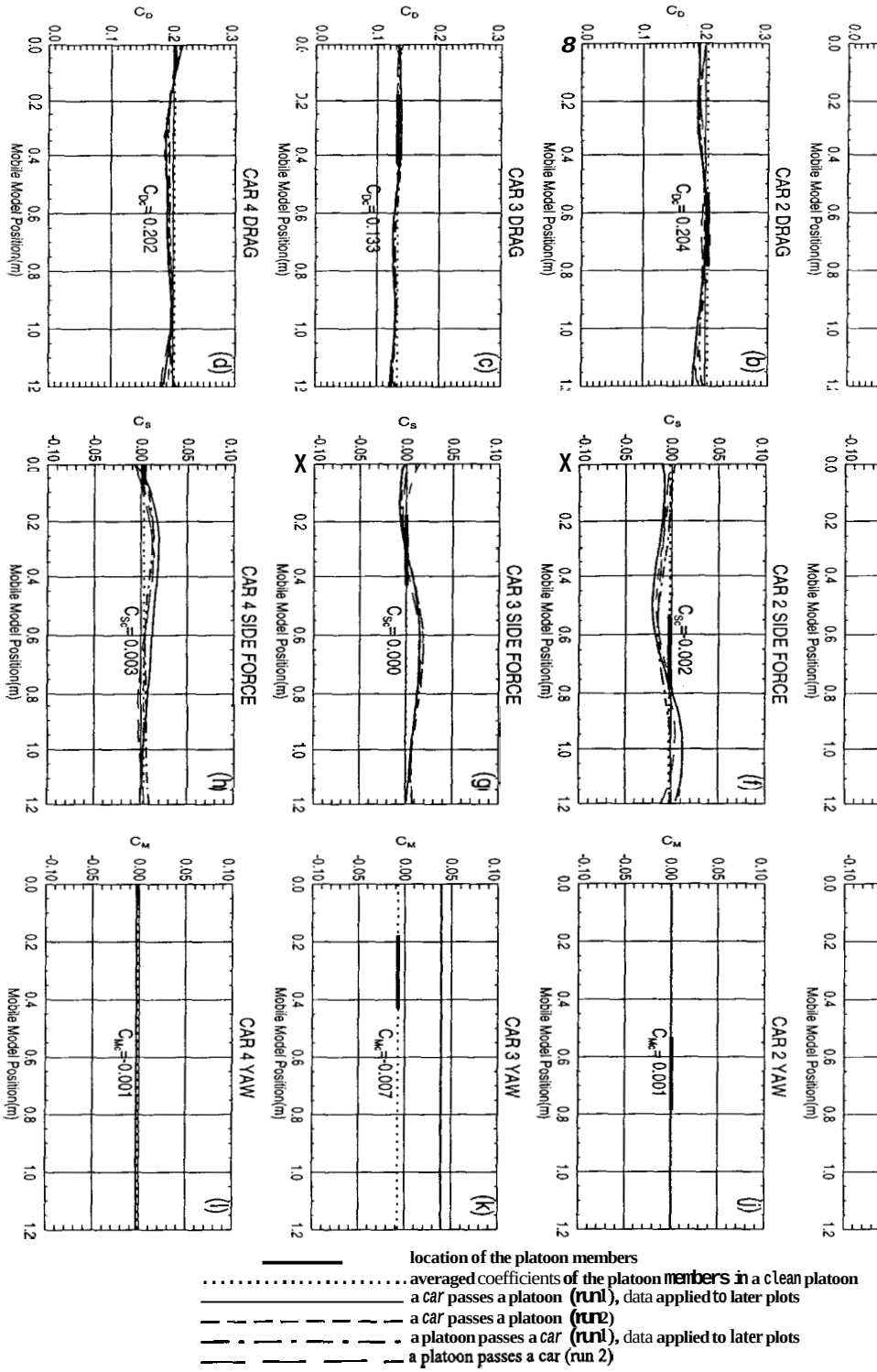

Figure **3.24:** Comparison of passing directions - a car vs. a platoon $(d = \frac{3}{2}W, v = 3.75m/s)$. The drag [frames (a)-(d)], side force [frames (e)-(h)], and yaw moment [frames (i)-(l)] coefficients on each car in the platoon are shown with respect to the position of mobile model.

Chapter 4

Effects of Passing Velocity

Aerodynamic forces experienced by every platoon member are compared for various relative velocities between the mobile model and the platoon. Forces measured on each of the four cars in the platoon are recorded simultaneously as the mobile model travels $1.2m$. The coefficients on each of the four cars are plotted with respect to the position of the front end of the mobile model. Transient data in five different velocities ($v = 1.25, 2.50, 3.75, 5.00,$ and $6.25m/s$) are taken when the mobile model is in forward motion, and three velocities ($v = -1.25, -2.50,$ and $-3.75m/s$) are recorded when the mobile model is in backward motion. Steady data are measured by placing the vehicle or box model at seven different locations, which represents the case that the fifth model is moving at the same speed as the platoon. The position of each platoon member and its coefficients determined in a clean platoon condition are also plotted for reference.

Figure 4.1 to figure 4.4 show the data while a rectangular box is used as the forward motion mobile model, and figure 4.5 to figure 4.8 show the data as the box model in backward motion. Figure 4.9 to figure 4.12 show the data while a vehicle is applied as the forward motion mobile model, and figure 4.13 to figure 4.16 show the data as the vehicle is in backward motion. Four lateral spacings ($d = \frac{1}{4}, \frac{1}{2}, 1,$ and $\frac{3}{2}W$, where $W = 10.2cm$ = box width) are examined for both mobile models and both directions.

Note that the passing velocities mentioned in this chapter are those assigned to the mobile model without considering the acceleration and deceleration in the beginning or at the end of the motion. The real mobile model's velocity data are shown in chapter 7.

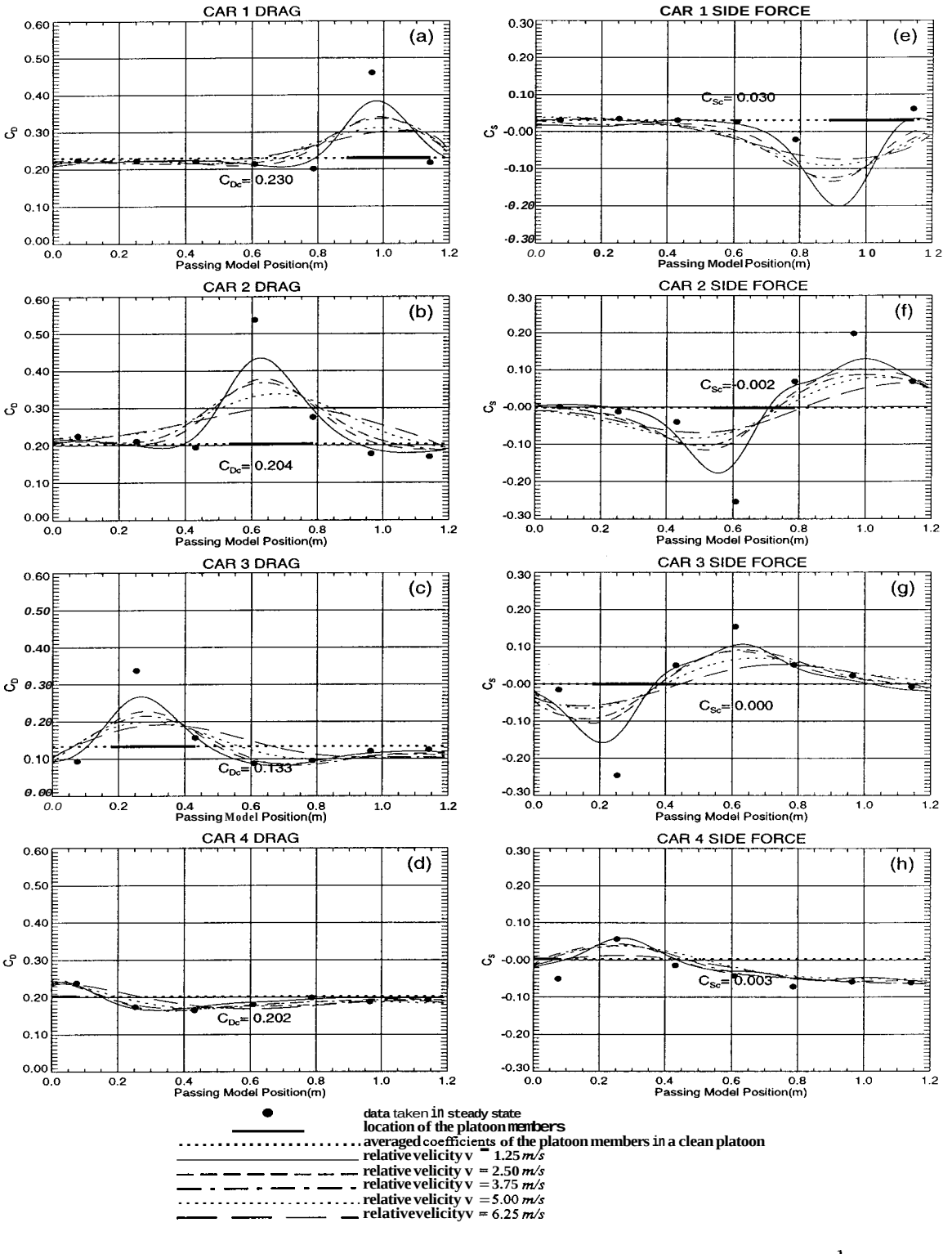

Figure **4.1:** Comparison of passing velocities - a box passes a platoon $(d = \frac{1}{4}W)$. The drag [frames (a)-(d)] and side force [frames (e)-(h)] coefficients on each car in the platoon are shown with respect to the position of mobile model.

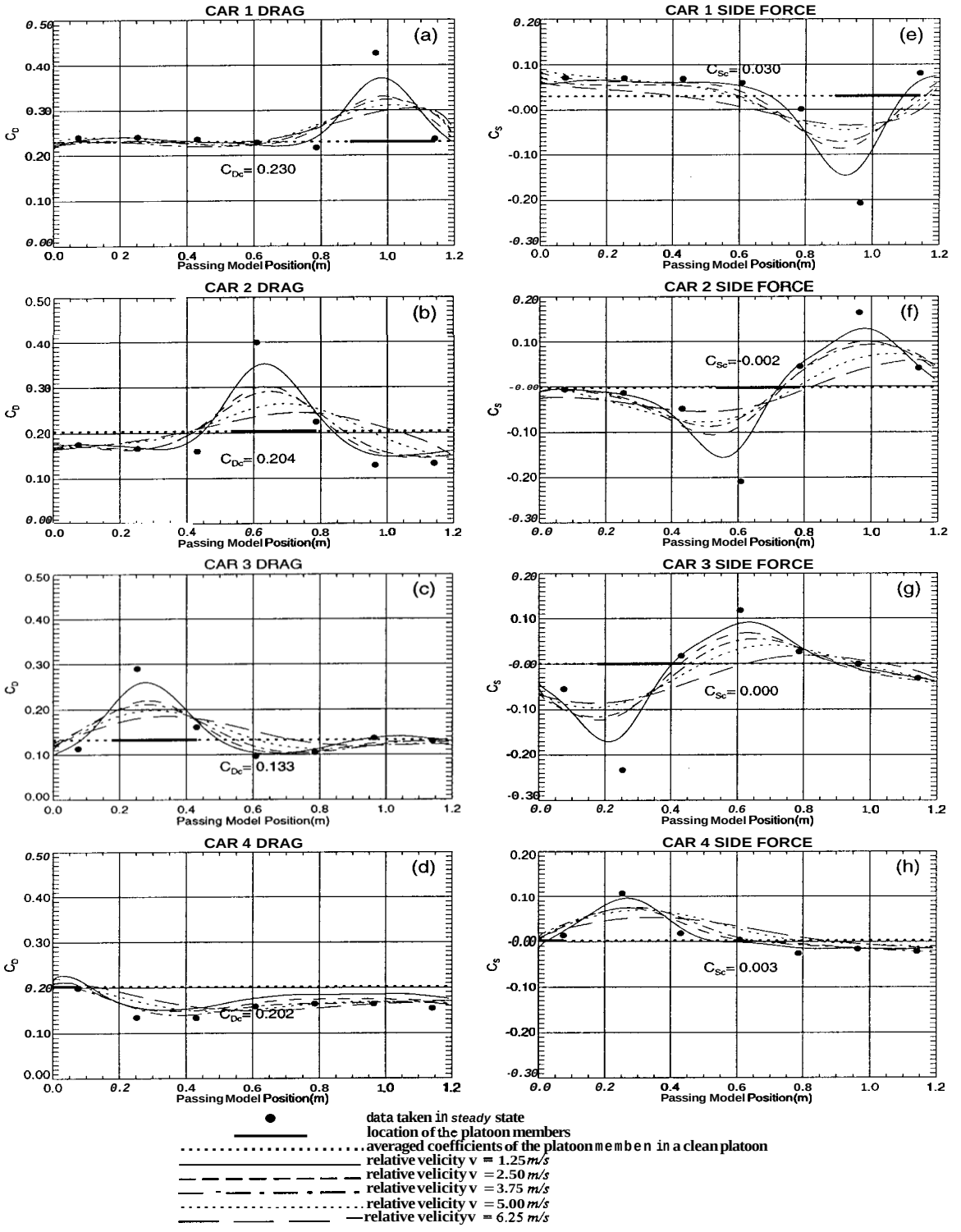

Figure 4.2: Comparison of passing velocities - a box passes a platoon ($d = \frac{1}{2}W$). The drag [frames (a)-(d)] and side force [frames (e)-(h)] coefficients on each car in the platoon are shown with respect to the position of mobile model.

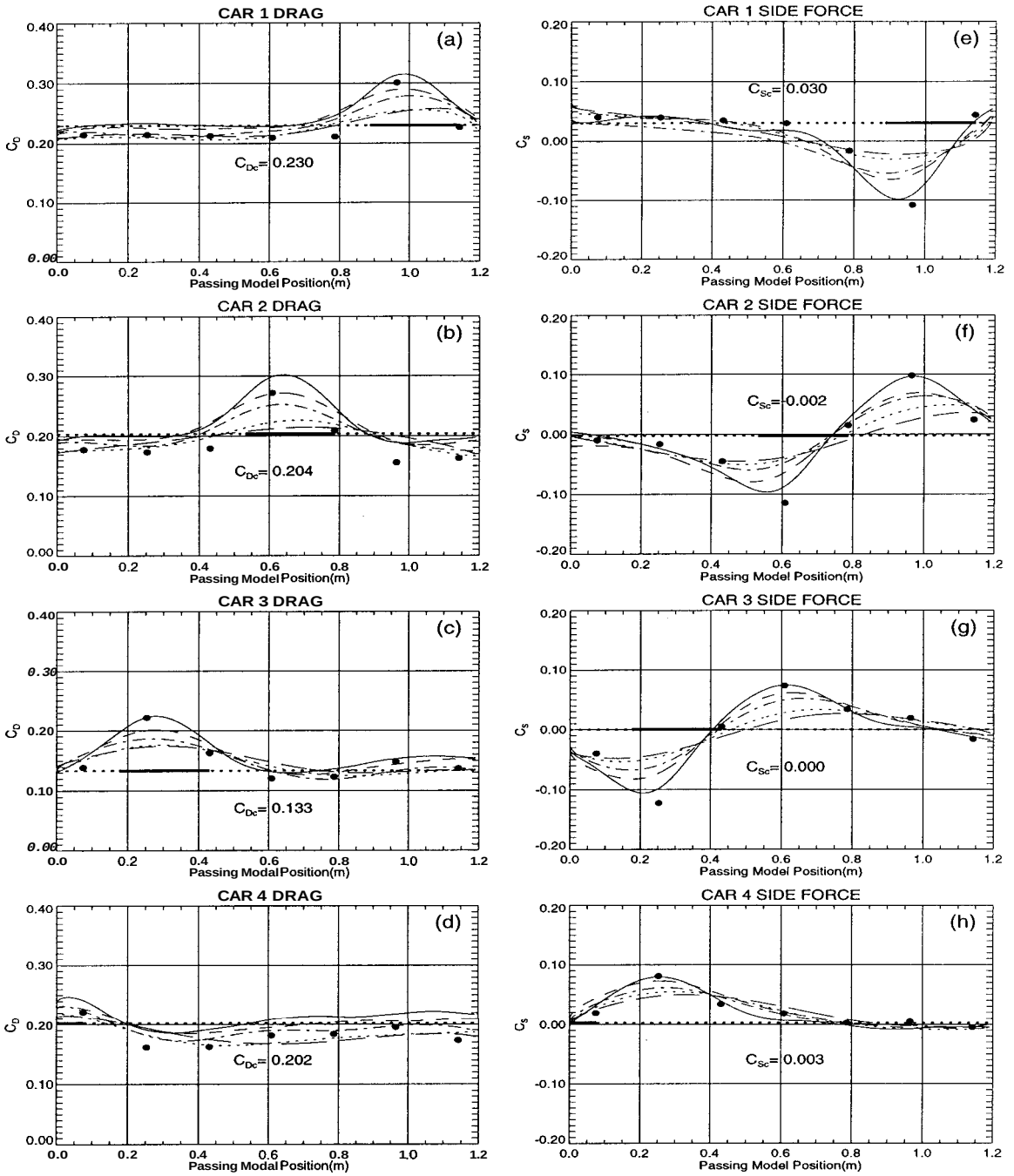

Figure **4.3:** Comparison of passing velocities - **a** box passes a platoon $(d = 1W)$. The drag [frames (a)-(d)] and side force [frames (e)-(h)] coefficients on each car in the platoon are shown with respect to the position of mobile model.

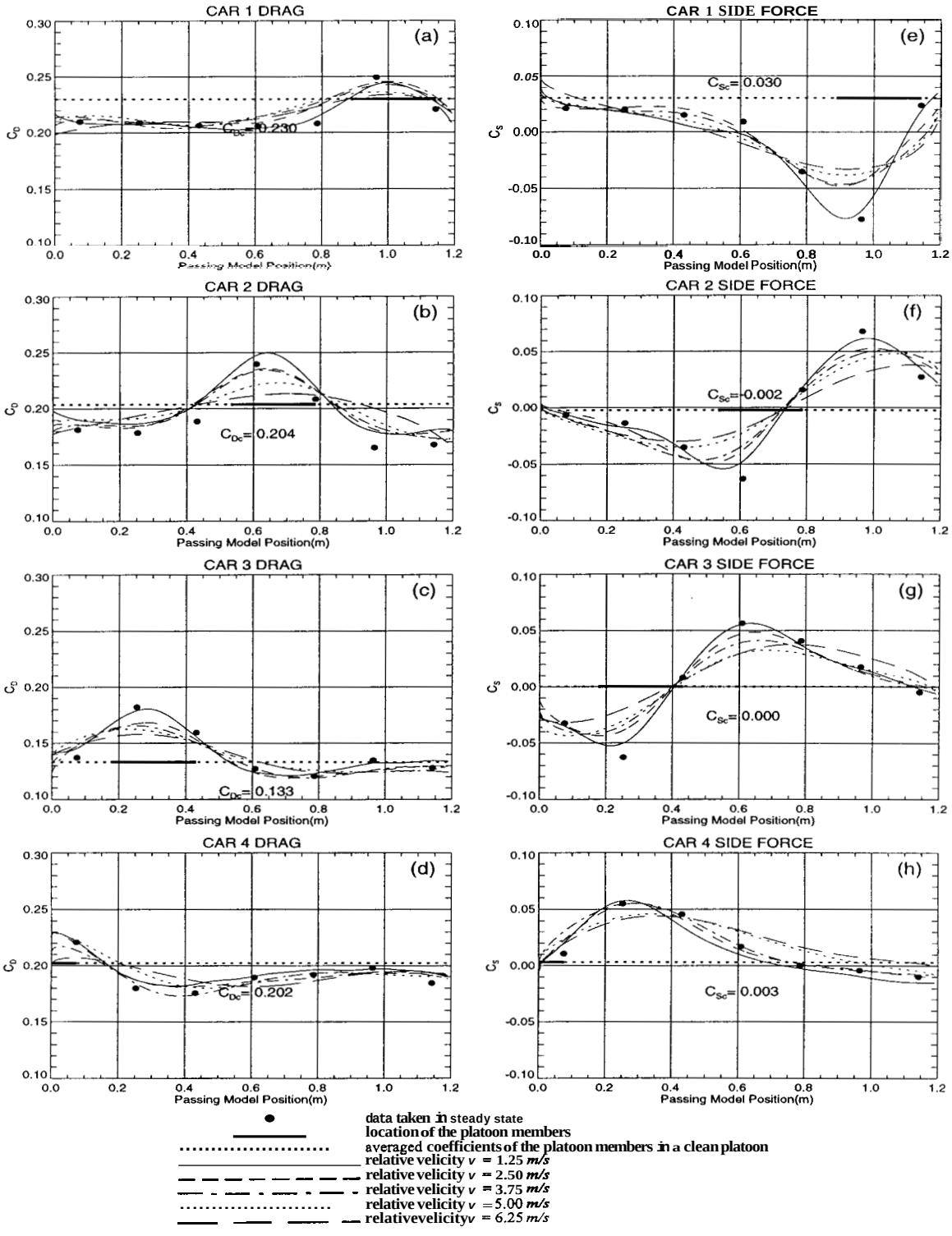

Figure **4.4:** Comparison of passing velocities - a box passes a platoon ($d = \frac{3}{2}W$). The drag [frames (a)-(d)] and side force [frames (e)-(h)] coefficients on each car in the platoon are shown with respect to the position of mobile model.

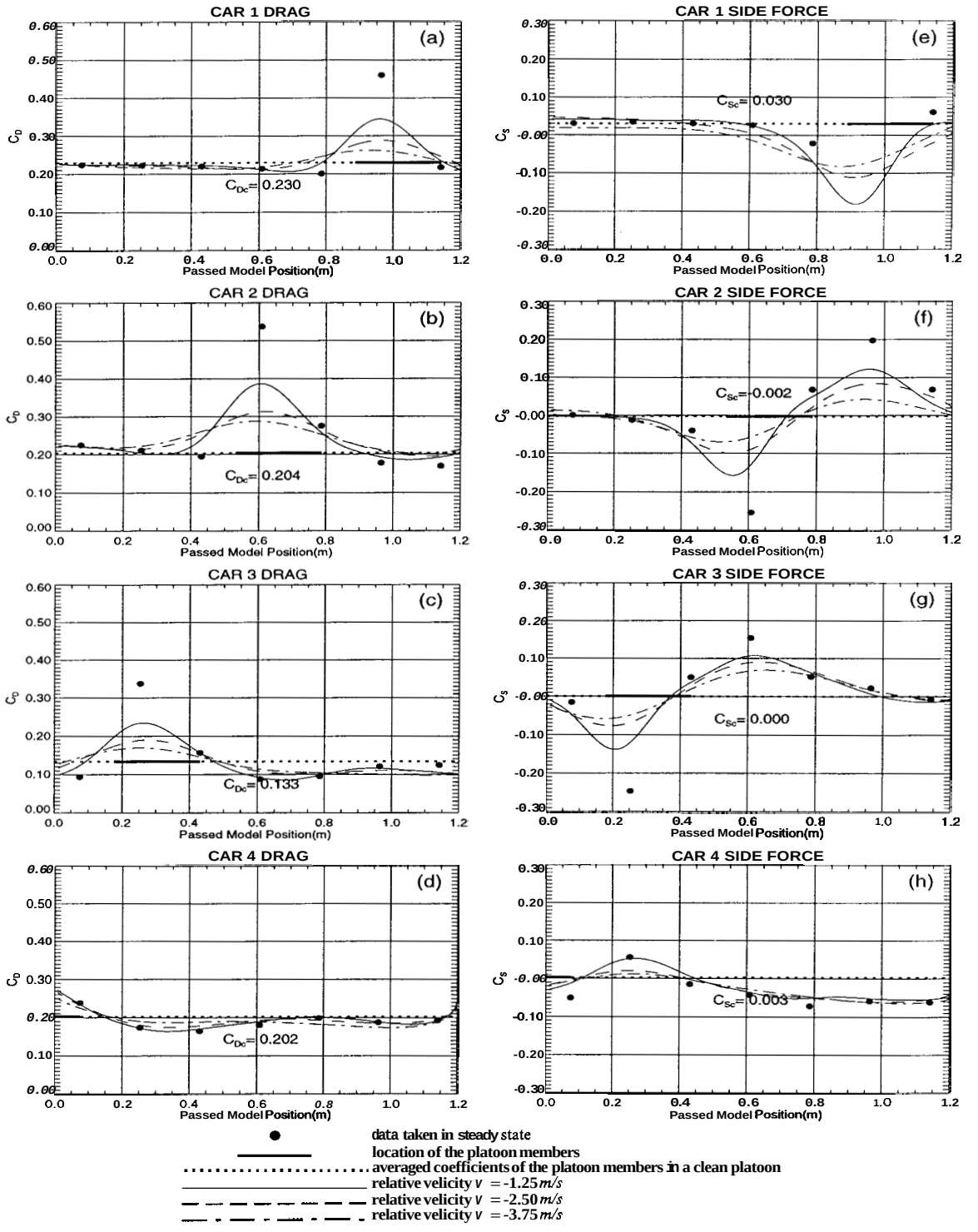

Figure 4.5: Comparison of passing velocities - a platoon passes a box ($d = \frac{1}{4}W$). The drag [frames (a)-(d)] and side force [frames (e)-(h)] coefficients on each car in the platoon are shown with respect to the position of mobile model.

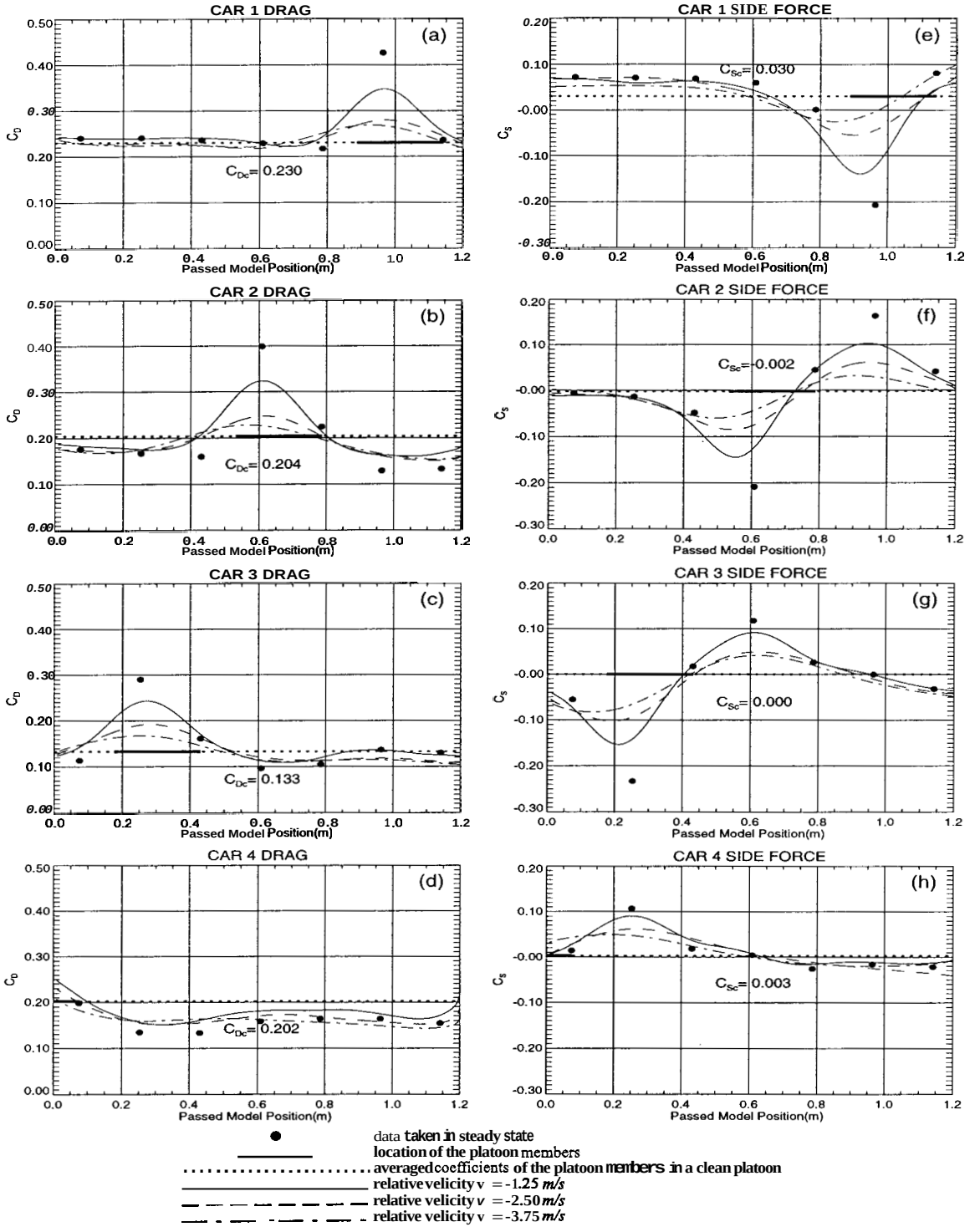

Figure 4.6: Comparison of passing velocities - a platoon passes a box ($d = \frac{1}{2}W$). The drag [frames (a)-(d)] and side force [frames (e)-(h)] coefficients on each car in the platoon are shown with respect to the position of mobile model.

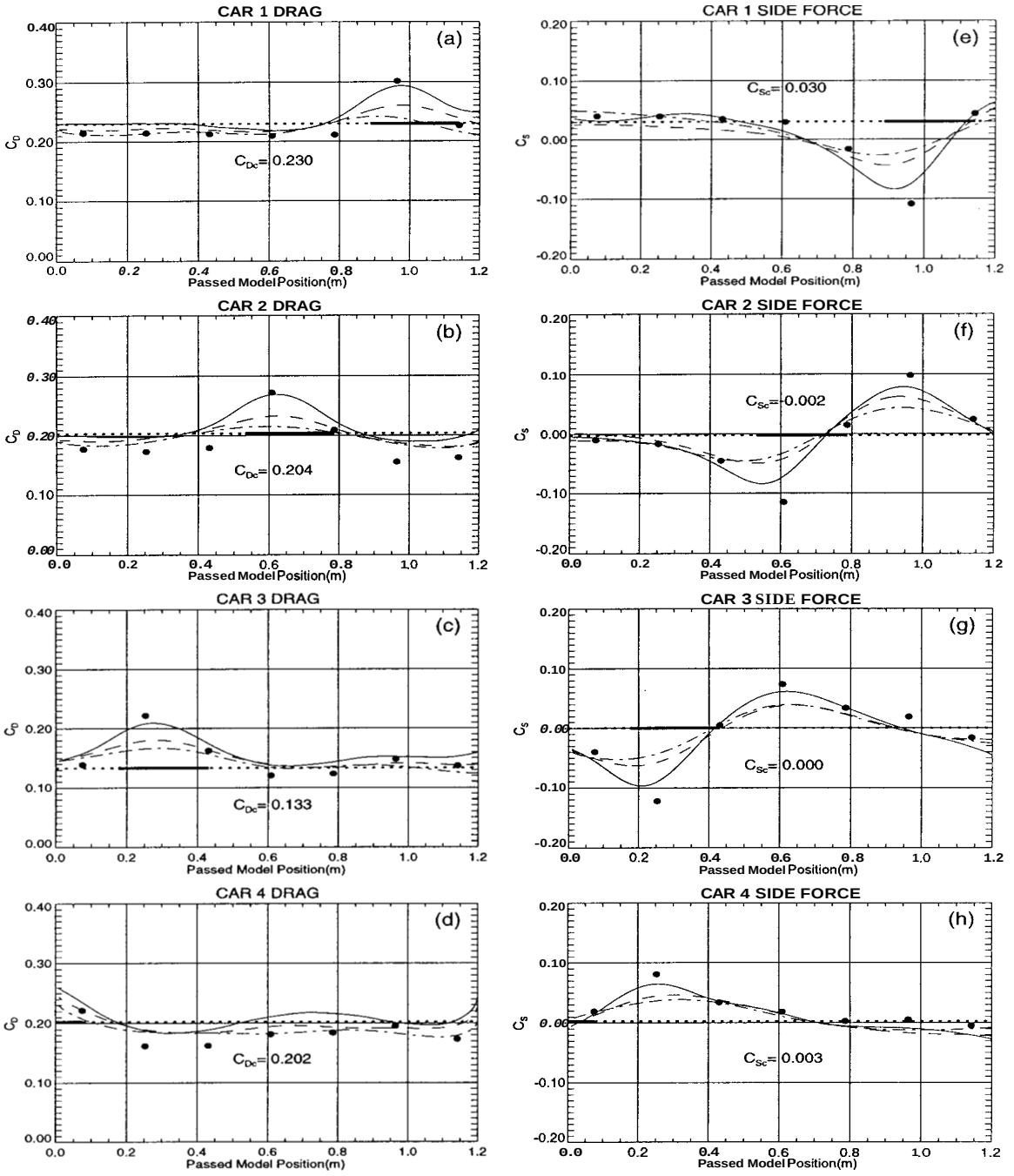

Figure 4.7: Comparison of passing velocities - a platoon passes a box ($d = 1W$). The drag [frames (a)-(d)] and side force [frames (e)-(h)] coefficients on each car in the platoon are shown with respect to the position of mobile model.

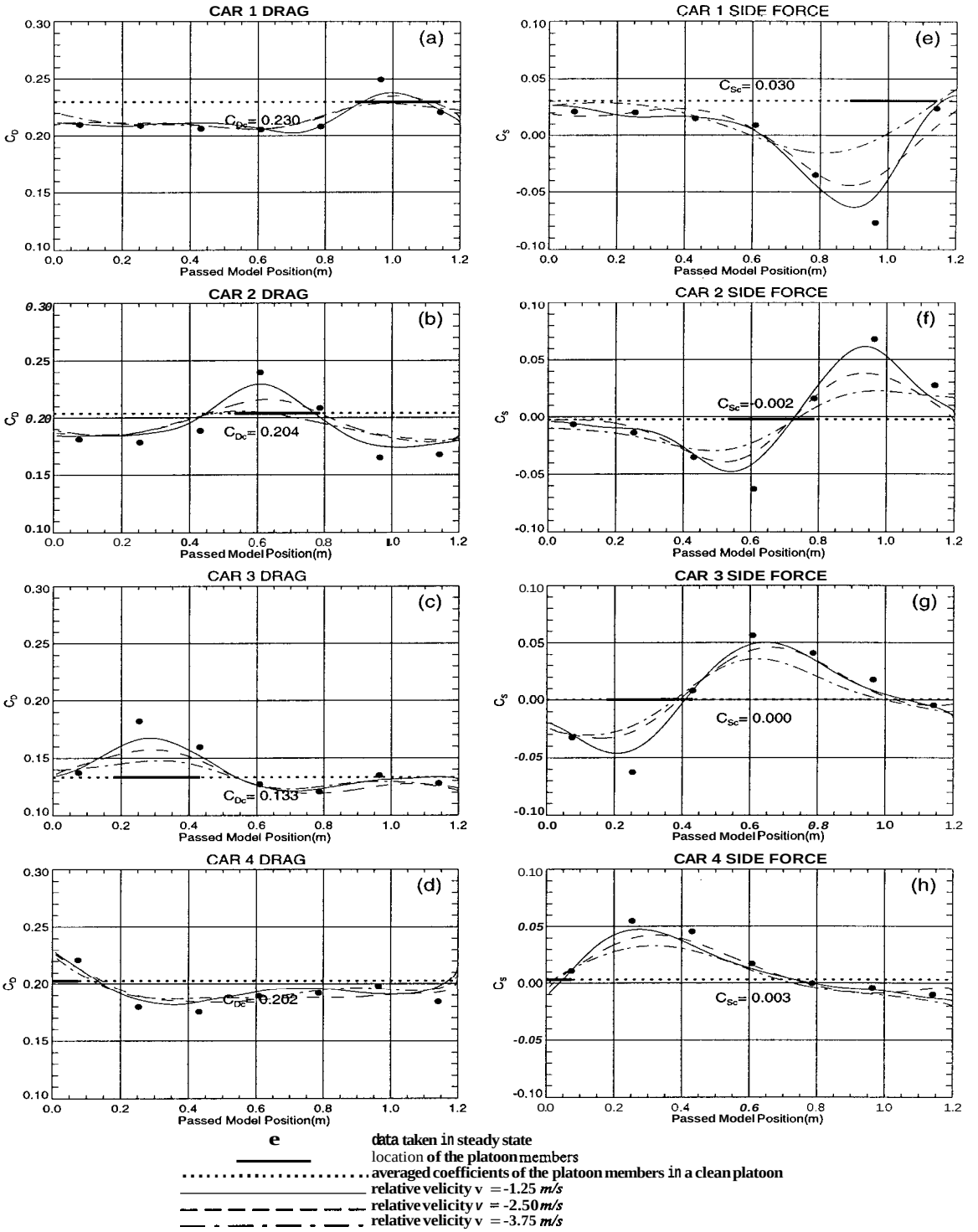

Figure 4.8: Comparison of passing velocities - a platoon passes a box ($d = \frac{3}{2}W$). The drag [frames (a)-(d)] and side force [frames (e)-(h)] coefficients on each car in the platoon are shown with respect to the position of mobile model.

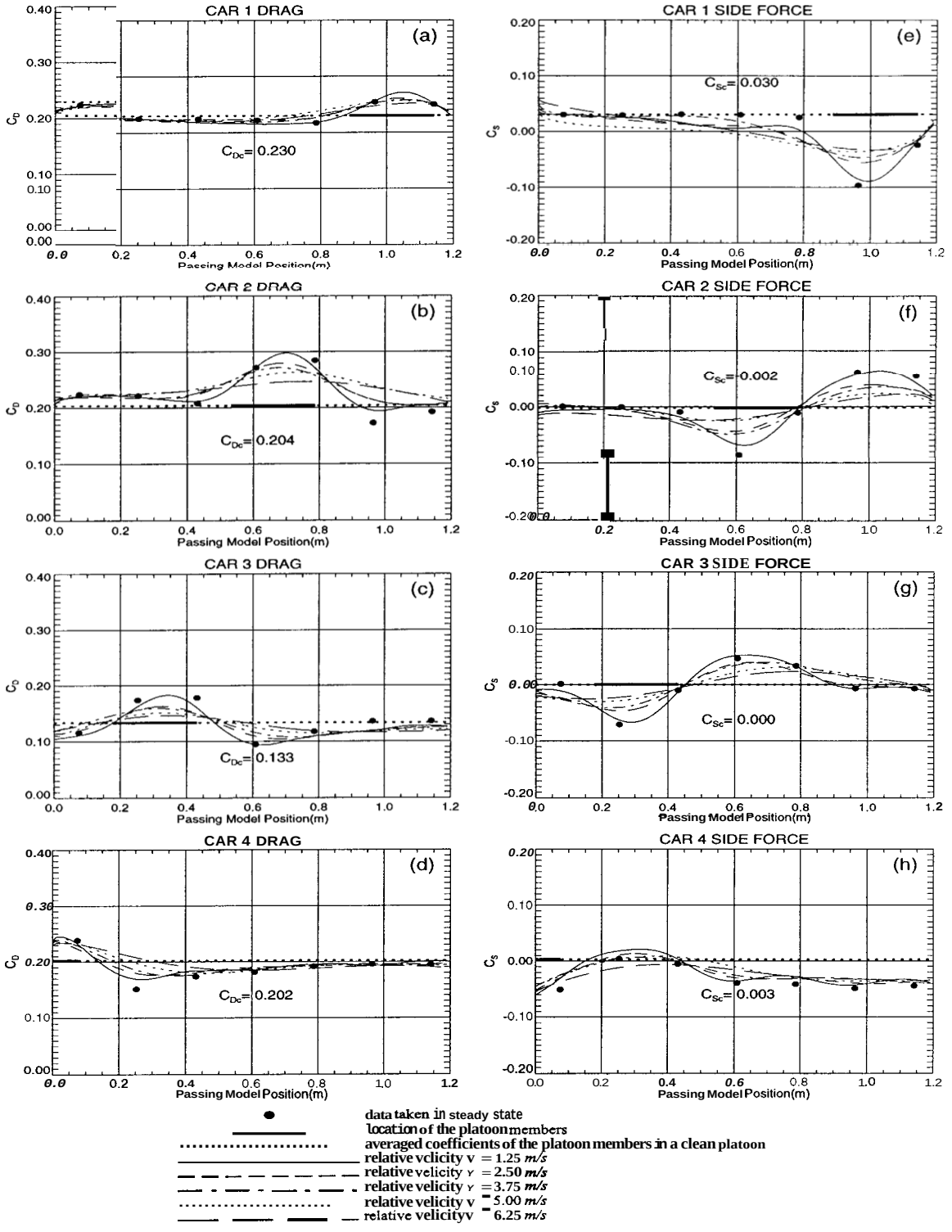

Figure **4.9:** Comparison of passing velocities - a car passes a platoon ($d = \frac{1}{4}W$). The drag [frames (a)-(d)] and side force [frames (e)-(h)] coefficients on each car in the platoon are shown with respect to the position of mobile model.

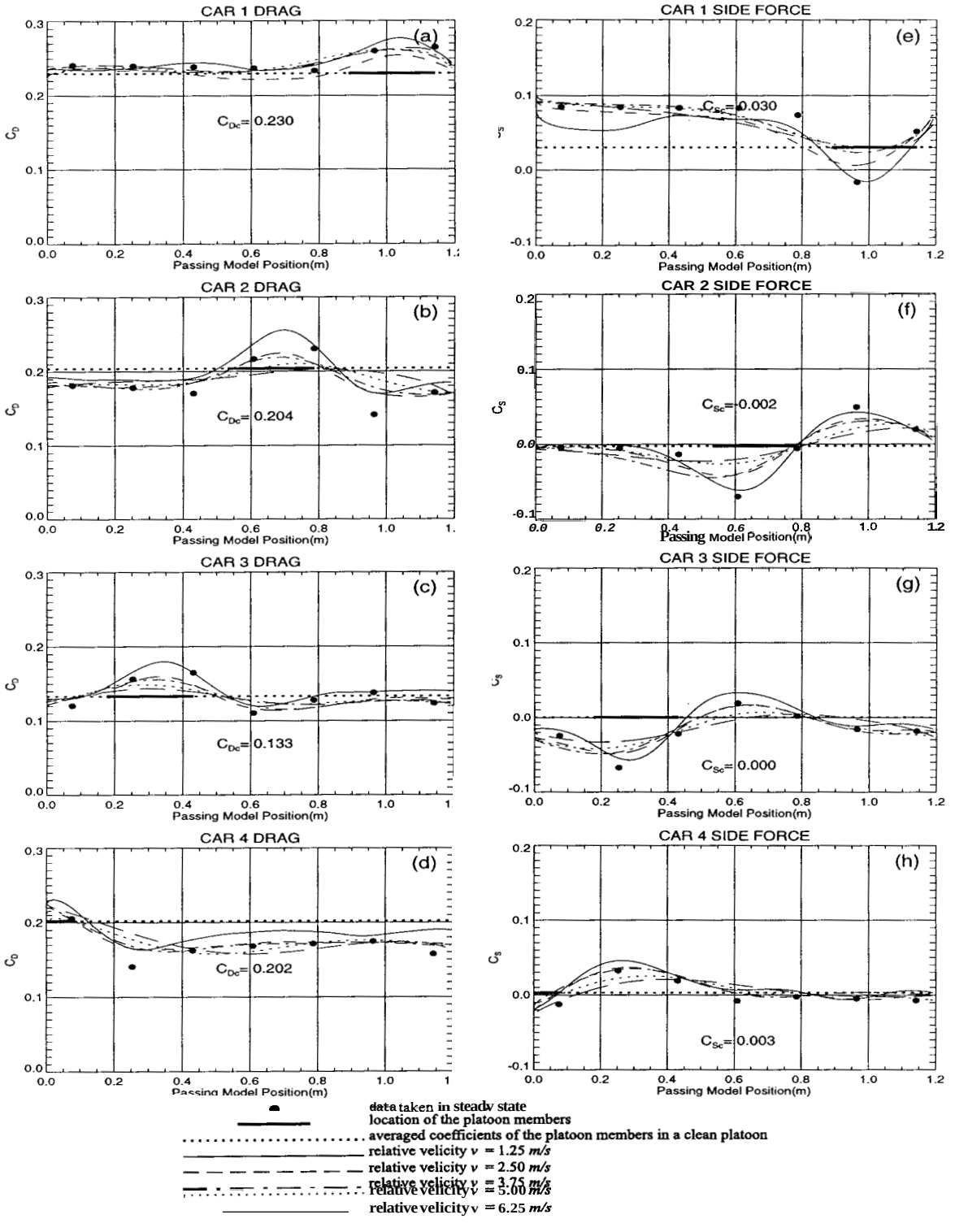

Figure 4.10: Comparison of passing velocities - **a** car passes **a** platoon $(d = \frac{1}{2}W)$. The drag [frames (a)-(d)] and side force [frames (e)-(h)] coefficients on each car in the platoon are shown with respect to the position of mobile model.

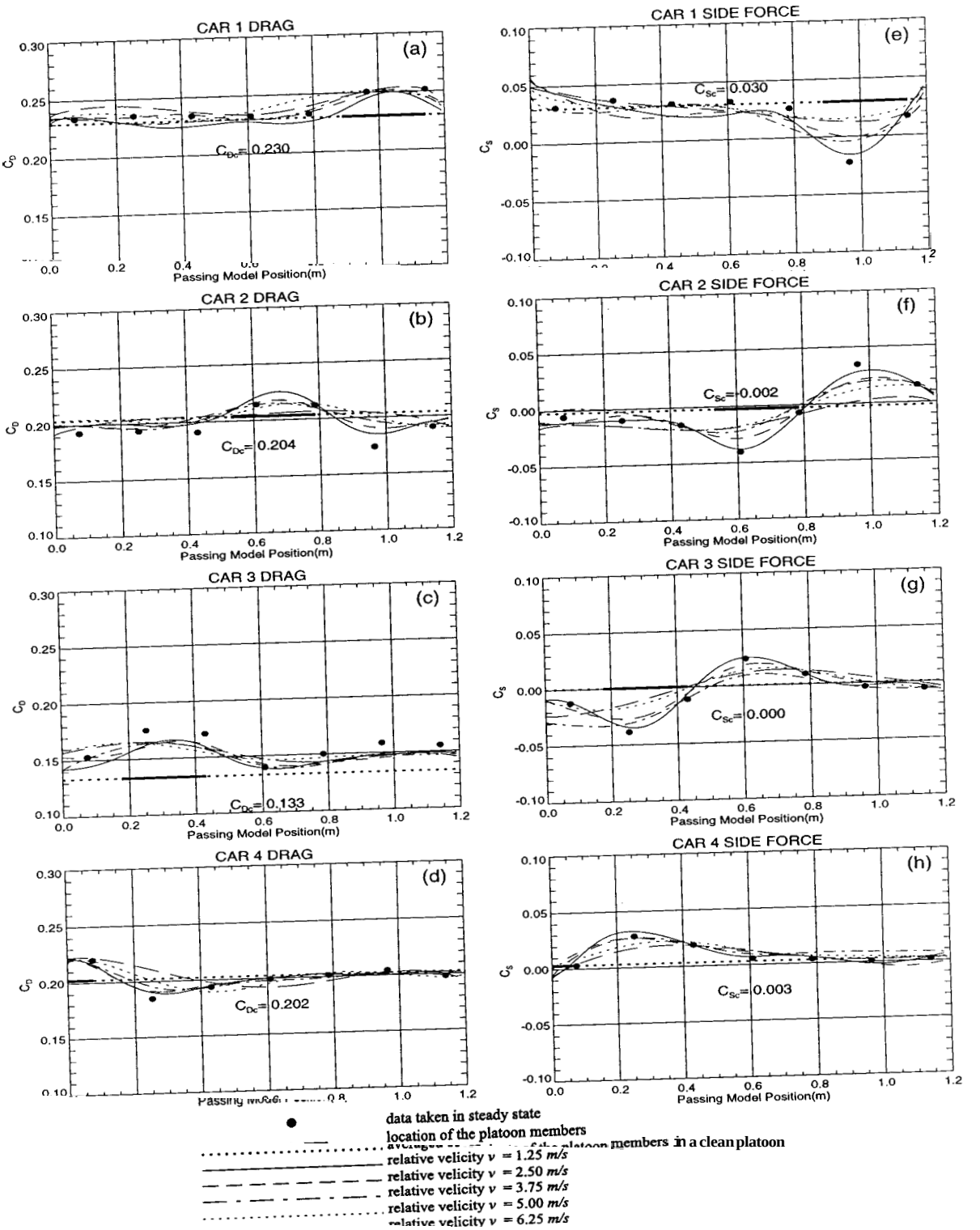

Figure 4.11: Comparison of passing velocities - a car passes a platoon ($d = 1W$). The drag [frames (a)-(d)] and side force [frames (e)-(h)] coefficients on each car in the platoon are shown with respect to the position of mobile model.

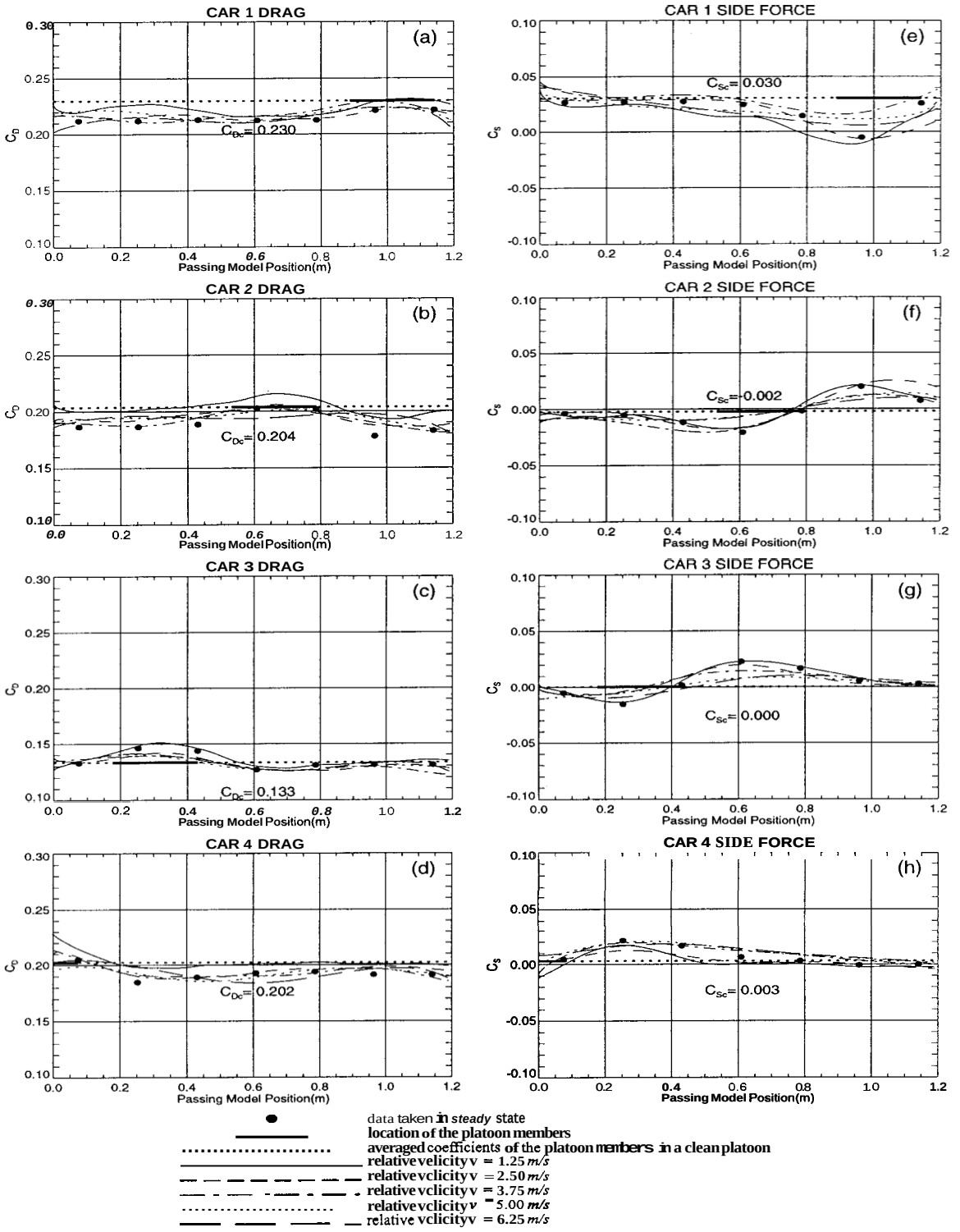

Figure 4.12: Comparison of passing velocities - a car passes a platoon ($d = \frac{3}{2}W$). The drag [frames (a)-(d)] and side force [frames (e)-(h)] coefficients on each car in the platoon are shown with respect to the position of mobile model.

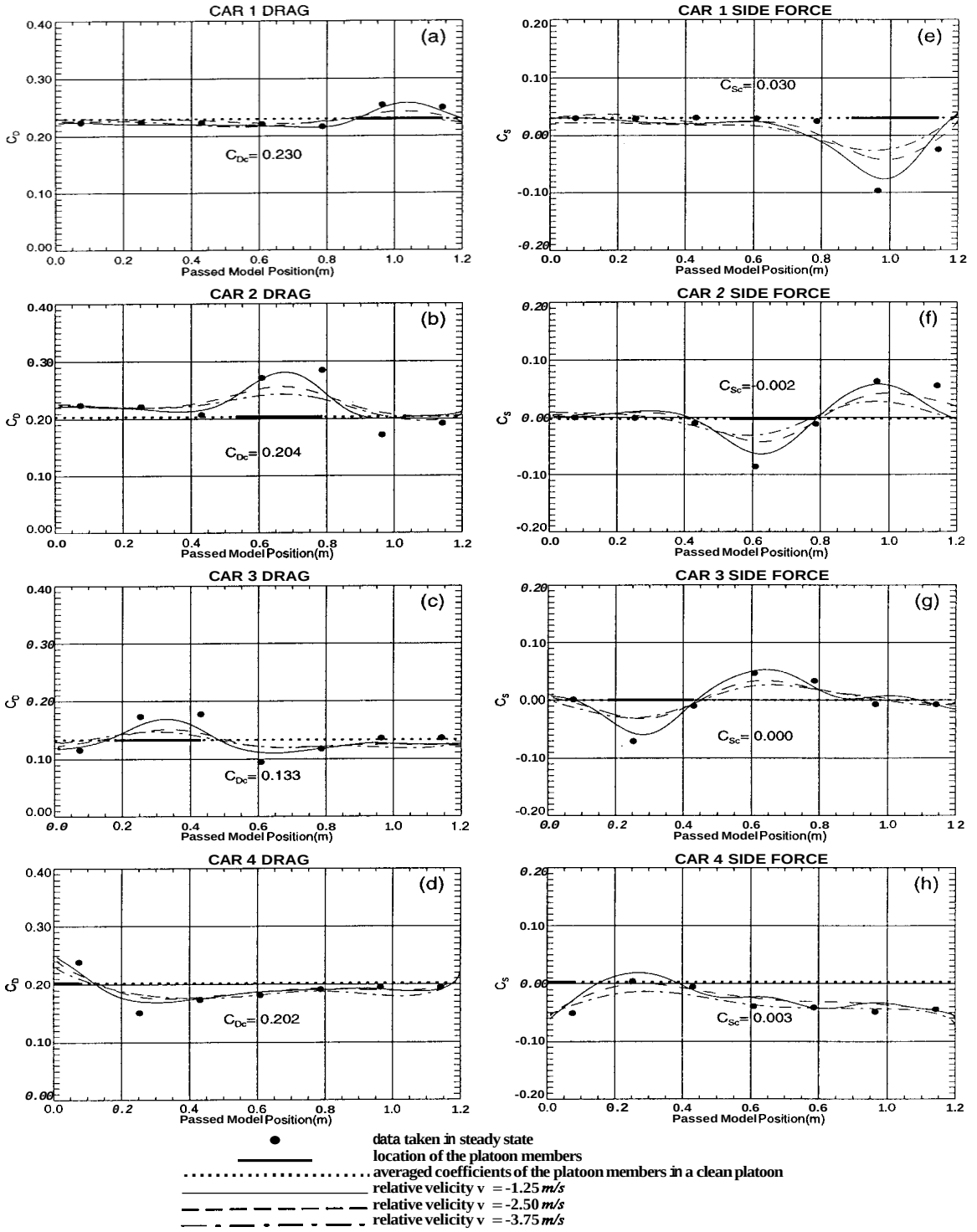

Figure **4.13:** Comparison of passing velocities - a platoon passes a car ($d = \frac{1}{4}W$). The drag [frames (a)-(d)] and side force [frames (e)-(h)] coefficients on each car in the platoon are shown with respect to the position of mobile model.

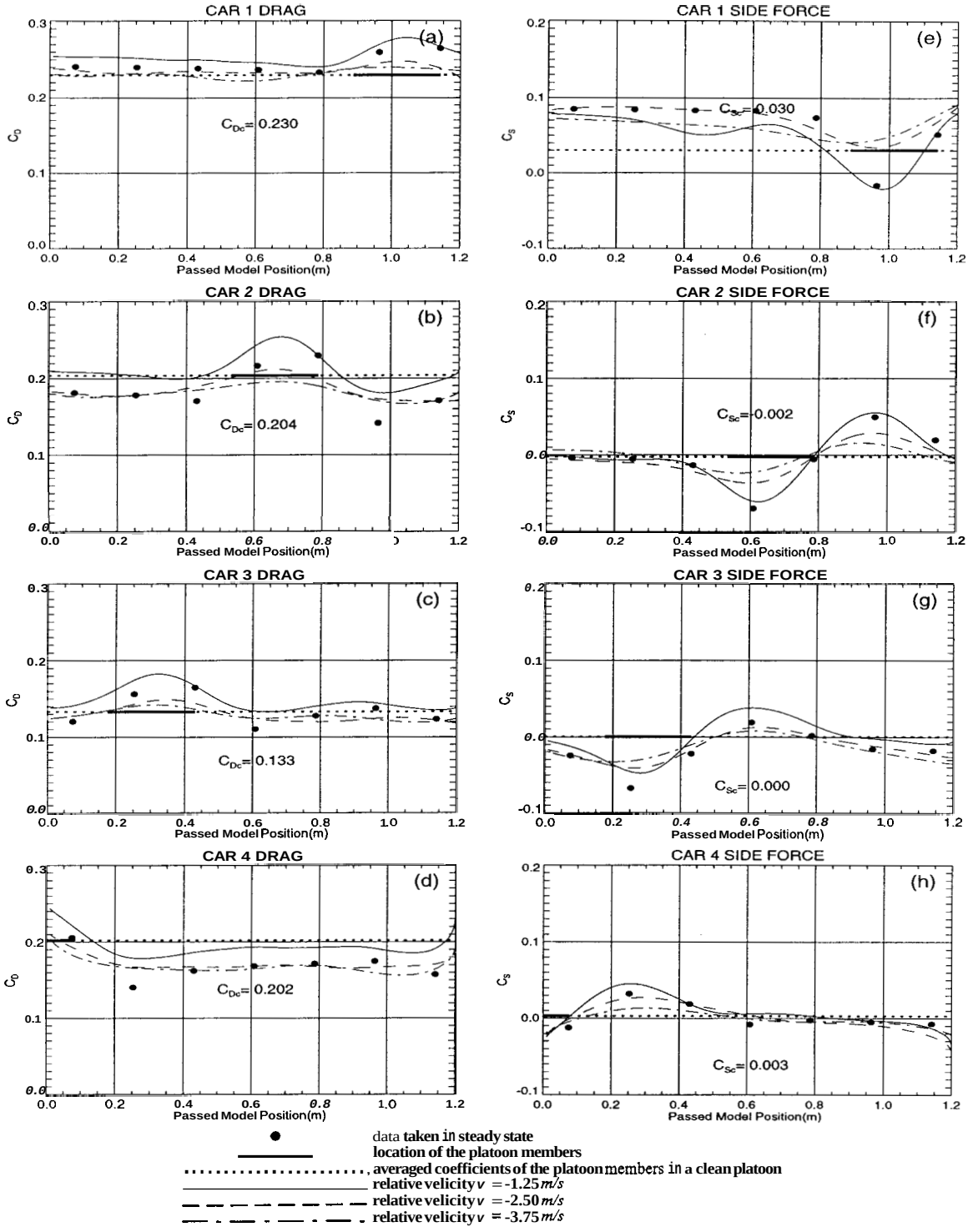

Figure **4.14:** Comparison of passing velocities - a platoon passes a car $(d = \frac{1}{2}W)$. The drag [frames (a)-(d)] and side force [frames (e)-(h)] coefficients on each car in the platoon are shown with respect to the position of mobile model.

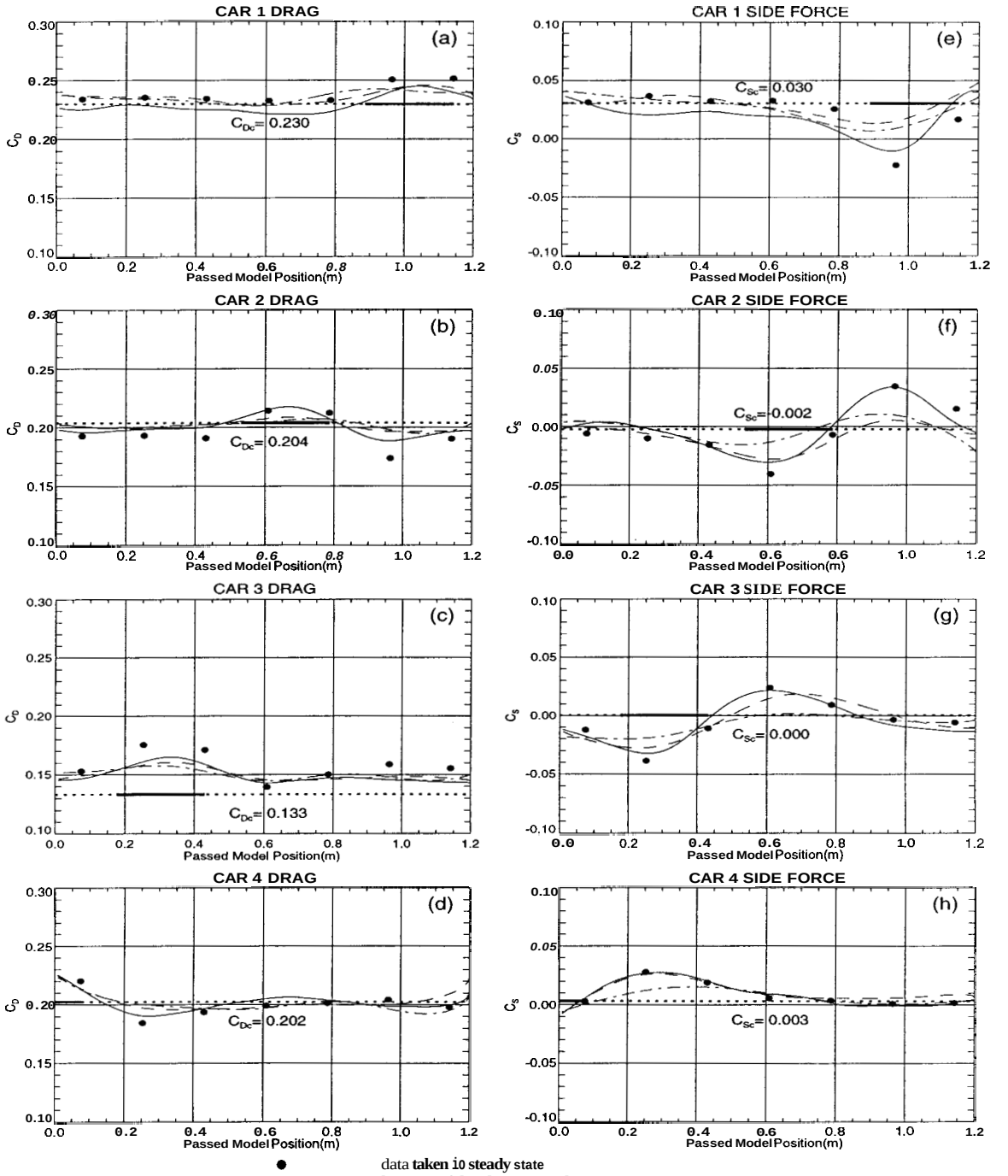

Figure **4.15:** Comparison of passing velocities - a platoon passes a car $(d = 1W)$. The drag [frames (a)-(d)] and side force [frames (e)-(h)] coefficients on each car in the platoon are shown with respect to the position of mobile model.

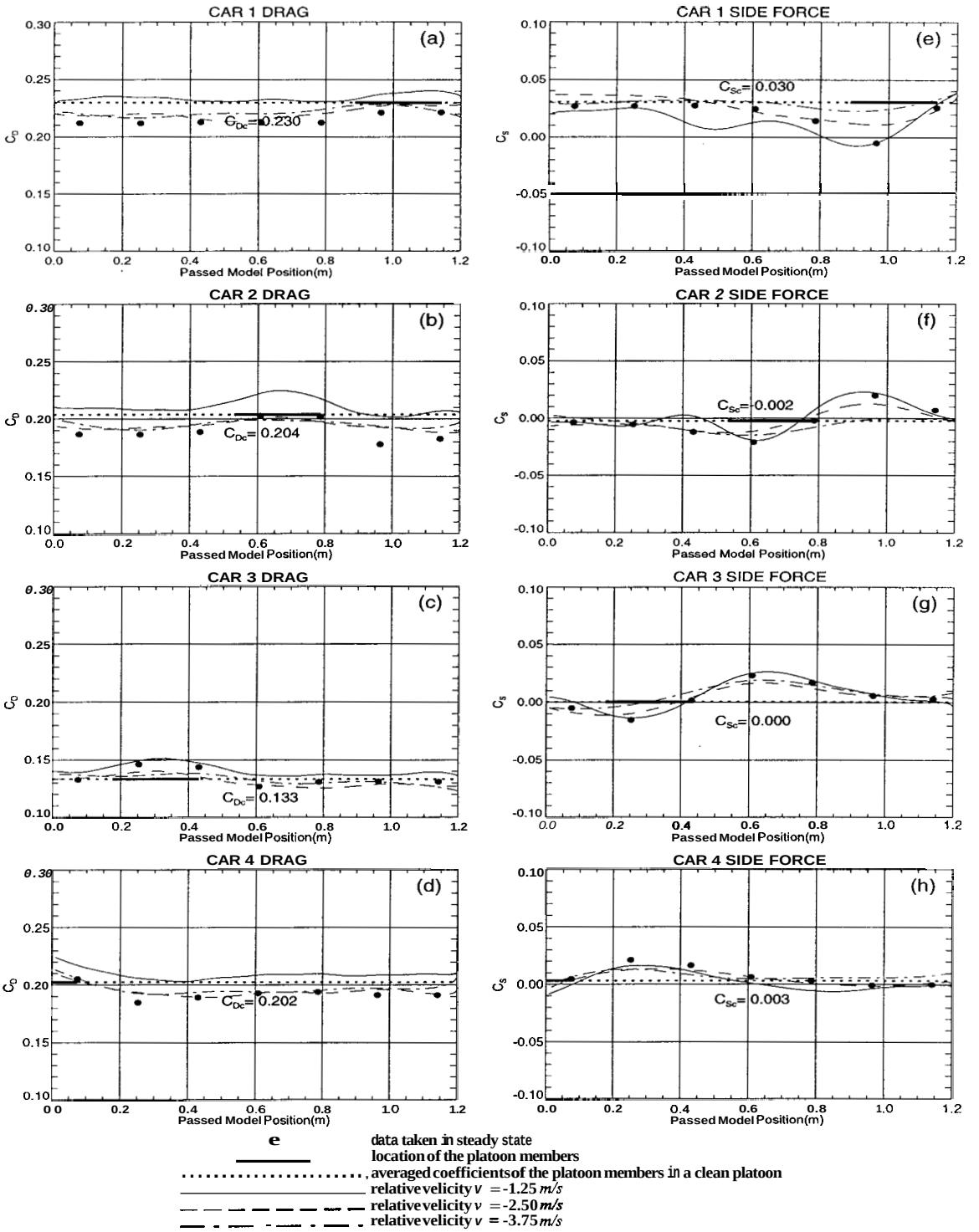

Figure 4.16: Comparison of passing velocities - a platoon passes a car ($d = \frac{3}{2}W$). The drag [frames (a)-(d)] and side force [frames (e)-(h)] coefficients on each car in the platoon are shown with respect to the position of mobile model.

Chapter 5

Effects of Lateral Spacing

Aerodynamic forces experienced by every platoon member are compared for various lateral spacings between the mobile model and the platoon. Forces measured on each of the four cars in the platoon are recorded simultaneously as the mobile model travels $1.2m$. The coefficients on each of the four cars are plotted with respect to the position of the front end of the mobile model. Transient data in four different lateral spacings ($d = \frac{1}{4}, \frac{1}{2}, 1$, and $\frac{3}{2}W$, where $W = 10.2cm$ = box width) are recorded. The position of each platoon member and its coefficients determined in a clean platoon condition are also plotted for reference.

Figure 5.1 to figure 5.5 show the data while a rectangular box is used as the forward motion mobile model, and figure 5.6 to figure 5.8 show the data as the box model in backward motion. Figure 5.9 to figure 5.13 show the data while a vehicle is applied as the forward motion mobile model, and figure 5.14 to figure 5.16 show the data as the vehicle is in backward motion. For both mobile models, five different velocities ($v = 1.25, 2.50, 3.75, 5.00$, and $6.25m/s$) are examined when model is in forward motion, and three velocities ($v = -1.25, -2.50$, and $-3.75m/s$) are investigated when mobile model is in backward motion.

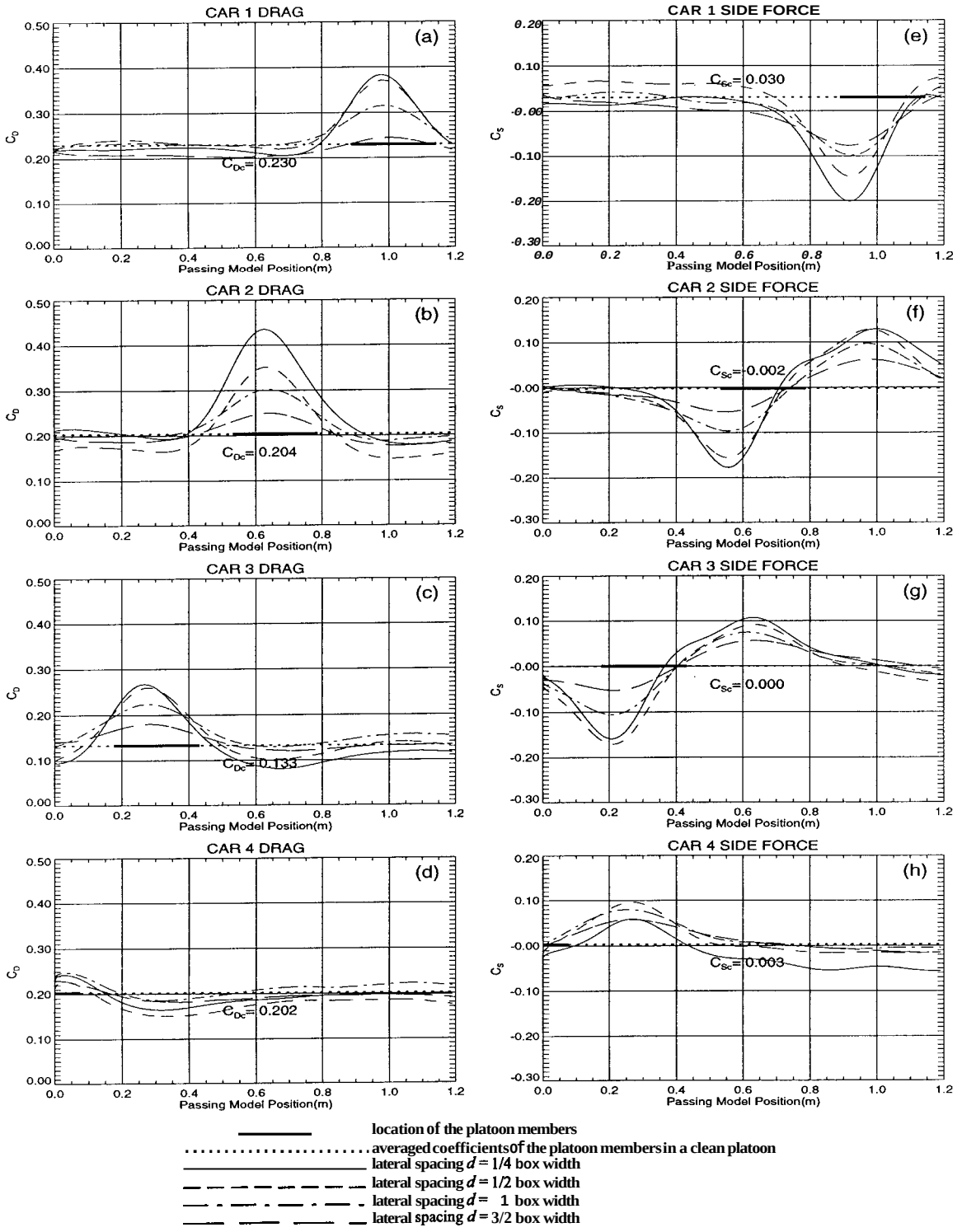

Figure 5.1: Comparison of lateral spacings - a box passes a platoon ($v = 1.25m/s$). The drag [frames (a)-(d)] and side force [frames (e)-(h)] coefficients on each car in the platoon are shown with respect to the position of mobile model.

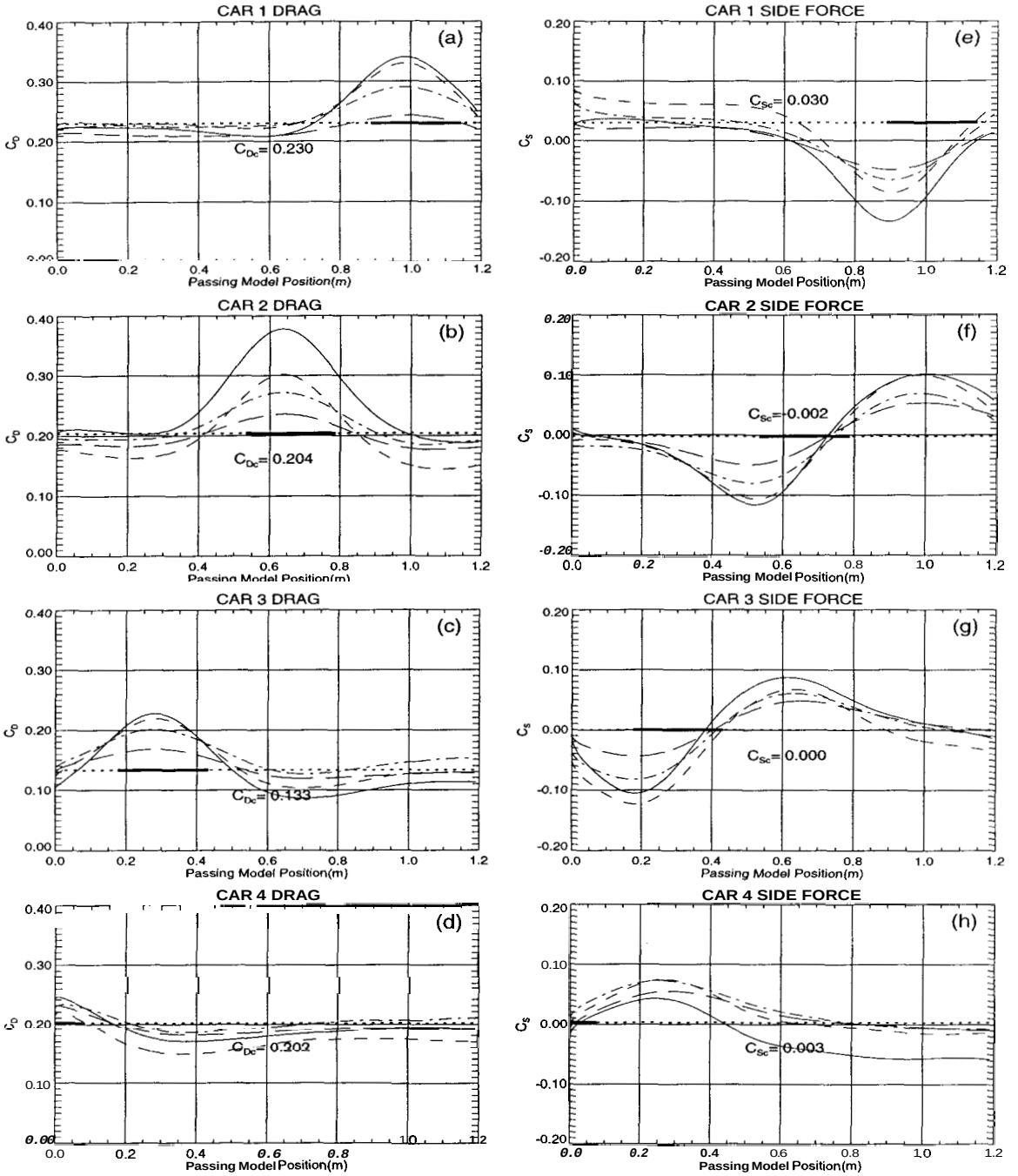

Figure 5.2: Comparison of lateral spacings - a box passes a platoon $(v = 2.50m/s)$. The drag [frames (a)-(d)] and side force [frames (e)-(h)] coefficients *on* each car in the platoon are shown with respect to the position of mobile model.

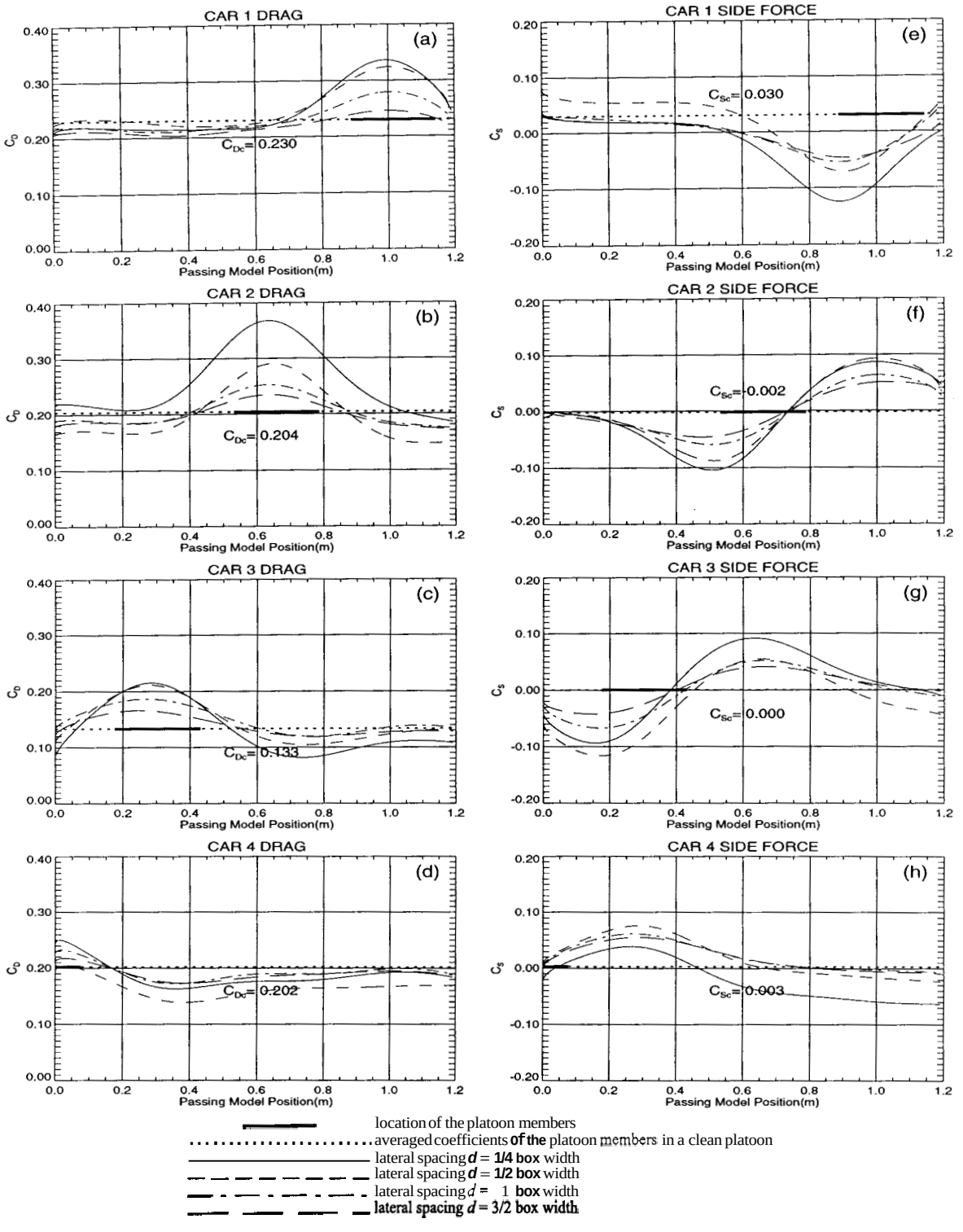

Figure 5.3: Comparison of lateral spacings - a box passes a platoon $(_{71} = 3.75m/s)$. The drag [frames (a)-(d)] and side force [frames (e)-(h)] coefficients on each car in the platoon are shown with respect to the position of mobile model.

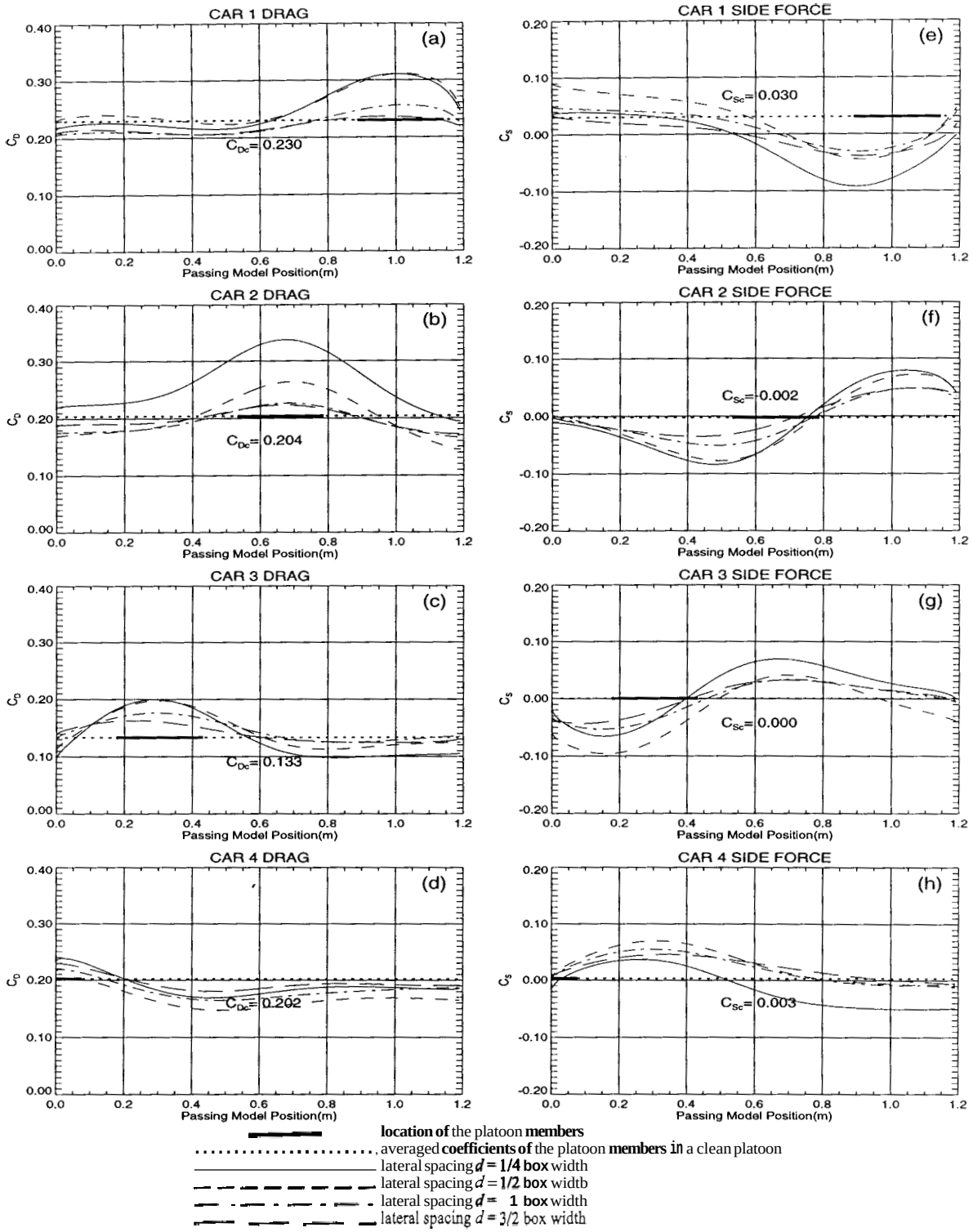

Figure 5.4: Comparison of lateral spacings - a box passes a platoon $(v = 5.00 m/s)$. The drag [frames (a)-(d)] and side force [frames (e)-(h)] coefficients on each car in the platoon are shown with respect to the position of mobile model.

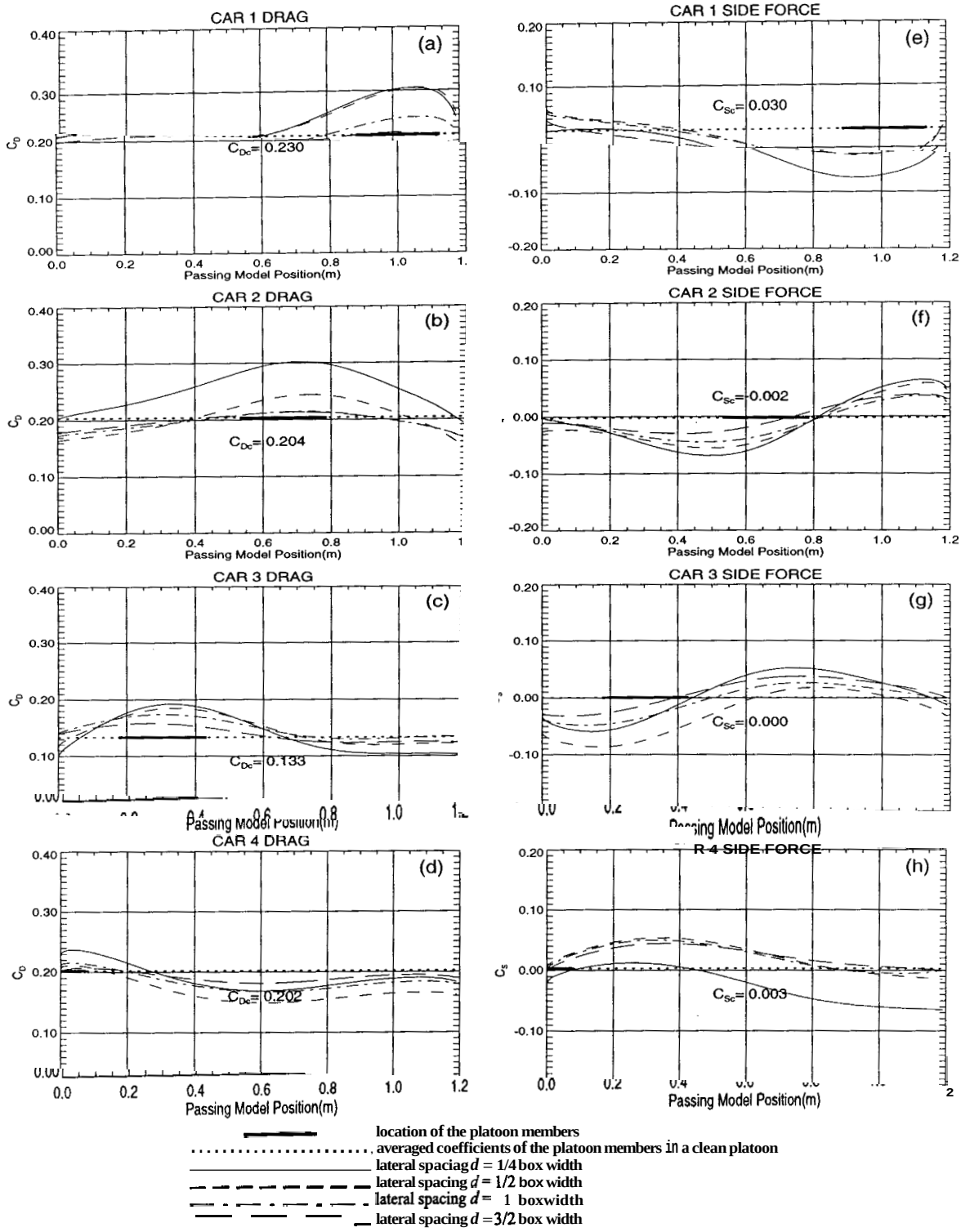

Figure 5.5: Comparison of lateral spacings - a box passes a platoon ($v = 6.25m/s$). The drag [frames (a)-(d)] and side force [frames (e)-(h)] coefficients on each car in the platoon are shown with respect to the position of mobile model.

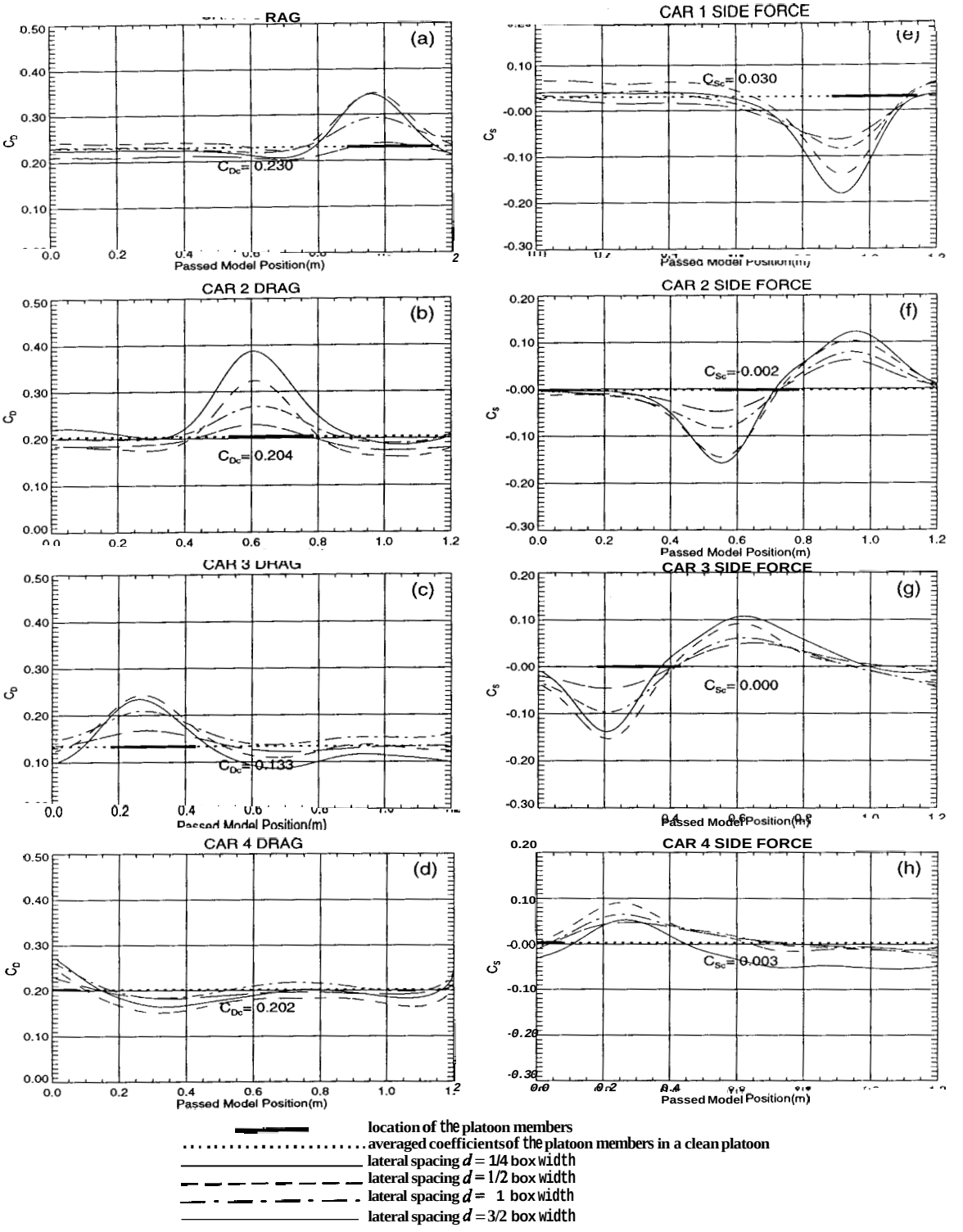

Figure 5.6: Comparison of lateral spacings - a platoon passes a box ($v = -1.25m/s$). The drag [frames (a)-(d)] and side force [frames (e)-(h)] coefficients on each car in the platoon are shown with respect to the position of mobile model.

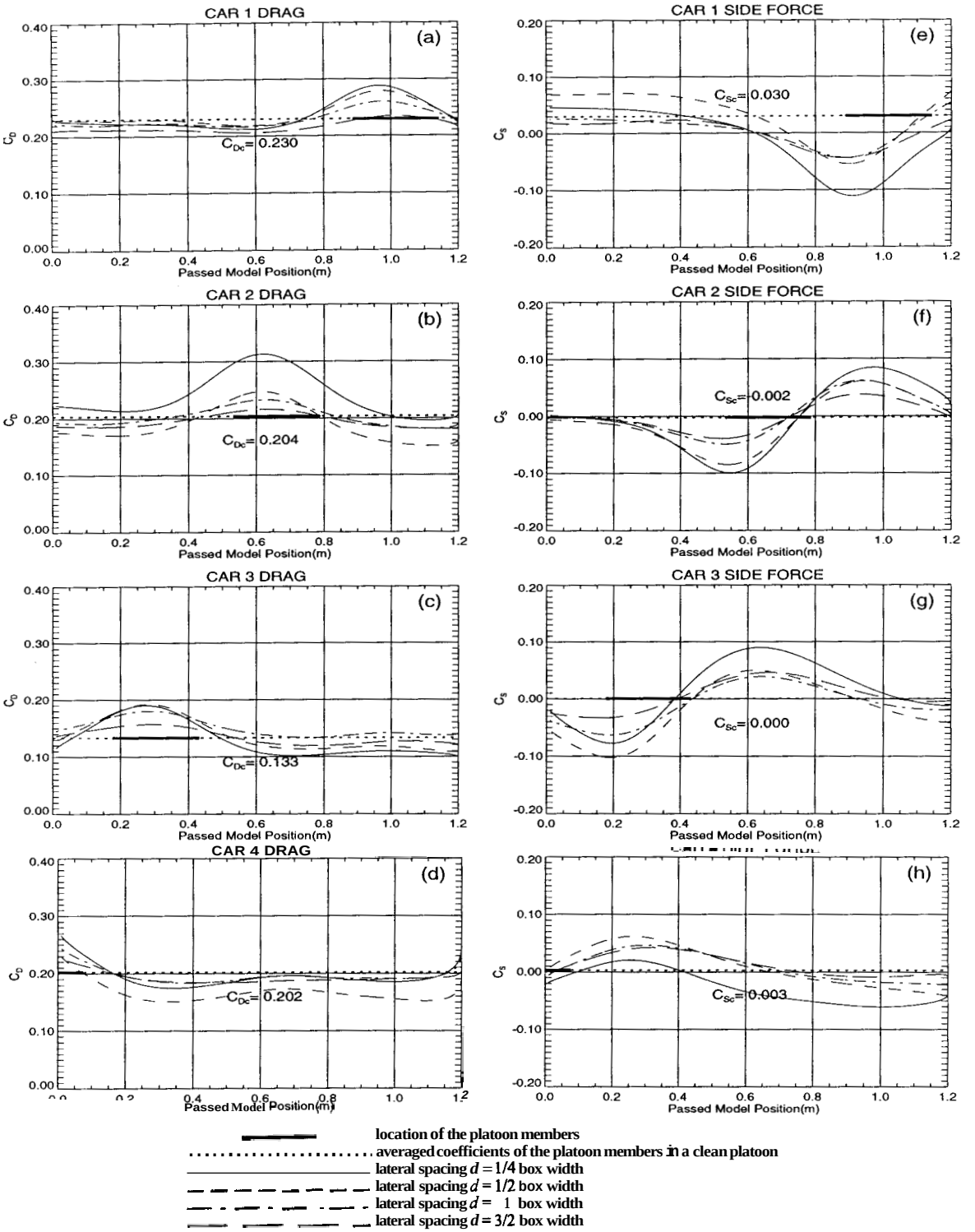

Figure 5.7: Comparison of lateral spacings - a platoon passes a box ($v = -2.50m/s$). The drag [frames (a)-(d)] and side force [frames (e)-(h)] coefficients on each car in the platoon are shown with respect to the position of mobile model.

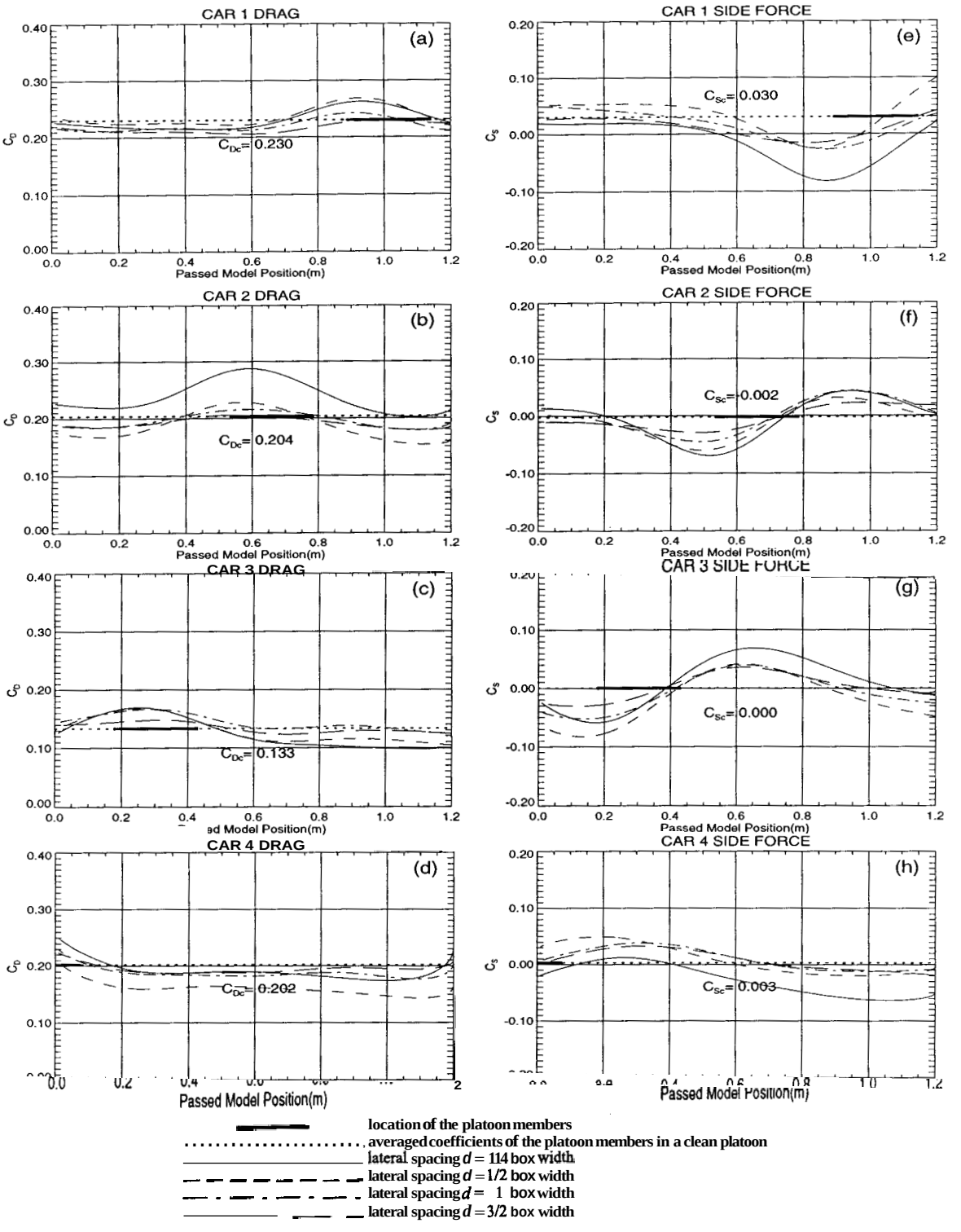

Figure 5.8: Comparison of lateral spacings - a platoon passes a box $(v = -3.75m/s)$. The drag [frames (a)-(d)] and side force [frames (e)-(h)] coefficients on each car in the platoon are shown with respect to the position of mobile model.

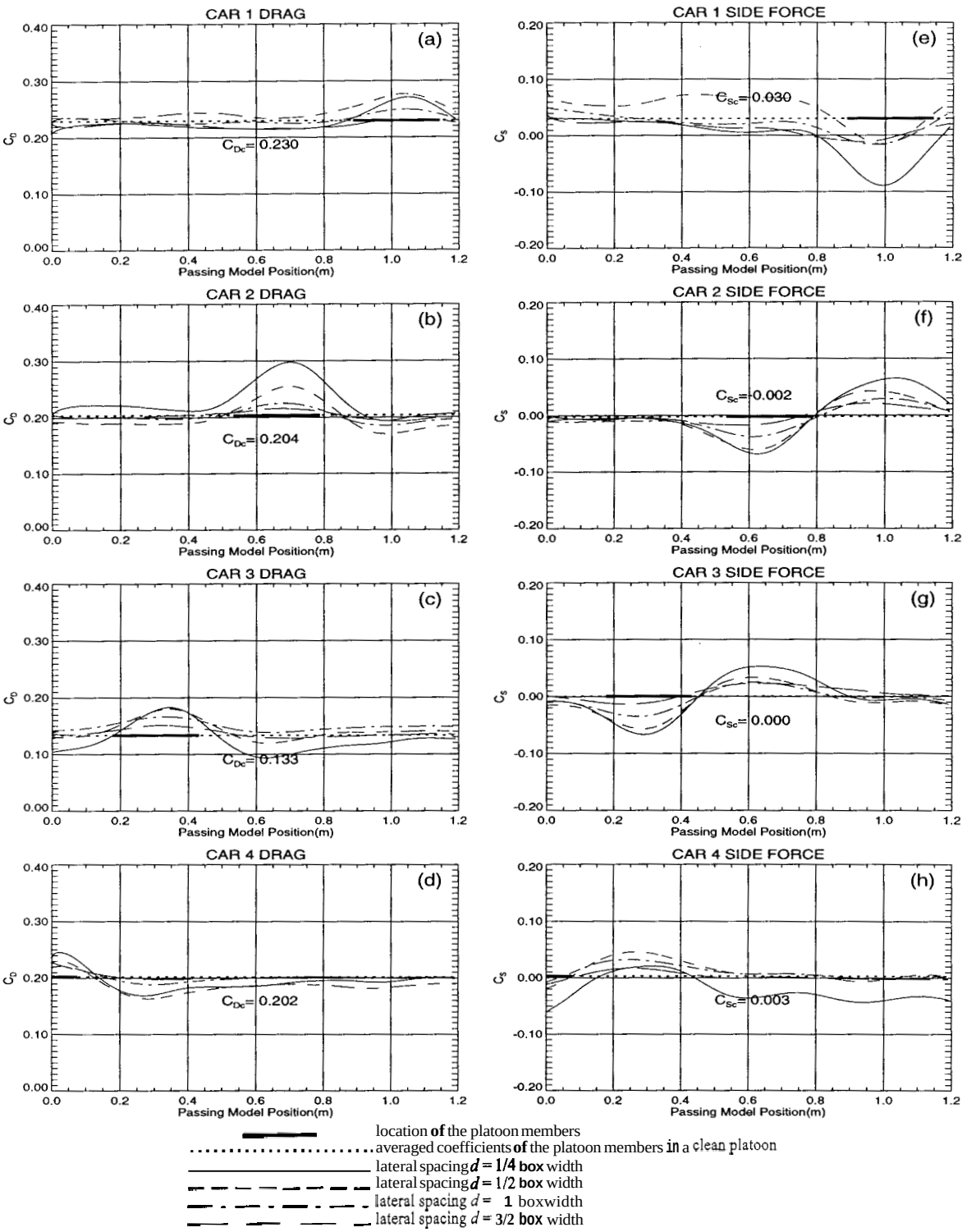

Figure 5.9: Comparison of lateral spacings - a car passes a platoon ($v = 1.25m/s$). The drag [frames (a)-(d)] and side force [frames (e)-(h)] coefficients on each car in the platoon are shown with respect to the position of mobile model.

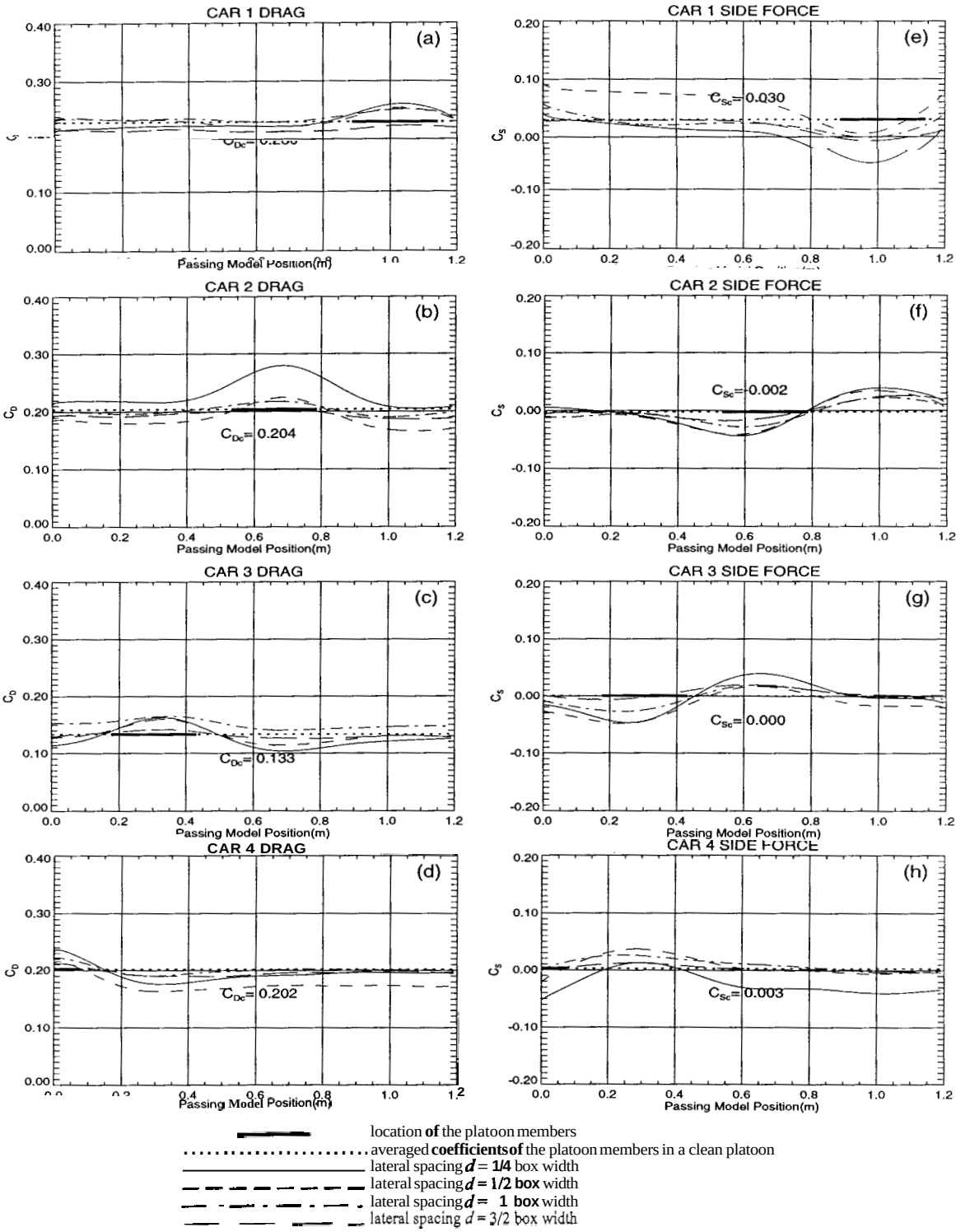

Figure 5.10: Comparison of lateral spacings - a car passes a platoon ($v = 2.50 m/s$). The drag [frames (a)-(d)] and side force [frames (e)-(h)] coefficients on each car in the platoon are shown with respect to the position of mobile model.

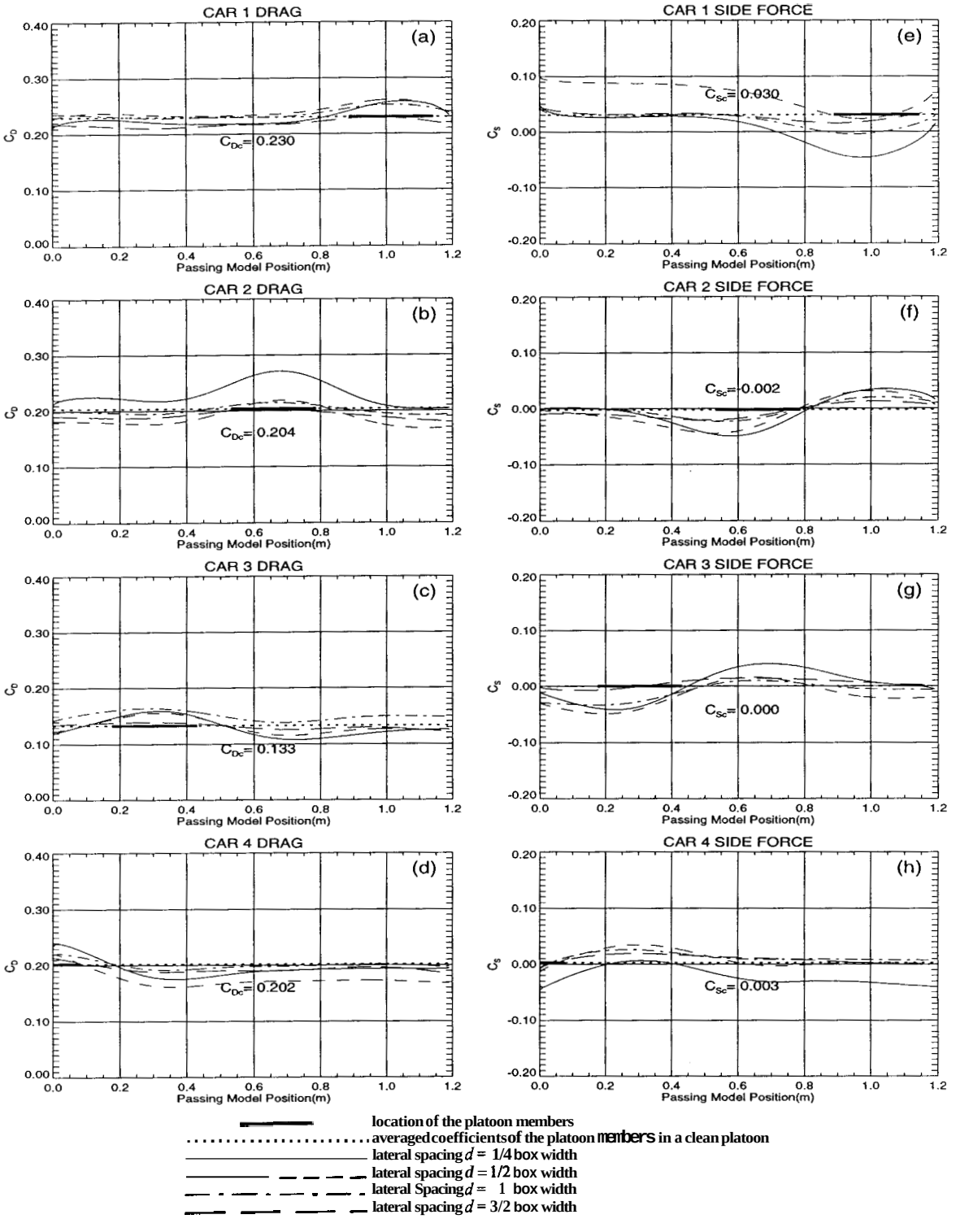

Figure 5.11: Comparison of lateral spacings - a car passes a platoon ($v = 3.75 m/s$). The drag [frames (a)-(d)] and side force [frames (e)-(h)] coefficients on each car in the platoon are shown with respect to the position of mobile model.

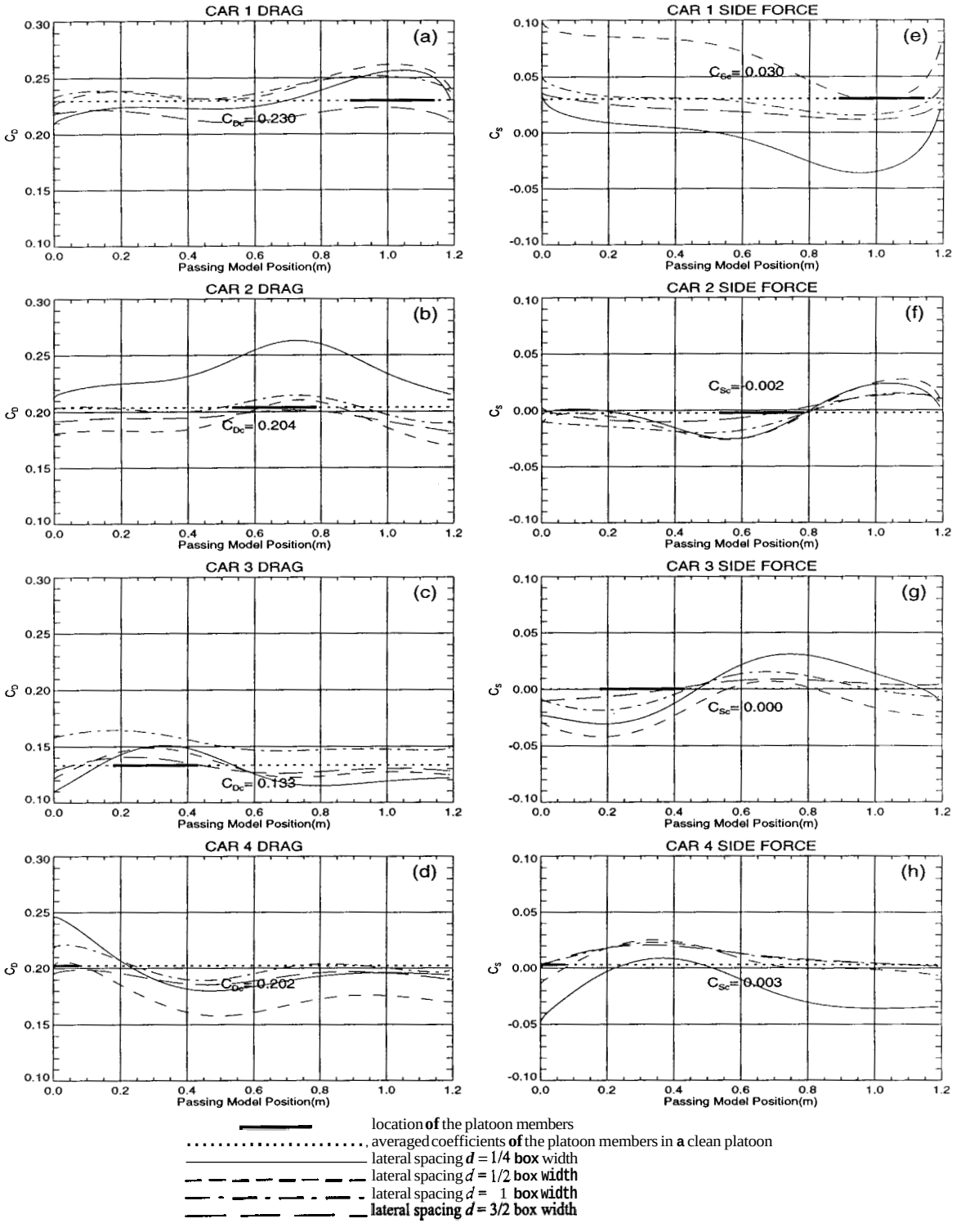

Figure 5.12: Comparison of lateral spacings - a car passes a platoon $(v = 5.00 m/s)$. The drag [frames (a)-(d)] and side force [frames (e)-(h)] coefficients on each car in the platoon are shown with respect to the position of mobile model.

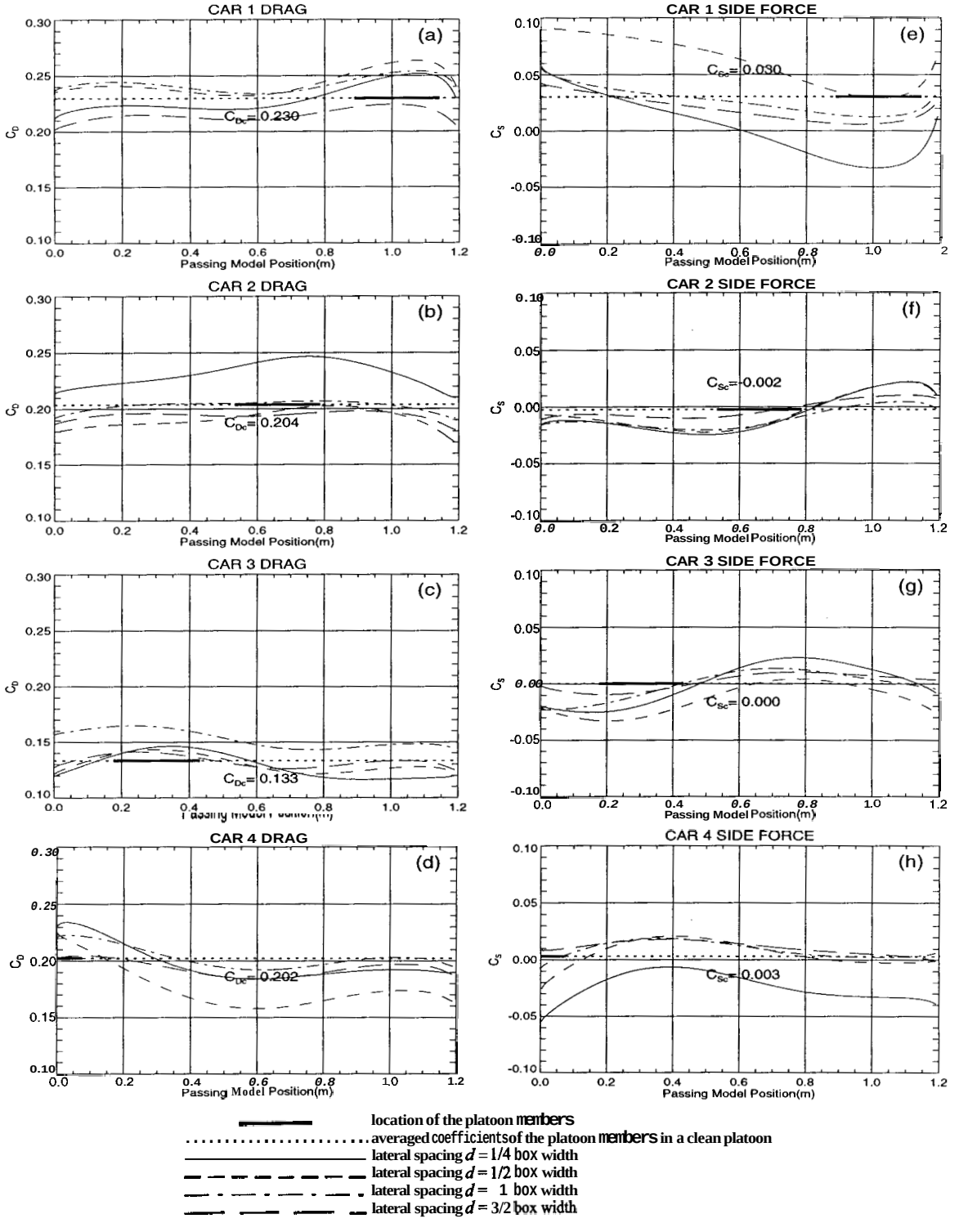

Figure 5.13: Comparison of lateral spacings - a car passes a platoon $(v = 6.25m/s)$. The drag [frames (a)-(d)] and side force [frames (e)-(h)] coefficients on each car in the platoon are shown with respect to the position of mobile model.

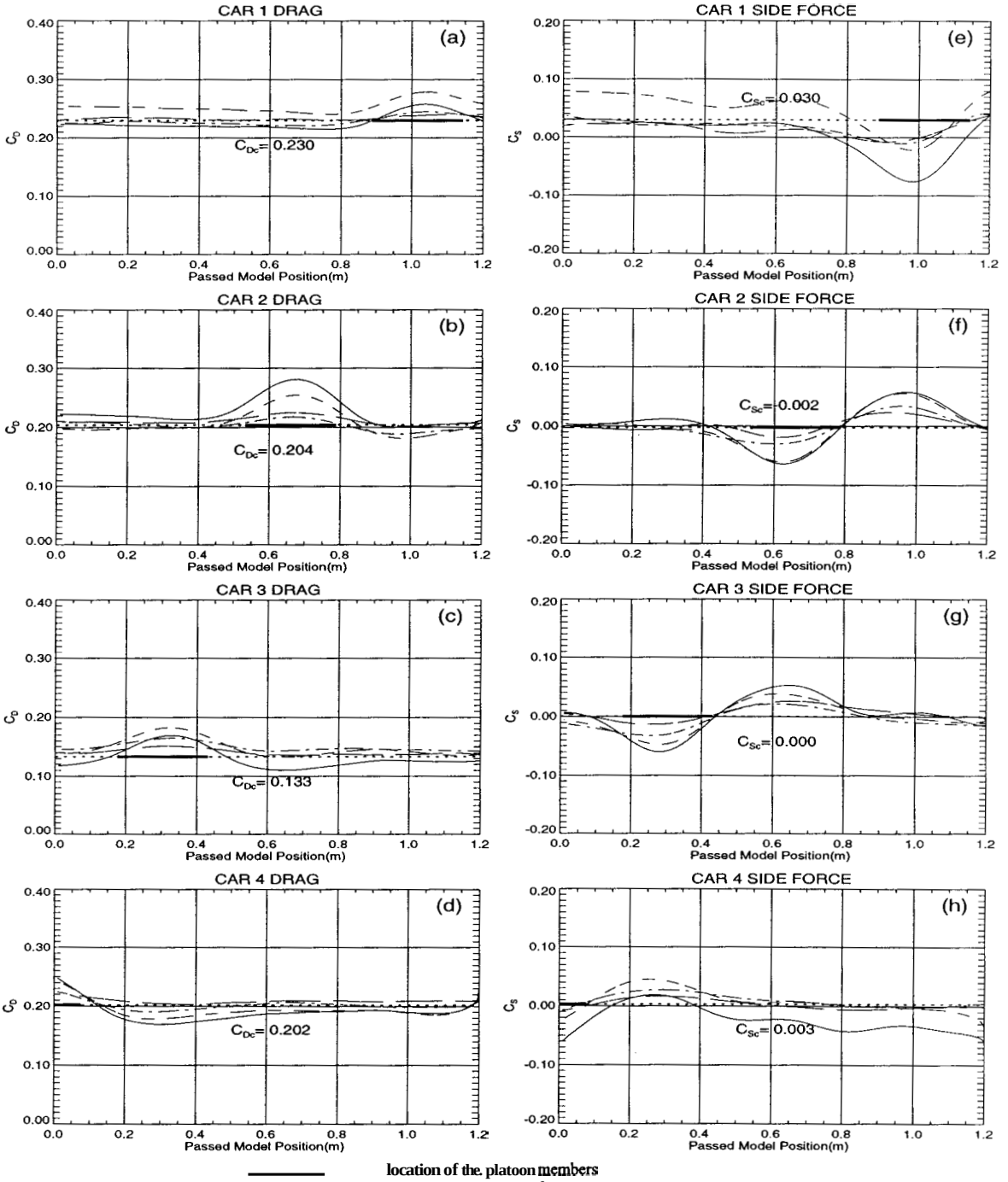

Figure 5.14: Comparison of lateral spacings - a platoon passes a car ($v = -1.25 m/s$). The drag [frames (a)-(d)] and side force [frames (e)-(h)] coefficients on each car in the platoon are shown with respect to the position of mobile model.

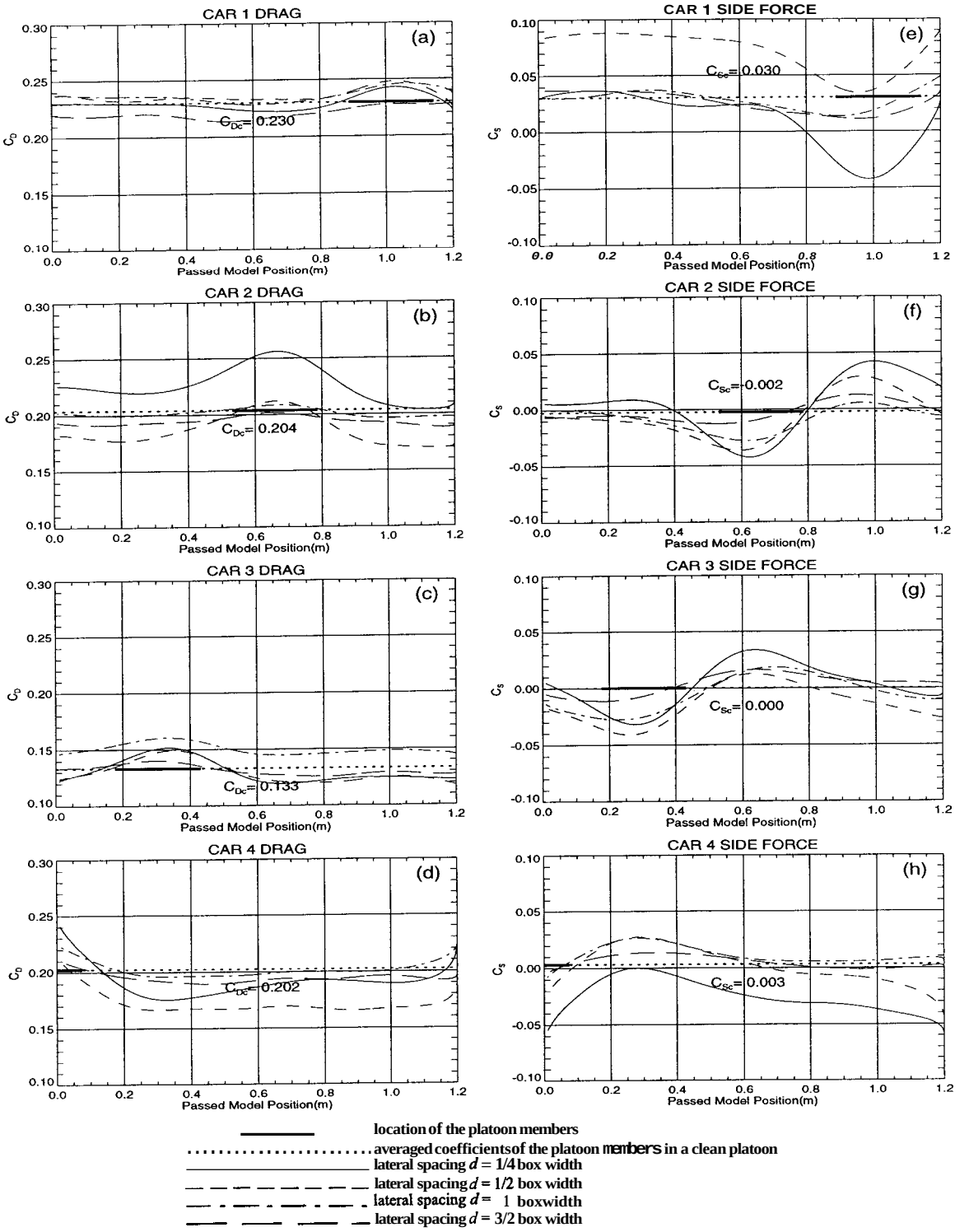

Figure 5.15: Comparison of lateral spacings - a platoon passes a car ($v = -2.50 m/s$). The drag [frames (a)-(d)] and side force [frames (e)-(h)] coefficients on each car in the platoon are shown with respect to the position of mobile model.

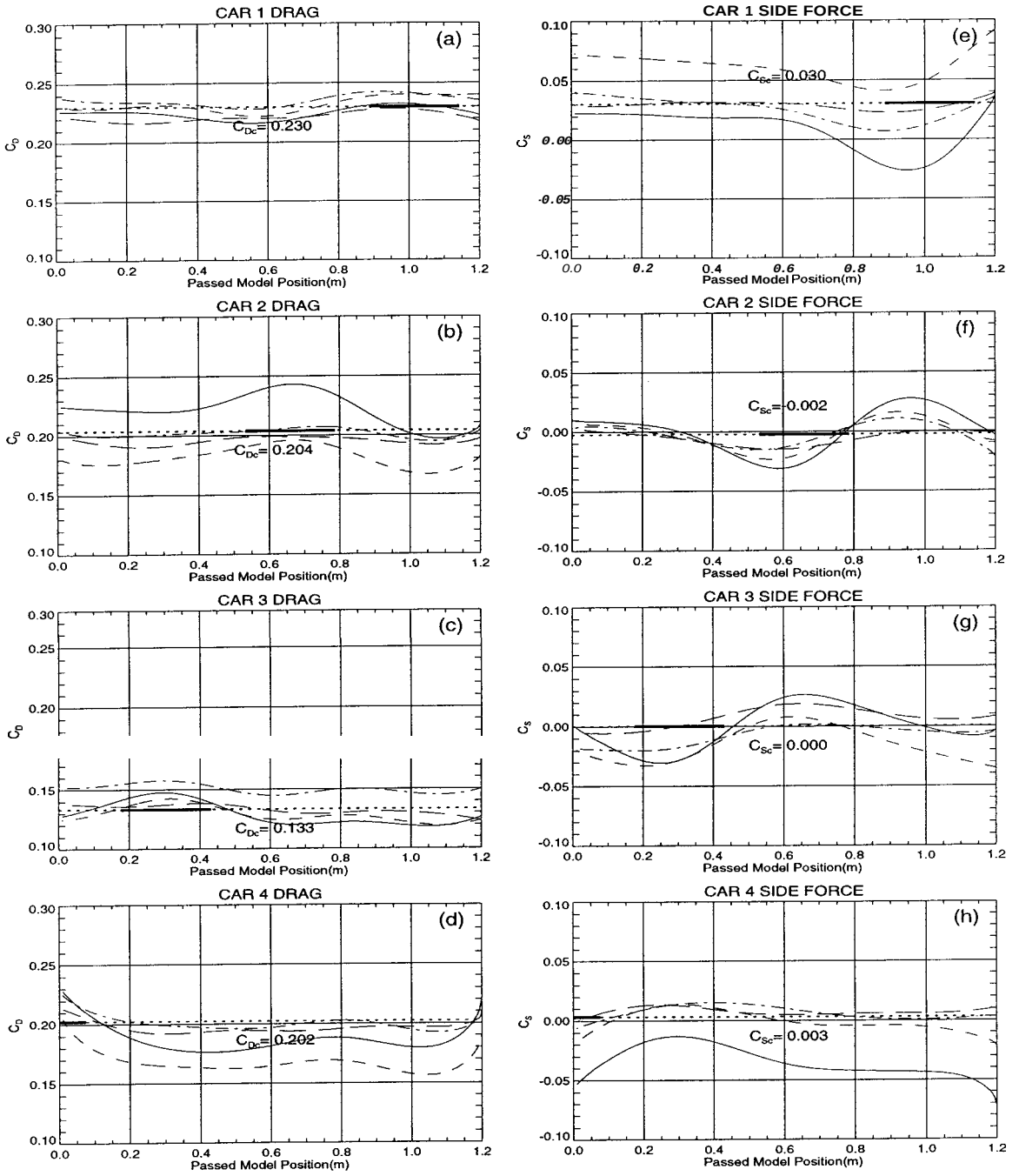

Figure 5.16: Comparison of lateral spacings - a platoon passes a car ($v = -3.75 m/s$). The drag [frames (a)-(d)] and side force [frames (e)-(h)] coefficients on each car in the platoon are shown with respect to the position of mobile model.

Chapter 6

Effects of Mobile Model

Aerodynamic forces experienced by every platoon member under the influence of the two different mobile models are compared. **A** passenger vehicle model and a similar sized rectangular box are applied. Compared with the streamlined front and rear ends of the passenger vehicle model, both ends of the rectangular box are flat with sharp corners, which provides a reasonable simulation of a mini van or bus. Forces measured on each of the four cars in the platoon are recorded simultaneously as the mobile model travels $1.2m$. The coefficients on each of the four cars are plotted with respect to the position of the front end of the mobile model. The peak values of drag and side force coefficients for each platoon members are shown, and the locations of the front end of the mobile model in which the peak values occur are determined. The position of each platoon member are also plotted for reference.

Four different lateral spacings ($d = \frac{1}{4}, \frac{1}{2}, 1$, and $\frac{3}{2}W$, where $W = 10.2cm$ = **box** width) are considered, while five different velocities ($v = 1.25, 2.50, 3.75, 5.00$, and $6.25m/s$) are examined when model is in forward motion, and three velocities ($v = -1.25, -2.50$, and $-3.75m/s$) are investigated when mobile model is in backward motion. Figure *6.1* to figure *6.20* show the data while the mobile models move forward, and figure 6.21 to figure *6.32* show the data when the models are in backward motion.

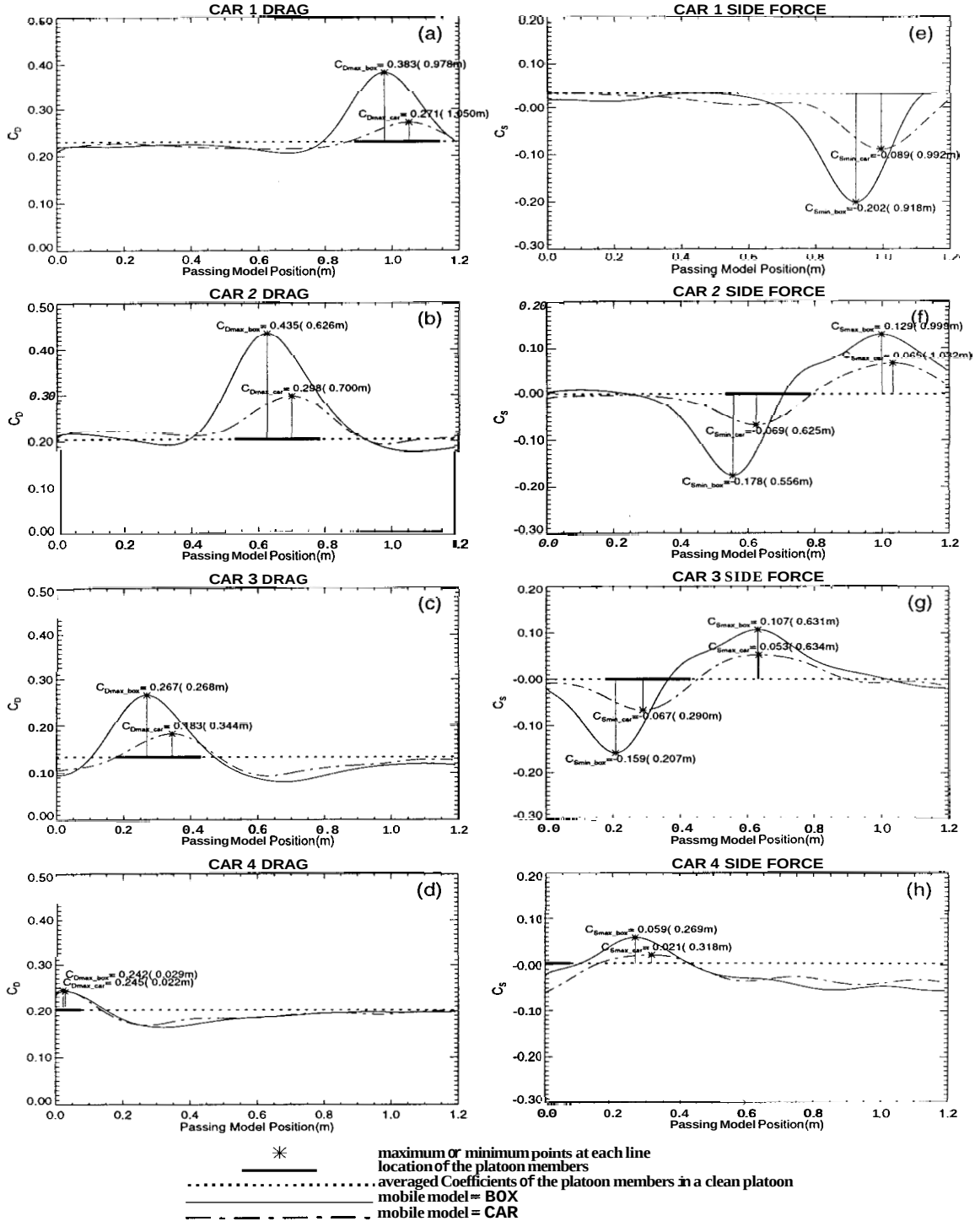

Figure 6.1: Comparison of mobile model ($d = \frac{1}{4}W, v = 1.25m/s$).
The drag [frames (a)-(d)] and side force [frames (e)-(h)] coefficients on each car in the platoon are shown with respect to the position of mobile model.

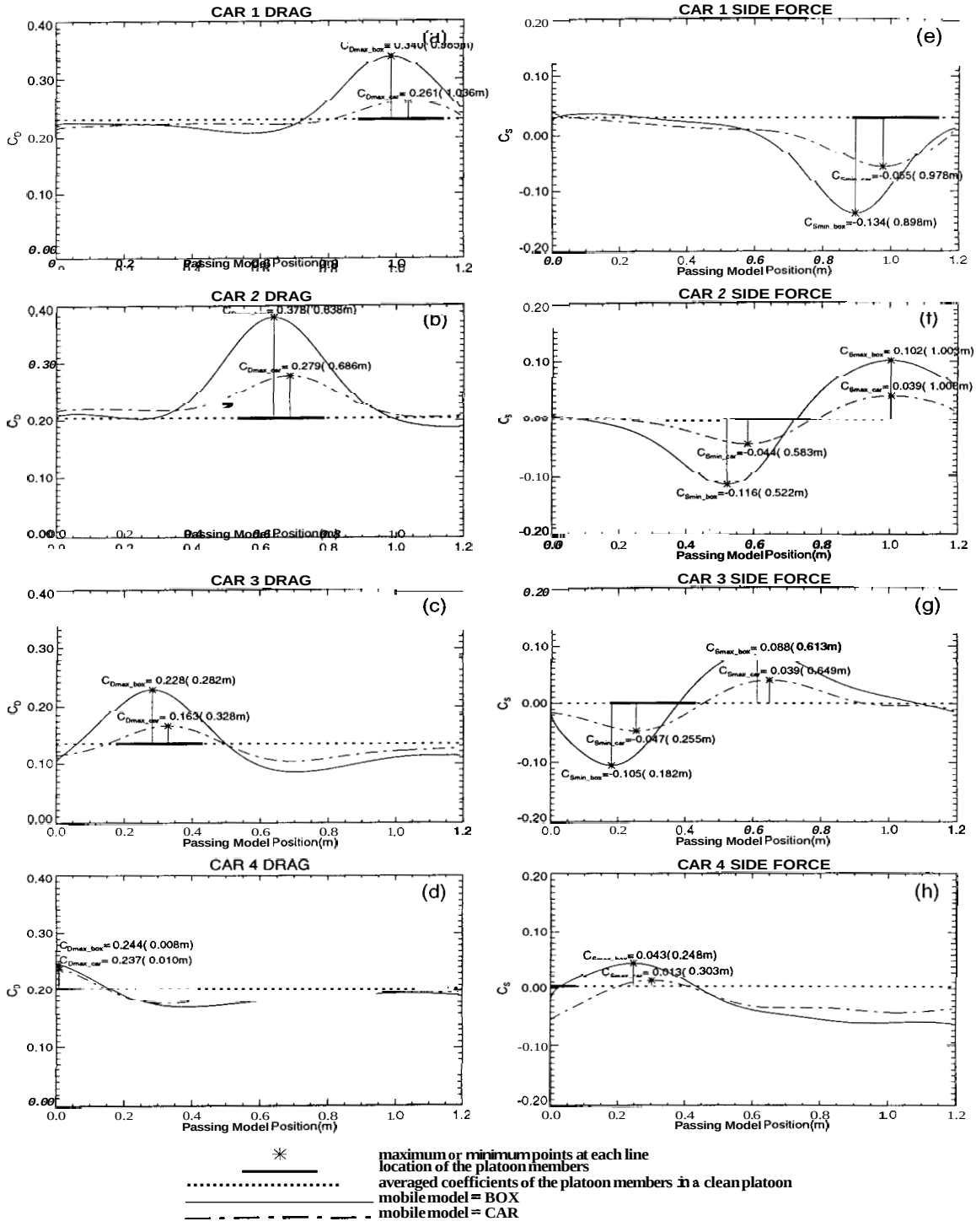

Figure 6.2: Comparison of mobile model ($d = \frac{1}{4}W, v = 2.50m/s$).
The drag [frames (a)-(d)] and side force [frames (e)-(h)] coefficients on each car in the platoon are shown with respect to the position of mobile model.

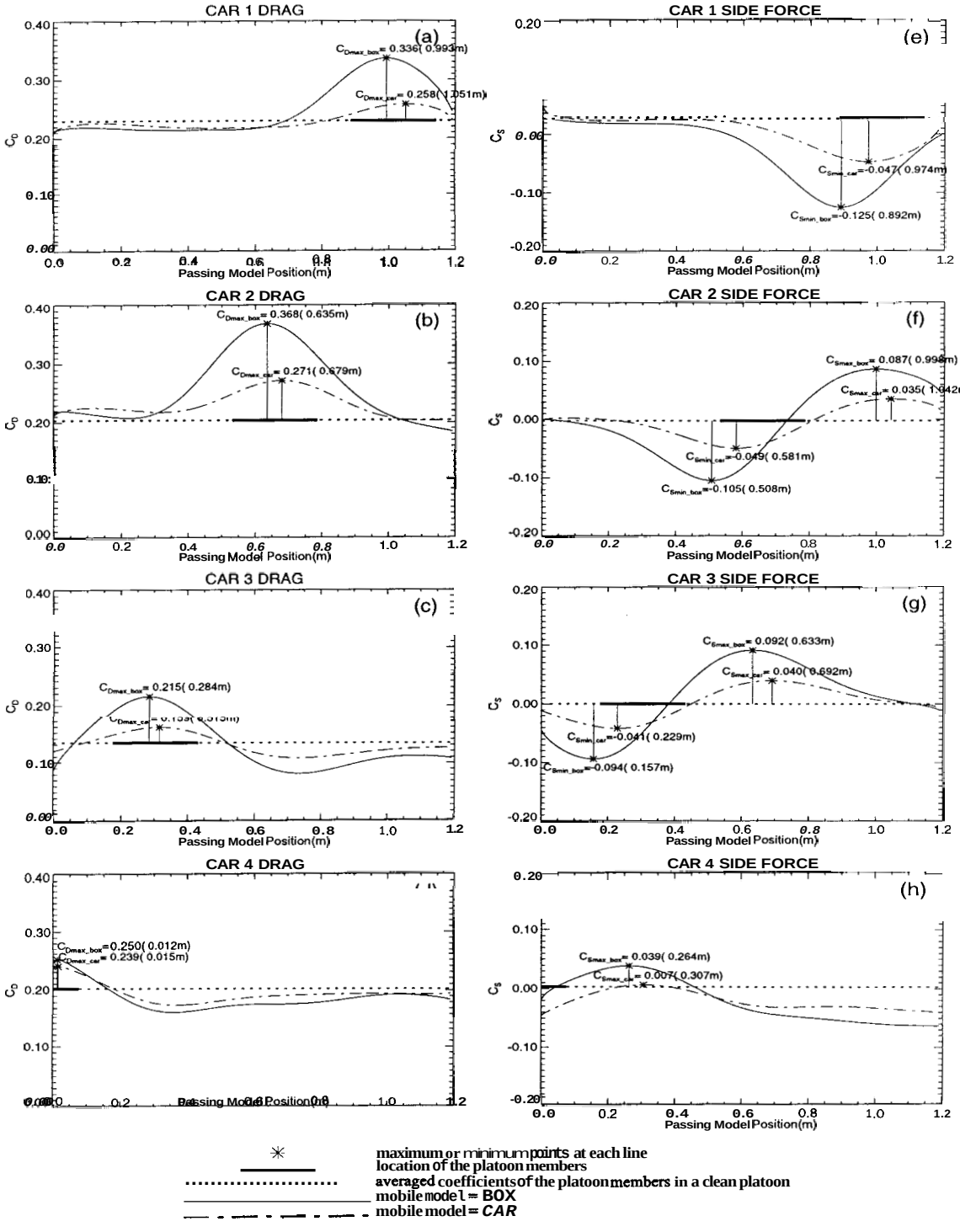

Figure *6.3:* Comparison of mobile model $(d = \frac{1}{4}W, v = 3.75m/s)$.
The drag [frames (a)-(d)] and side force [frames (e)-(h)] coefficients on each car in the platoon are shown with respect to the position of mobile model.

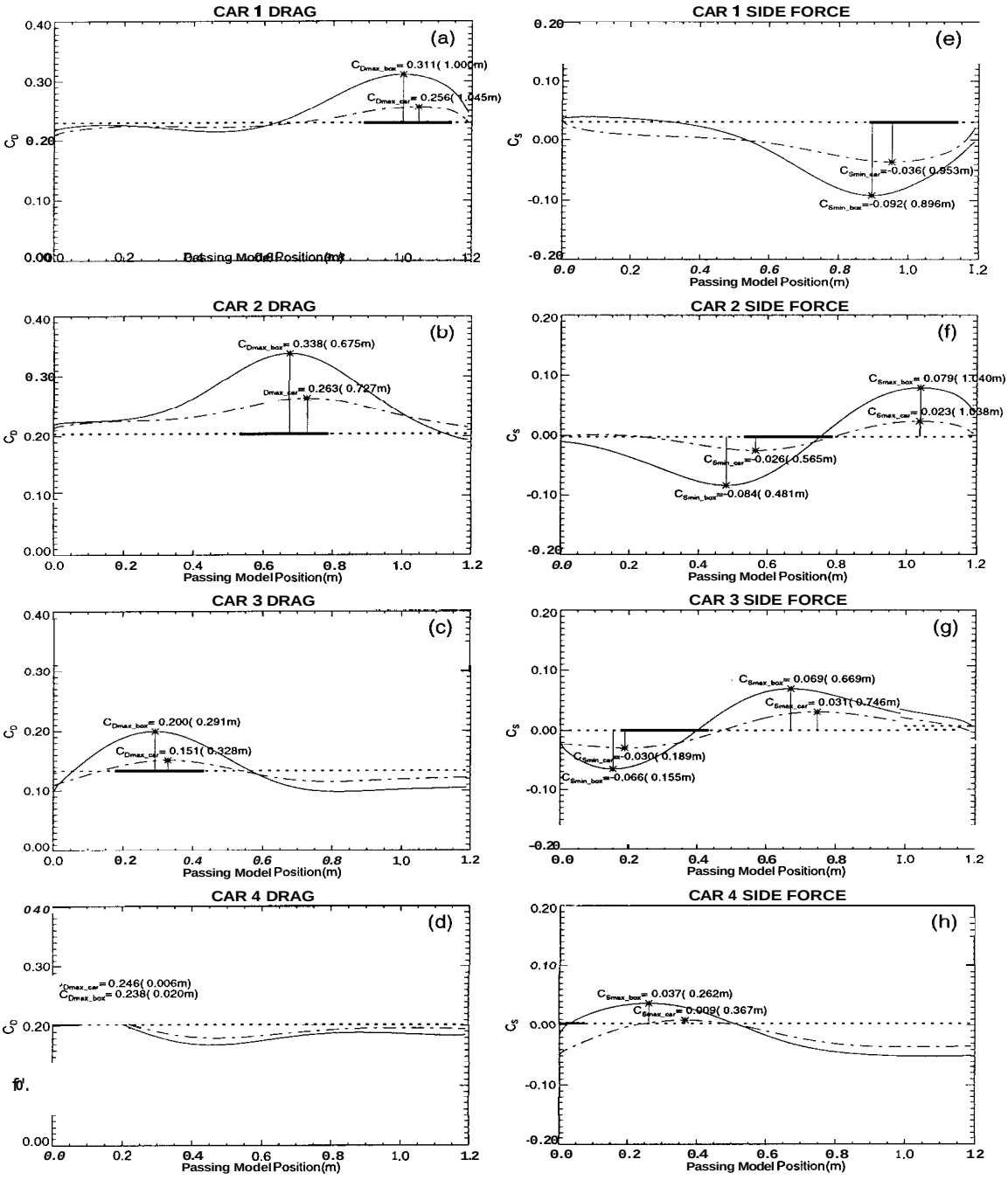

Figure **6.4:** Comparison of mobile model $(d = \frac{1}{4}W, v = 5.00m/s)$.
The drag [frames (a)-(d)] and side force [frames (e)-(h)] coefficients on each car in the platoon are shown with respect to the position of mobile model.

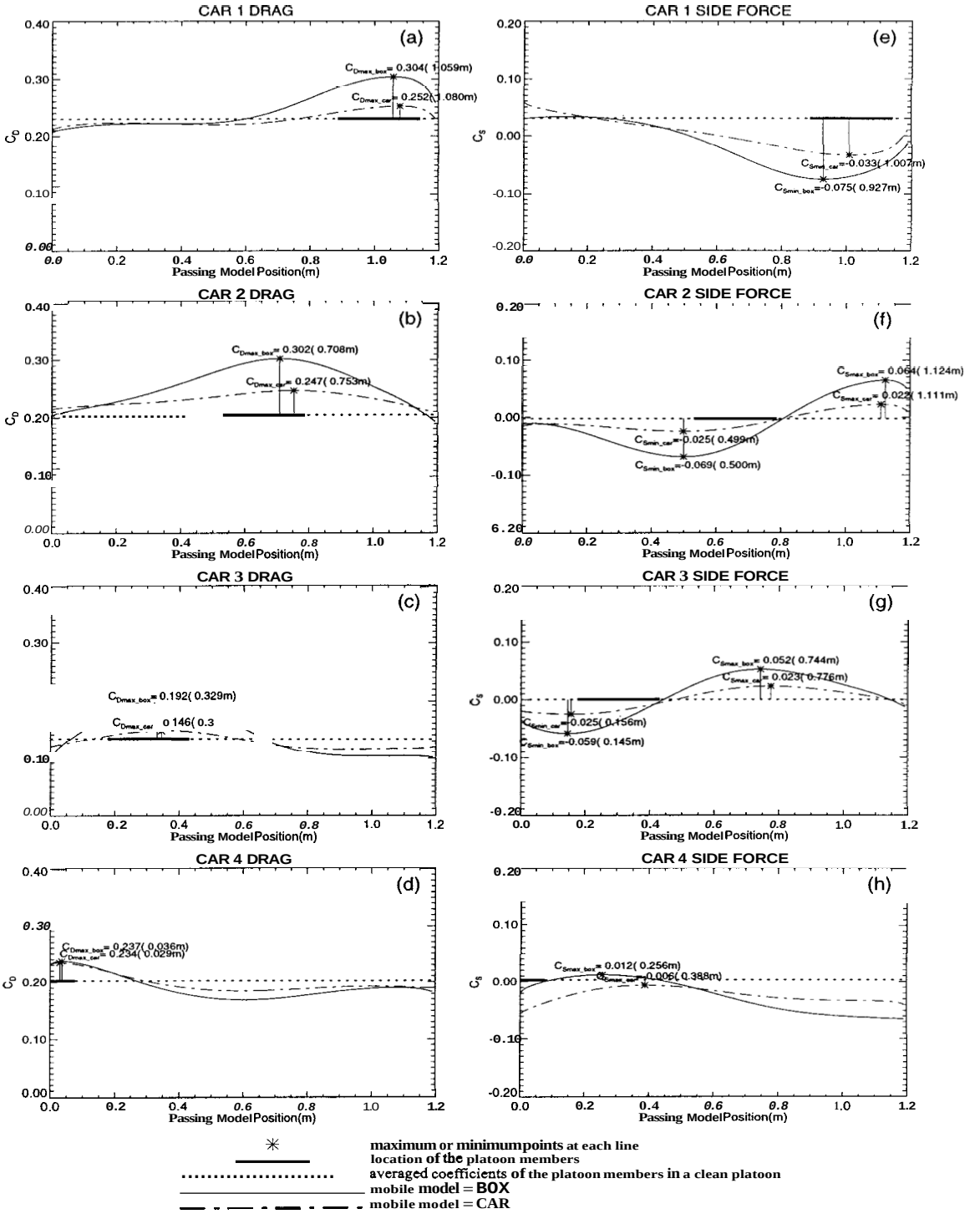

Figure 6.5: Comparison of mobile model ($d = \frac{1}{4}W, v = 6.25m/s$).
The drag [frames (a)-(d)] and side force [frames (e)-(h)] coefficients on each car in the platoon are shown with respect to the position of mobile model.

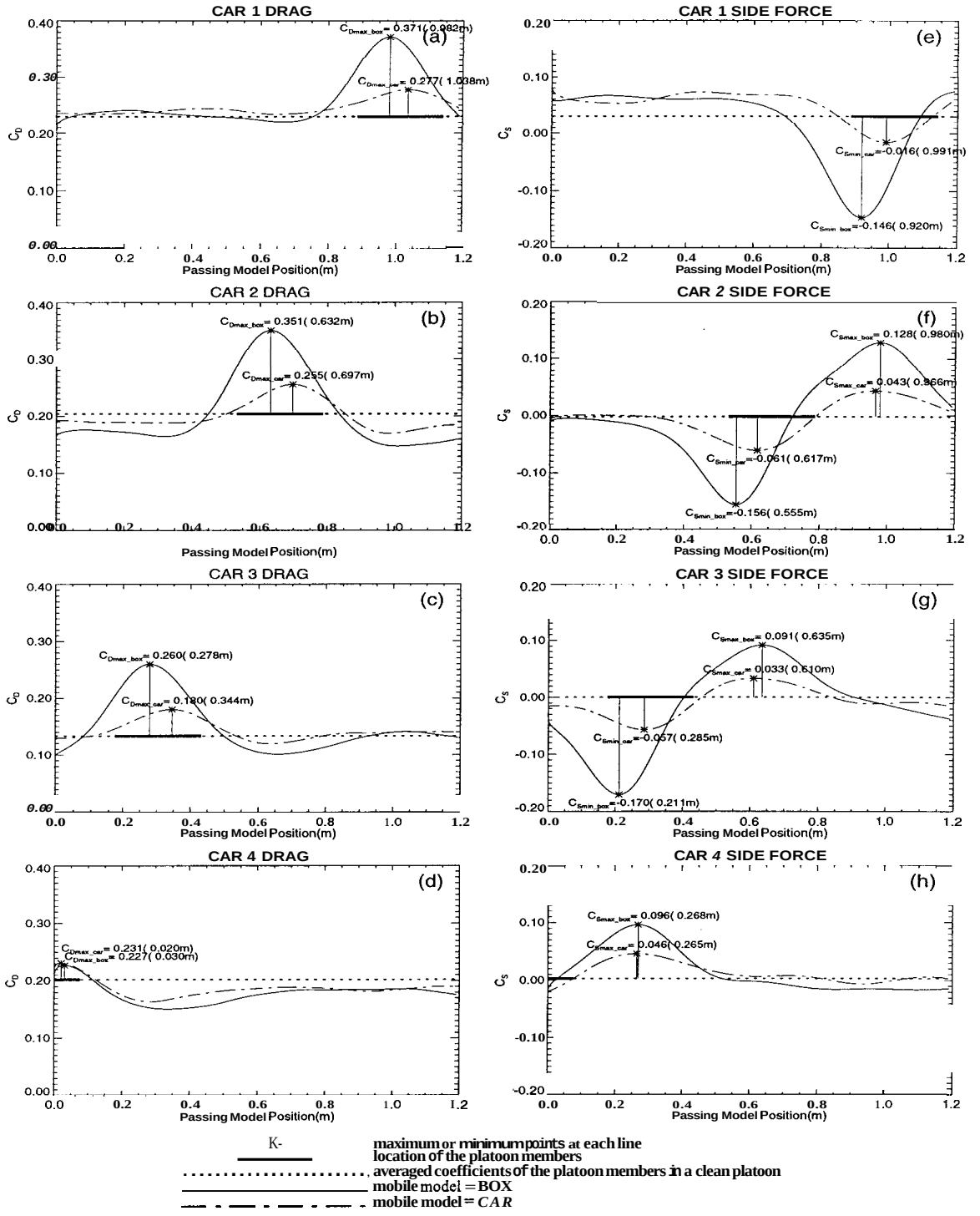

Figure **6.6:** Comparison of mobile model $(d = \frac{1}{2}W, \text{PI} = 1.25m/s)$.
The drag [frames (a)-(d)] and side force [frames (e)-(h)] coefficients on each car in the platoon are shown with respect to the position of mobile model.

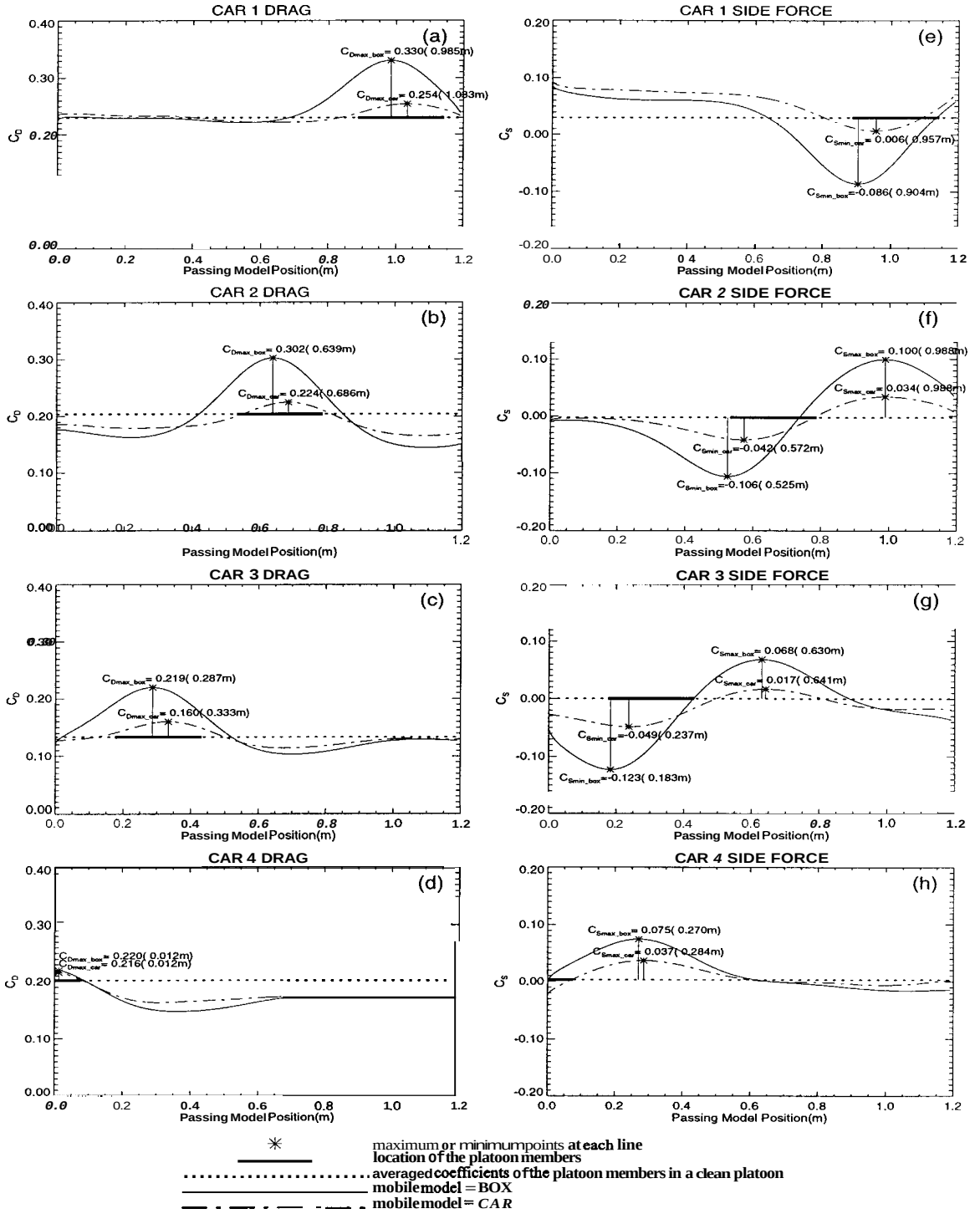

Figure 6.7: Comparison of mobile model ($d = \frac{1}{2}W, v = 2.50m/s$).
The drag [frames (a)-(d)] and side force [frames (e)-(h)] coefficients on each car in the platoon are shown with respect to the position of mobile model.

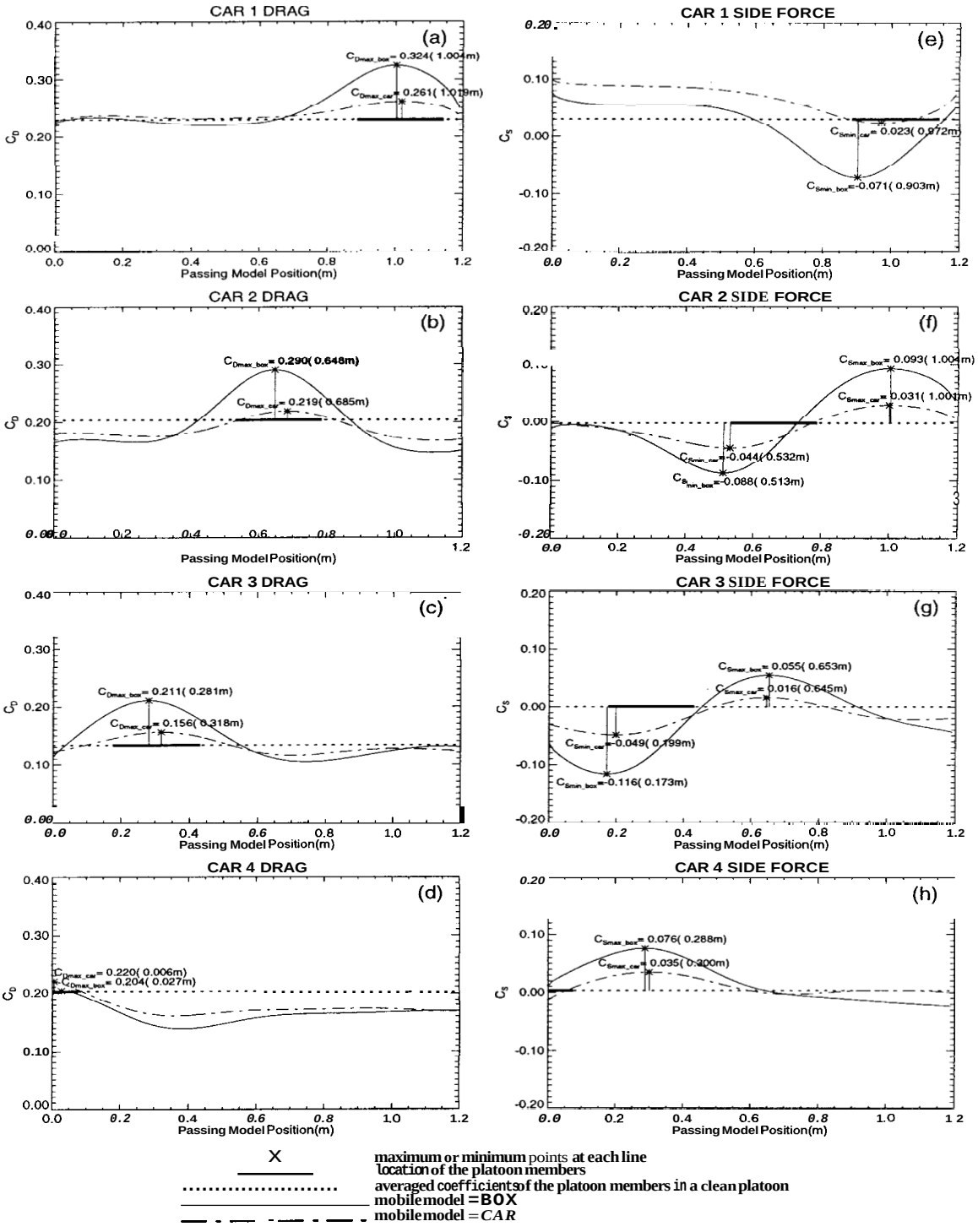

Figure *6.8:* Comparison of mobile model ($d = \frac{1}{2}W, v = 3.75m/s$).
The drag [frames (a)-(d)] and side force [frames (e)-(h)] coefficients on each car in the platoon are shown with respect to the position of mobile model.

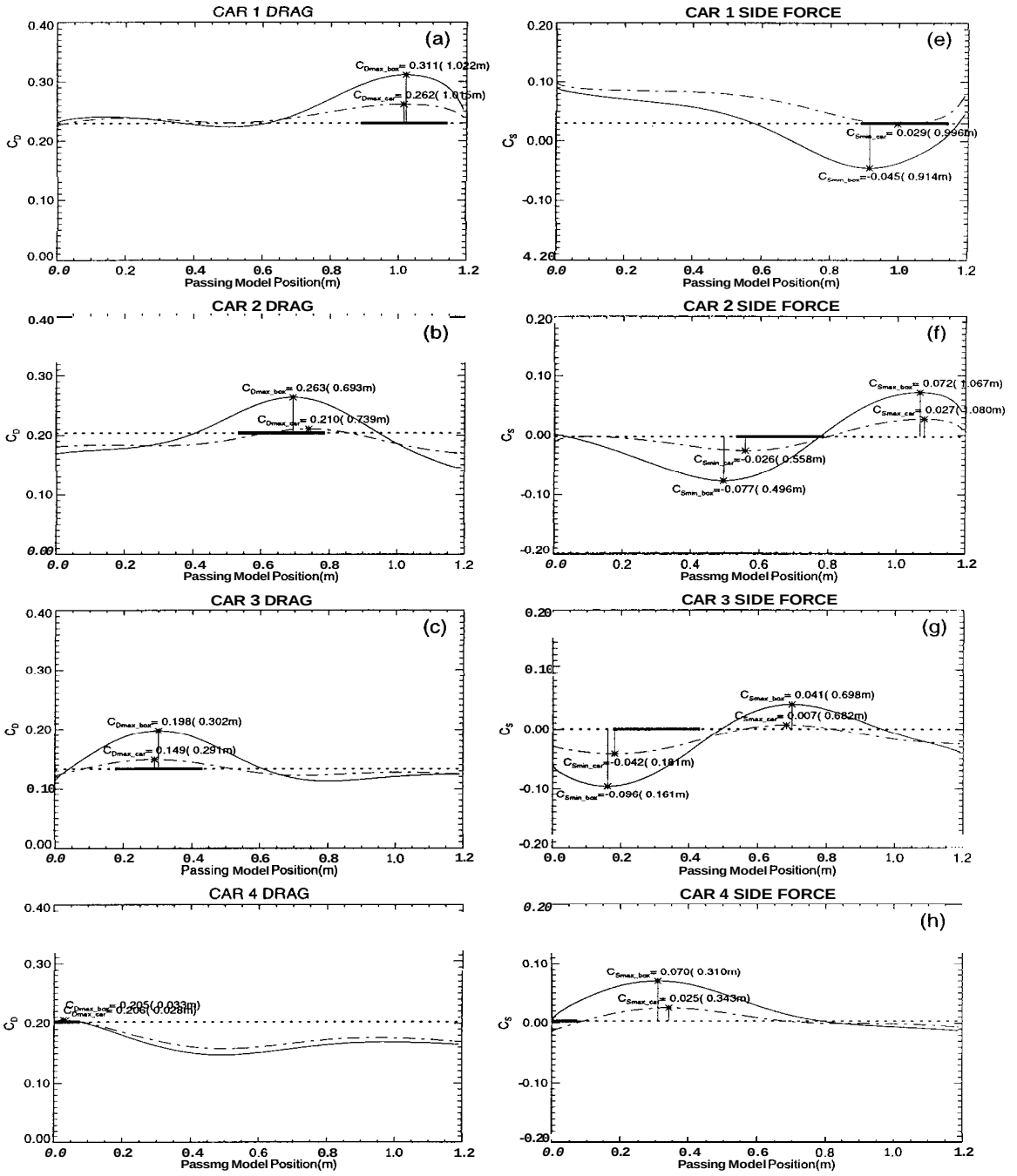

Figure 6.9: Comparison of mobile model ($d = \frac{1}{2}W, v = 5.00m/s$).
The drag [frames (a)-(d)] and side force [frames (e)-(h)] coefficients on each car in the platoon are shown with respect to the position of mobile model.

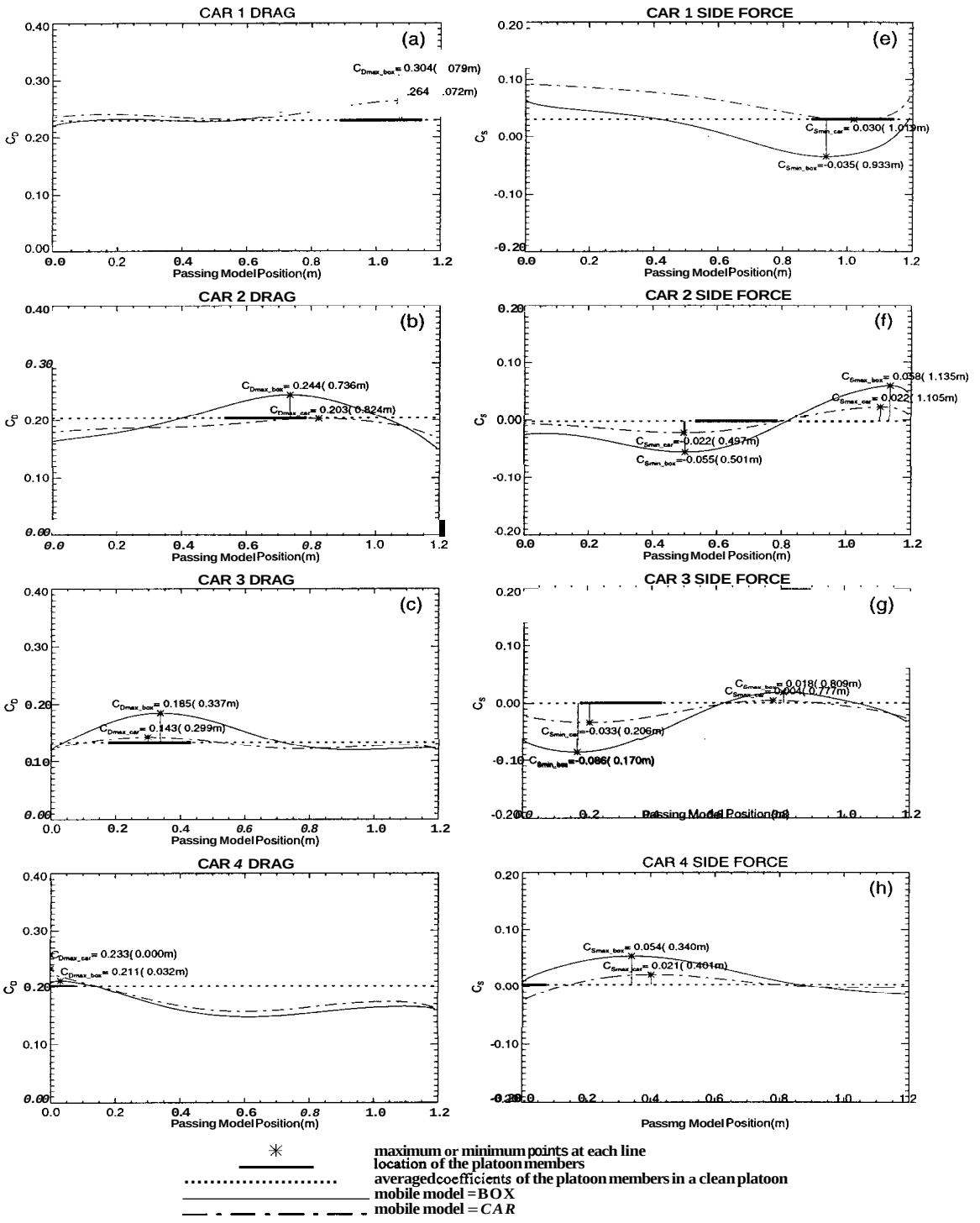

Figure 6.10: Comparison of mobile model $(d = \frac{1}{2}W, v = 6.25m/s)$.
The drag [frames (a)-(d)] and side force [frames (e)-(h)] coefficients on each car in the platoon are shown with respect to the position of mobile model.

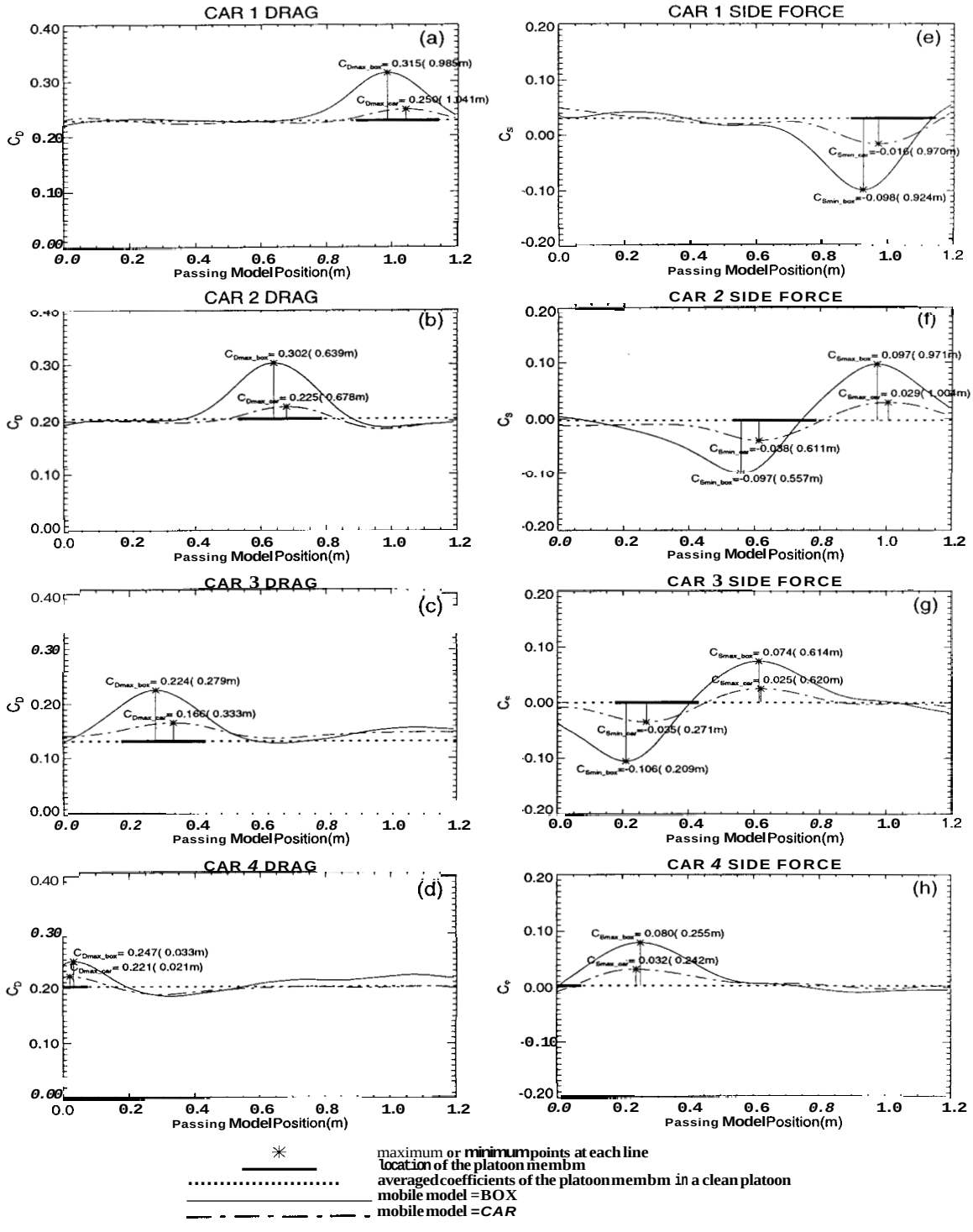

Figure 6.11: Comparison of mobile model $(d = 1W, v = 1.25m/s)$.
The drag [frames (a)-(d)] and side force [frames (e)-(h)] coefficients on each car in the platoon are shown with respect to the position of mobile model.

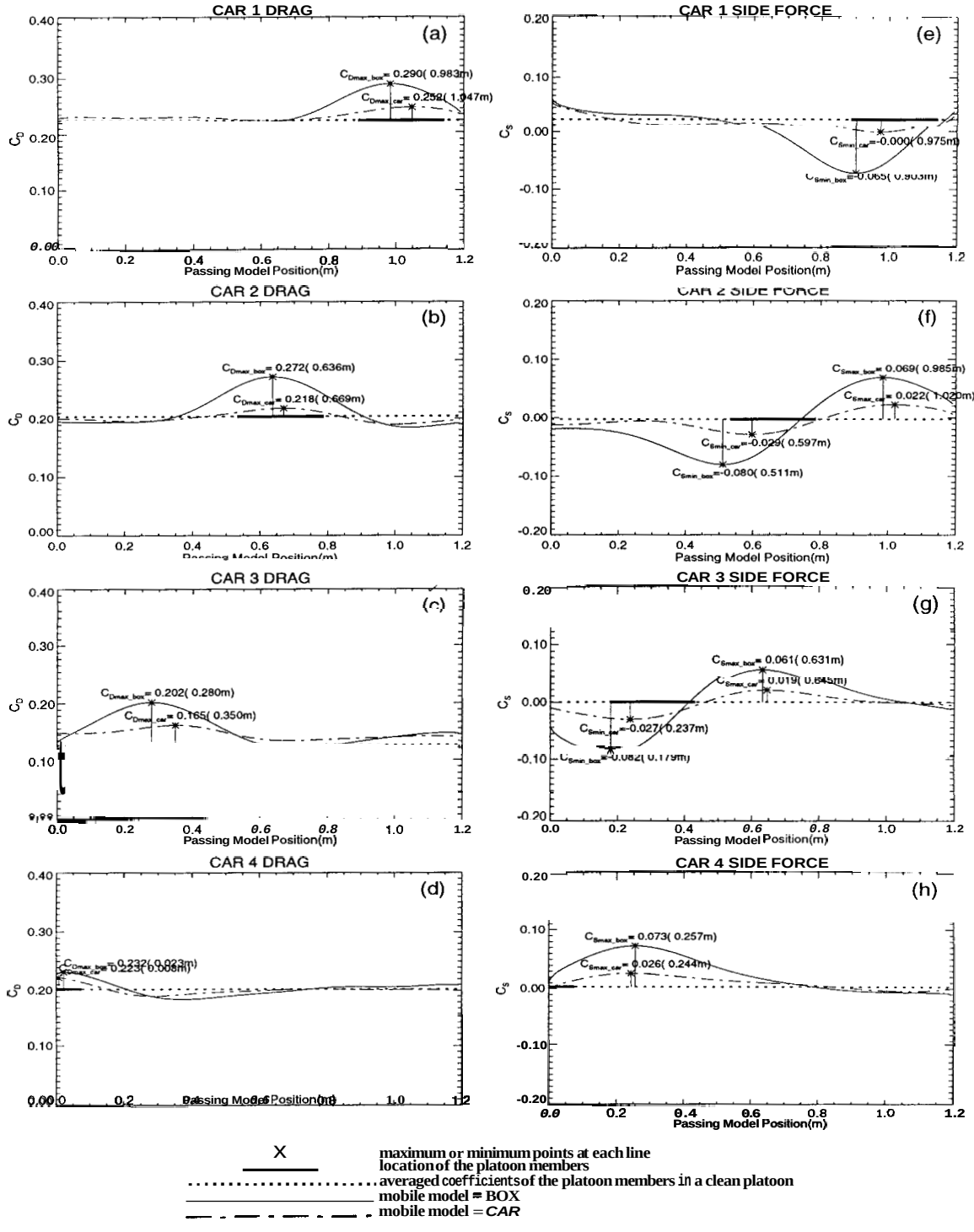

Figure 6.12: **Comparison of mobile model** $(d = 1W, v = 2.50m/s)$.
The drag [frames (a)-(d)] and side force [frames (e)-(h)] coefficients on each car in the platoon are shown with respect to the position of mobile model.

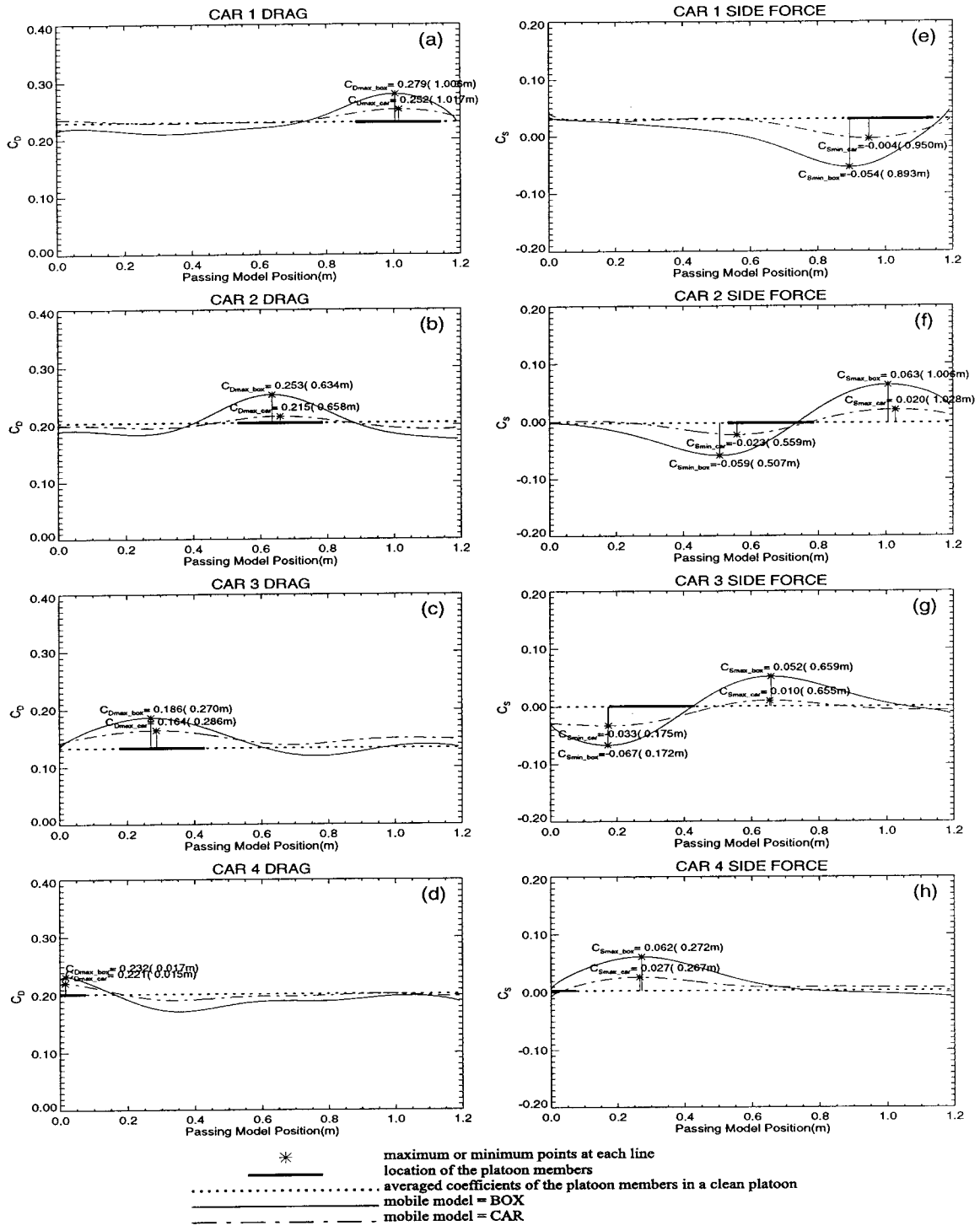

Figure 6.13: Comparison of mobile model ($d = 1W, v = 3.75m/s$).
The drag [frames (a)-(d)] and side force [frames (e)-(h)] coefficients on each car in the platoon are shown with respect to the position of mobile model.

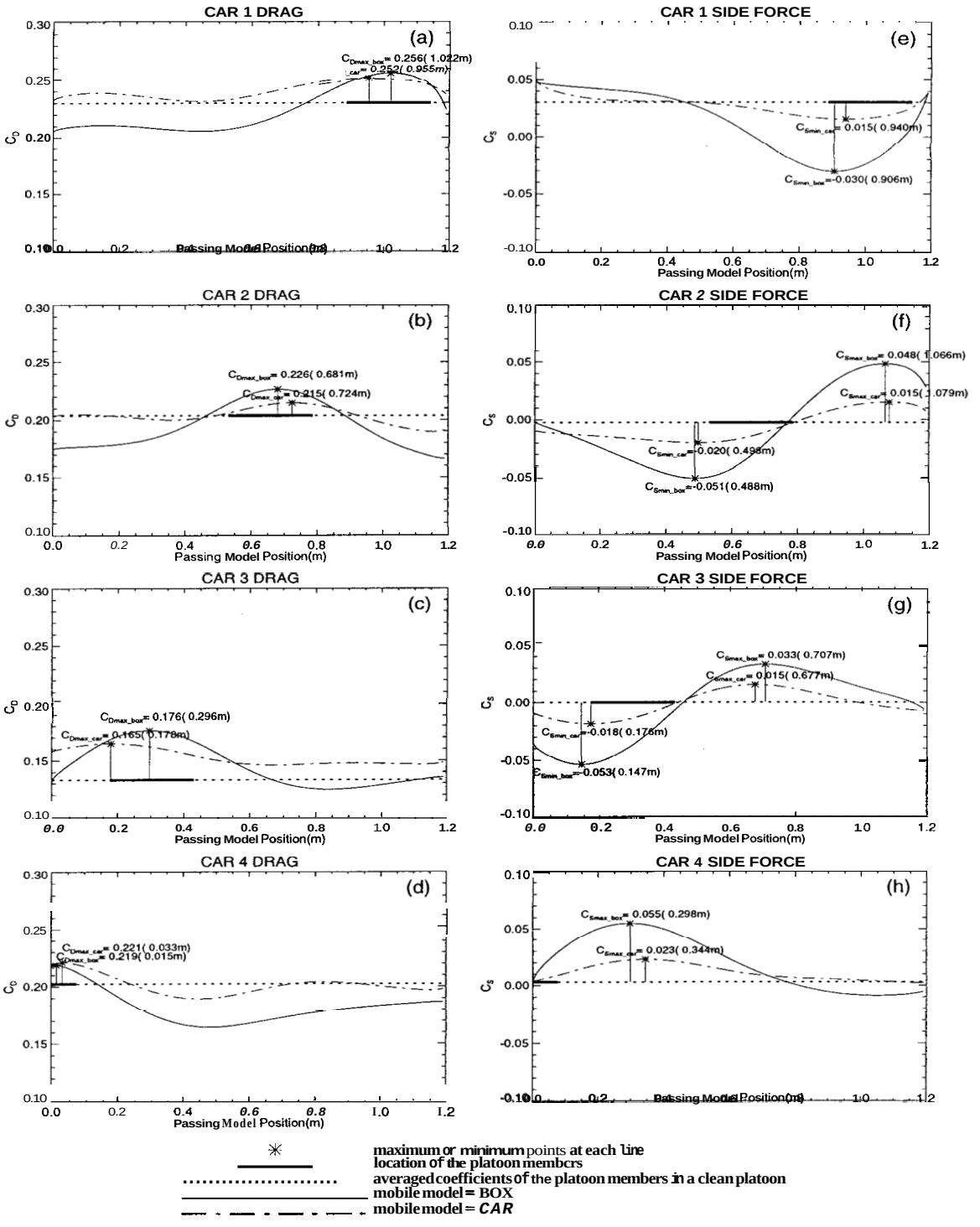

Figure 6.14: Comparison of mobile model $(d = 1W, v = 5.00m/s)$.
The drag [frames (a)-(d)] and side force [frames (e)-(h)] coefficients on each car in the platoon are shown with respect to the position of mobile model.

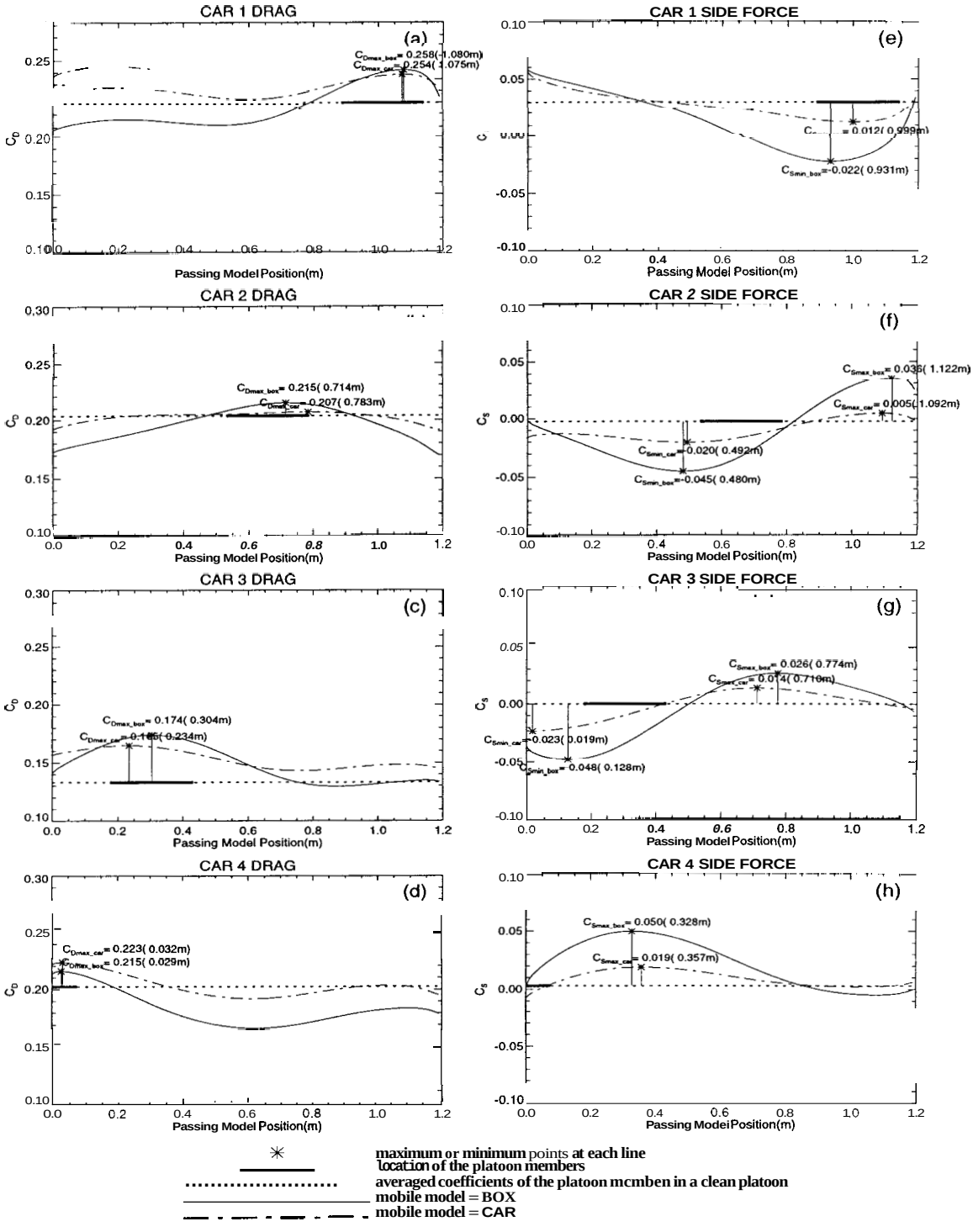

Figure 6.15: Comparison of mobile model $(d = 1W, v = 6.25m/s)$.
The drag [frames (a)-(d)] and side force [frames (e)-(h)] coefficients on each car in the platoon are shown with respect to the position of mobile model.

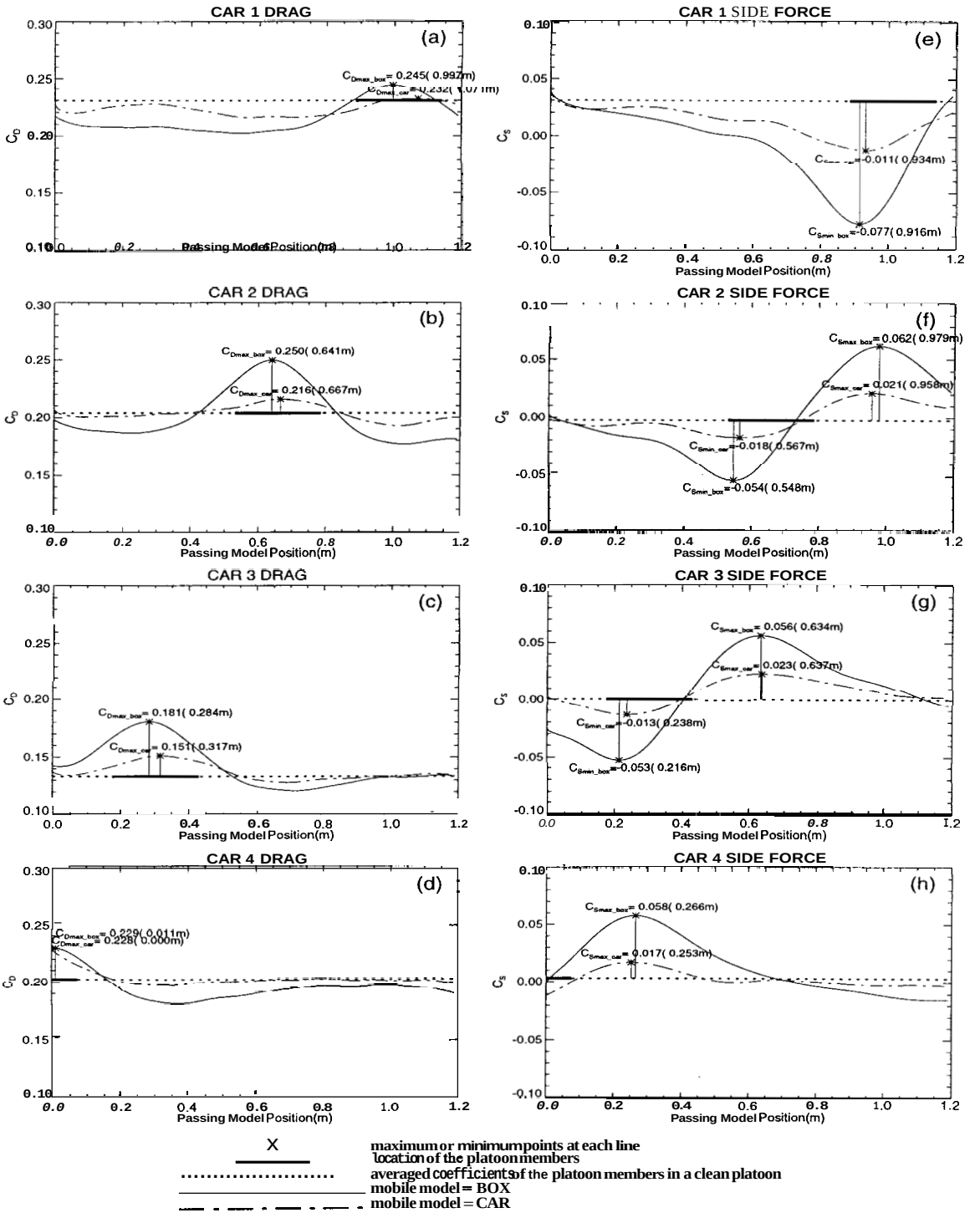

Figure 6.16: Comparison of mobile model ($d = \frac{3}{2}W, v = 1.25m/s$).
The drag [frames (a)-(d)] and side force [frames (e)-(h)] coefficients on each car in the platoon are shown with respect to the position of mobile model.

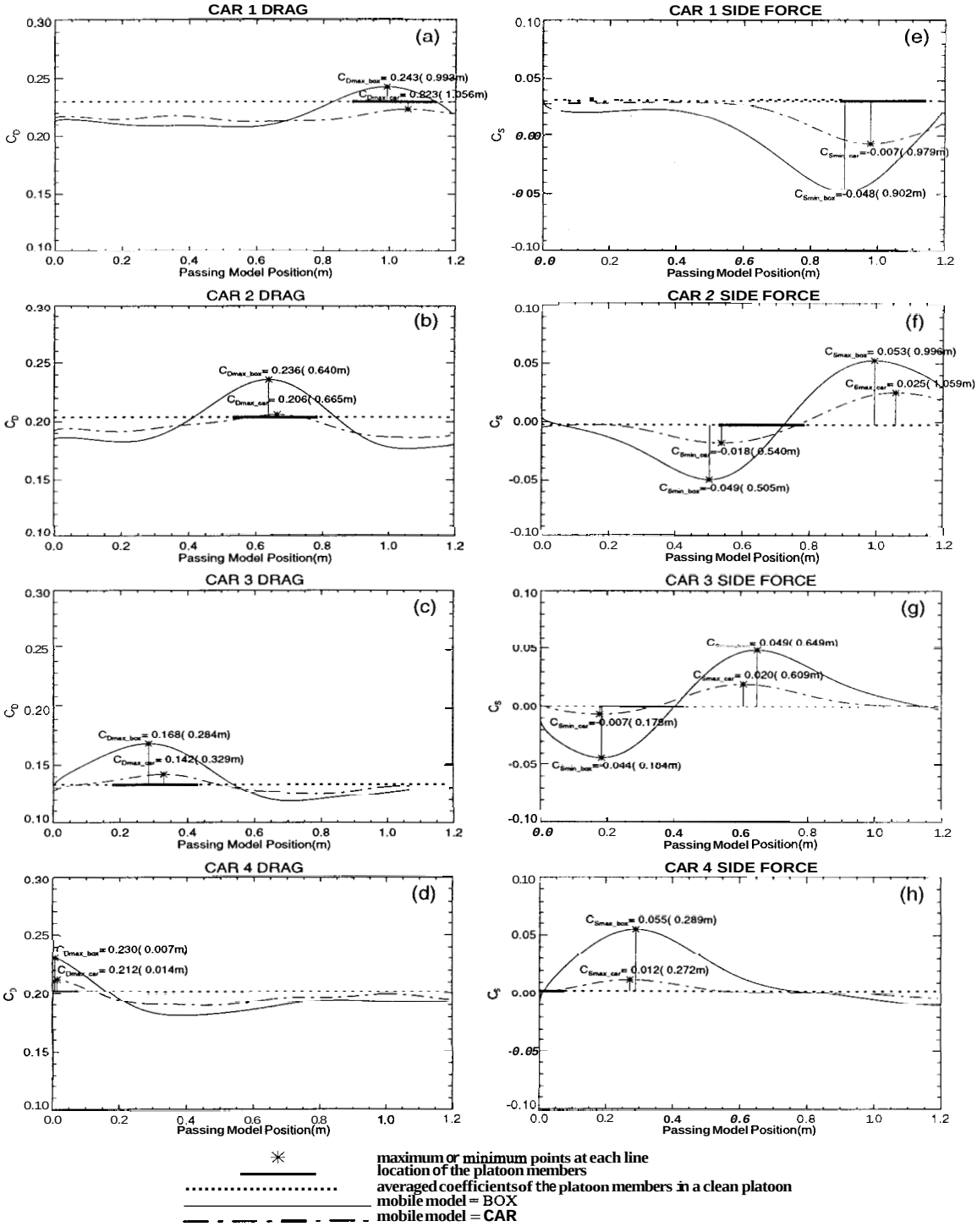

Figure 6.17: Comparison of mobile model ($d = \frac{3}{2}W, v = 2.50m/s$).
The drag [frames (a)-(d)] and side force [frames (e)-(h)] coefficients on each car in the platoon are shown with respect to the position of mobile model.

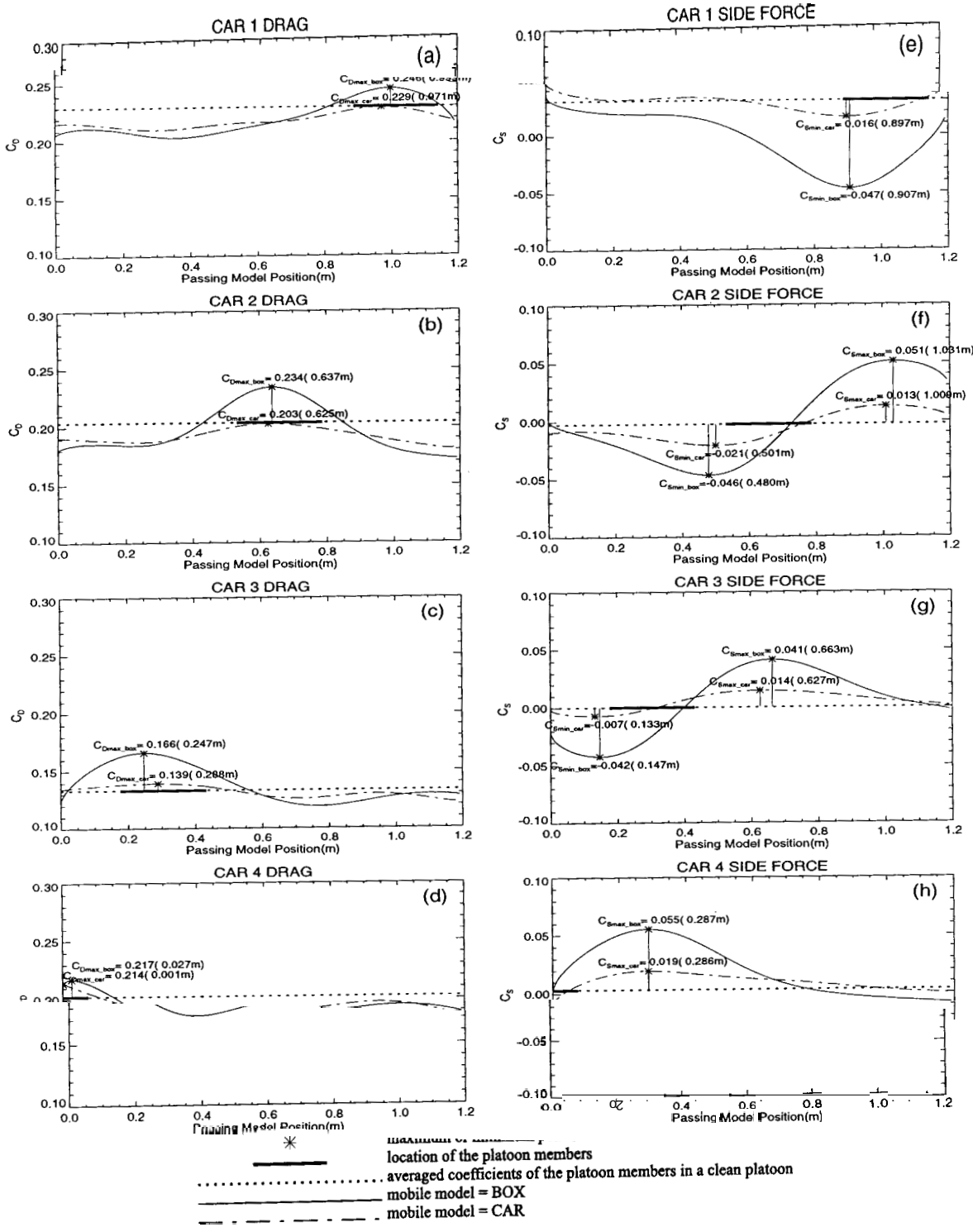

Figure 6.18: Comparison of mobile model ($d = \frac{3}{2}W, v = 3.75m/s$).
The drag [frames (a)-(d)] and side force [frames (e)-(h)] coefficients on each car in the platoon are shown with respect to the position of mobile model.

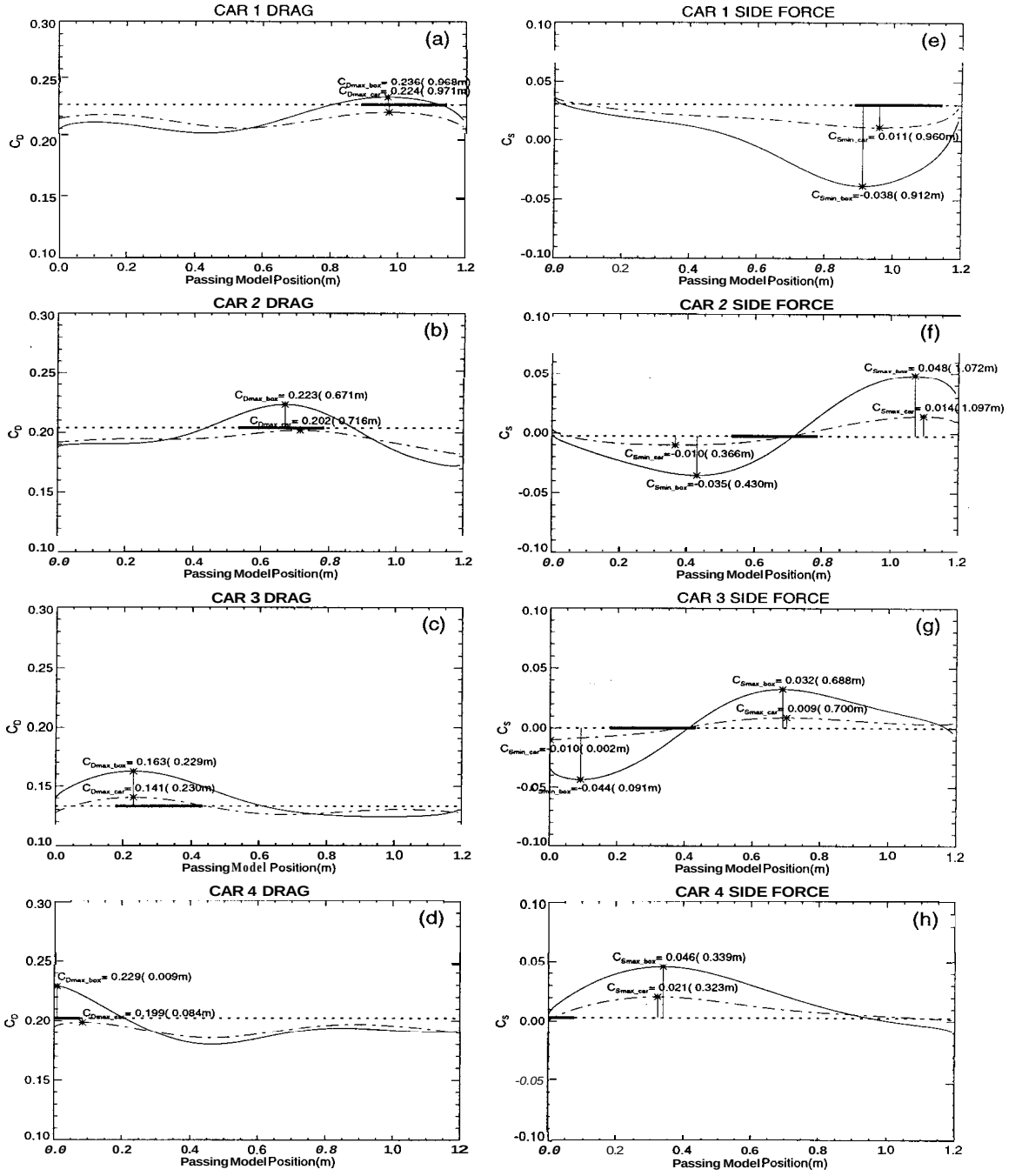

Figure 6.19: Comparison of mobile model ($d = \frac{3}{2}W, v = 5.00m/s$).
The drag [frames (a)-(d)] and side force [frames (e)-(h)] coefficients on each car in the platoon are shown with respect to the position of mobile model.

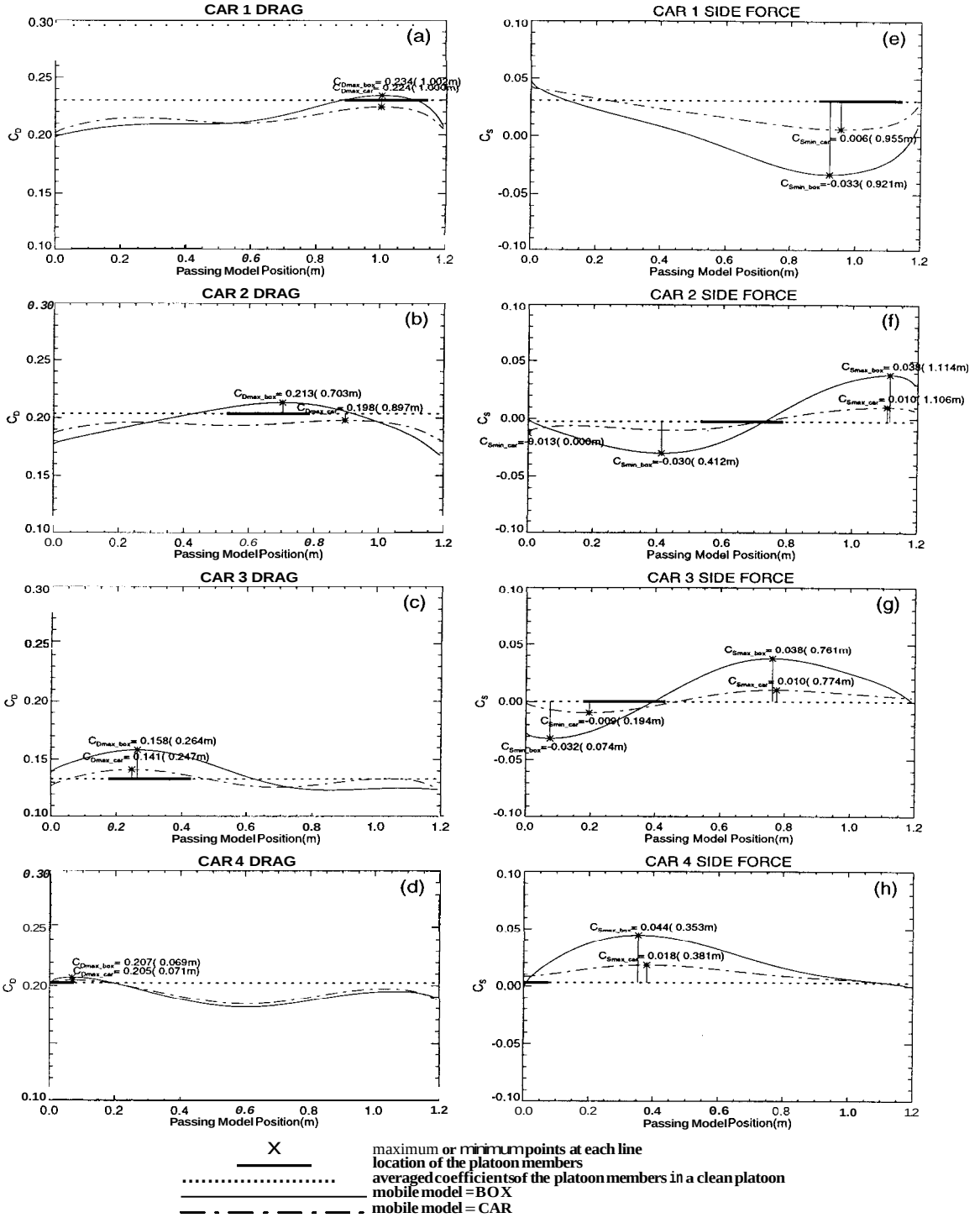

Figure 6.20: Comparison of mobile model ($d = \frac{3}{2}W, v = 6.25m/s$).
The drag [frames (a)-(d)] and side force [frames (e)-(h)] coefficients on each car in the platoon are shown with respect to the position of mobile model.

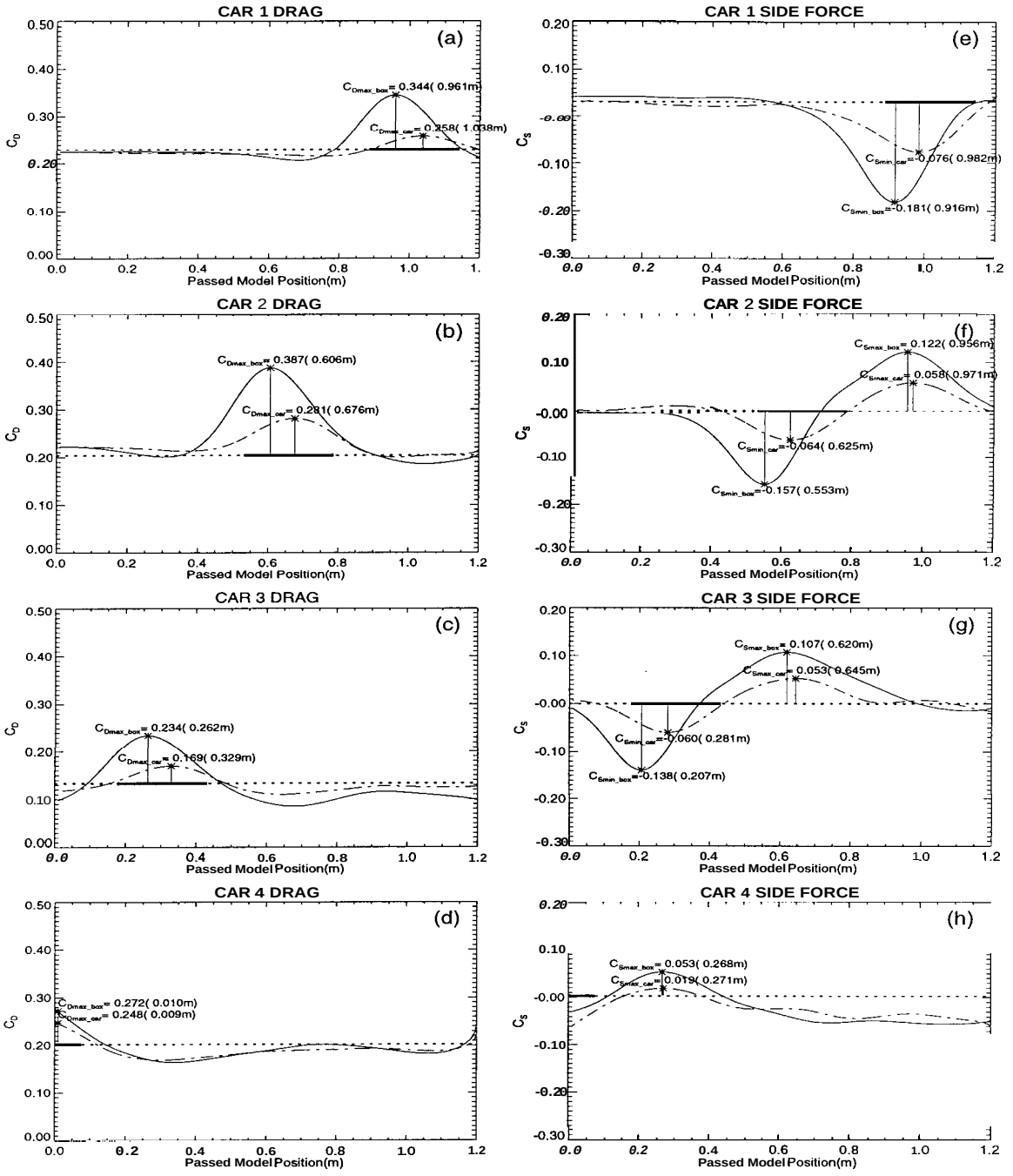

Figure 6.21: Comparison of mobile model $(d = \frac{1}{4}W, v = -1.25m/s)$.
The drag [frames (a)-(d)] and side force [frames (e)-(h)] coefficients on each car in the platoon are shown with respect to the position of mobile model.

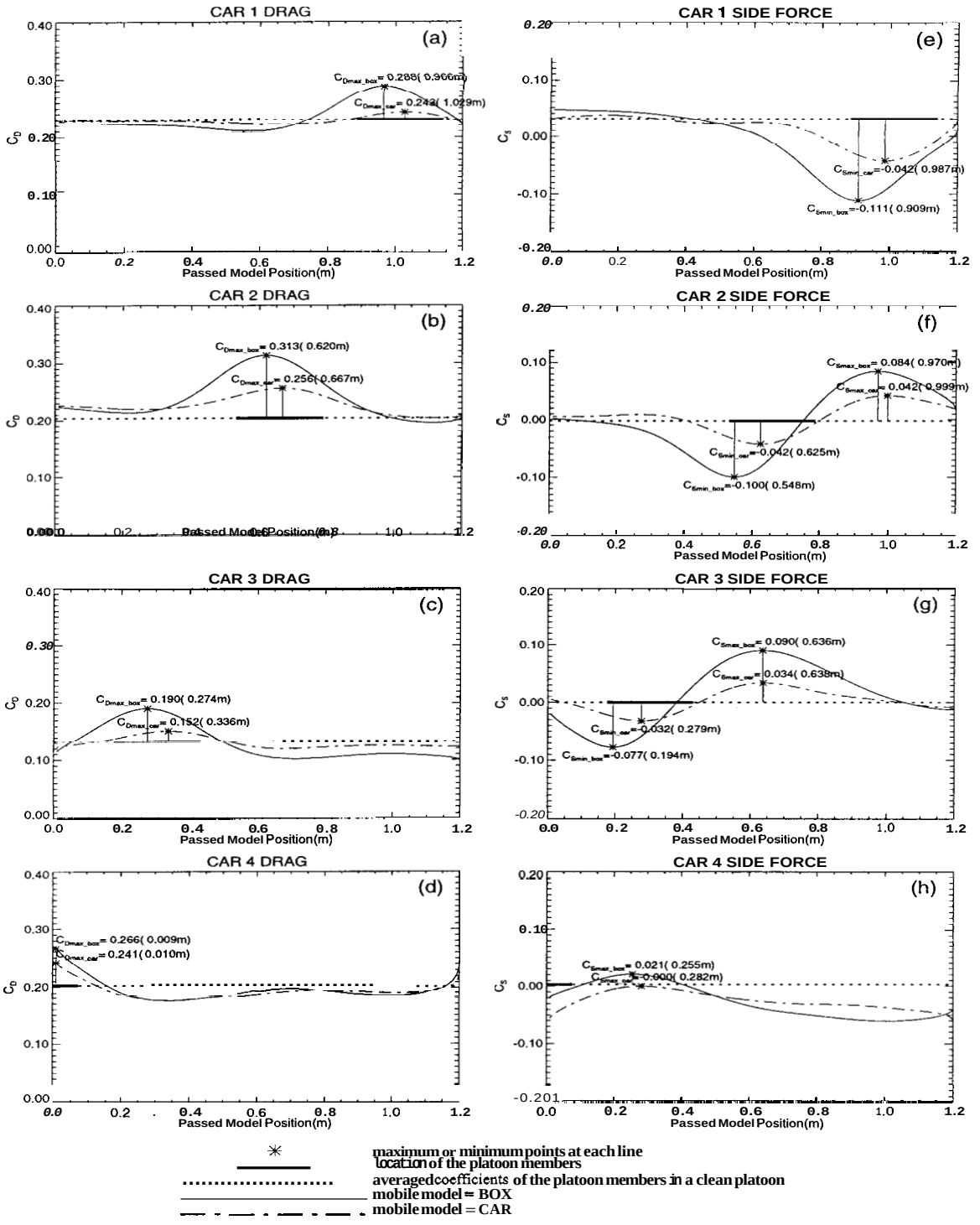

Figure 6.22: Comparison of mobile model $(d = \frac{1}{4}W, v = -2.50m/s)$.
The drag [frames (a)-(d)] and side force [frames (e)-(h)] coefficients on each car in the platoon are shown with respect to the position of mobile model.

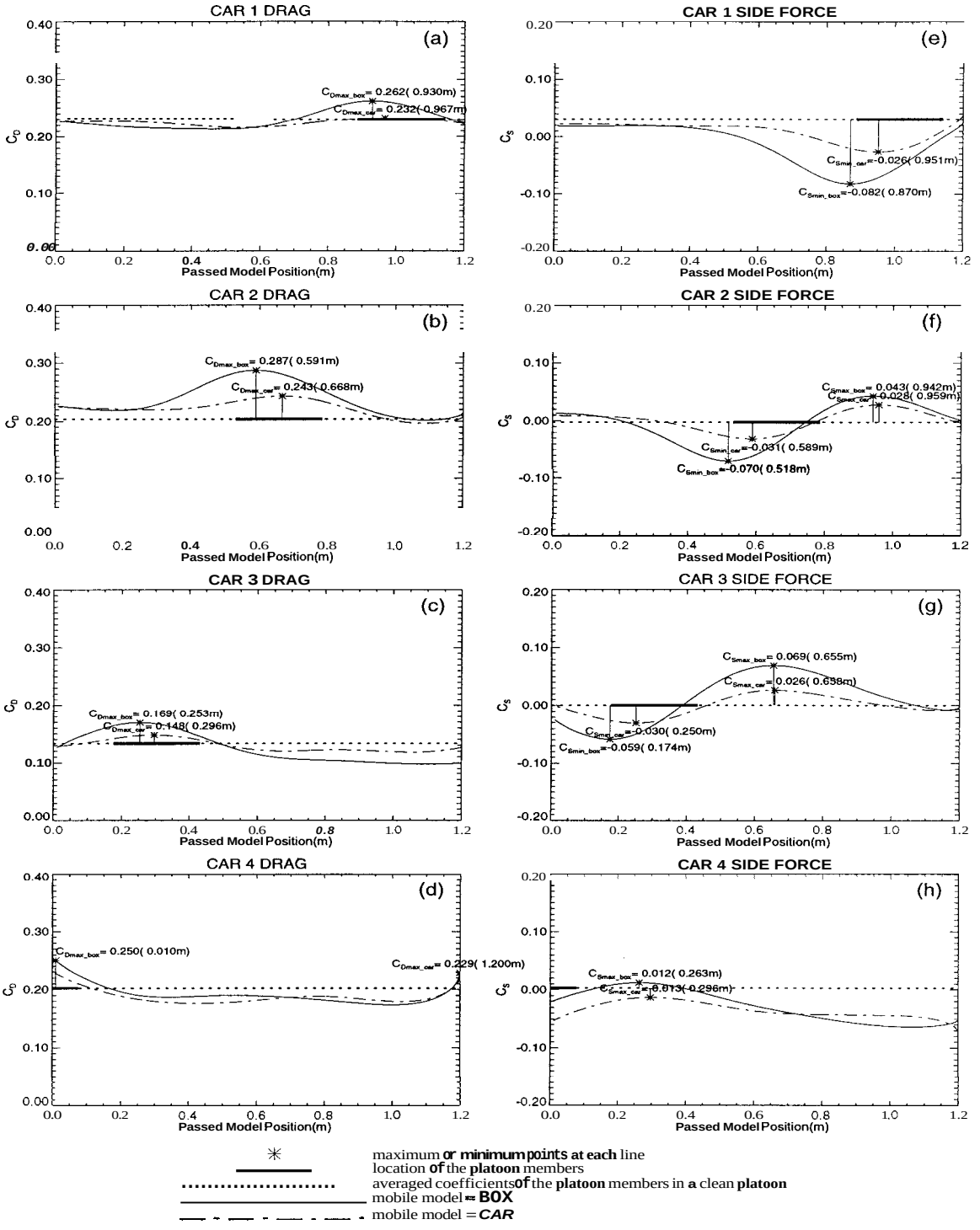

Figure **6.23:** Comparison of mobile model $(d = \frac{1}{4}W, v = -3.75m/s)$.
The drag [frames (a)-(d)] and side force [frames (e)-(h)] coefficients on each car in the platoon are shown with respect to the position of mobile model.

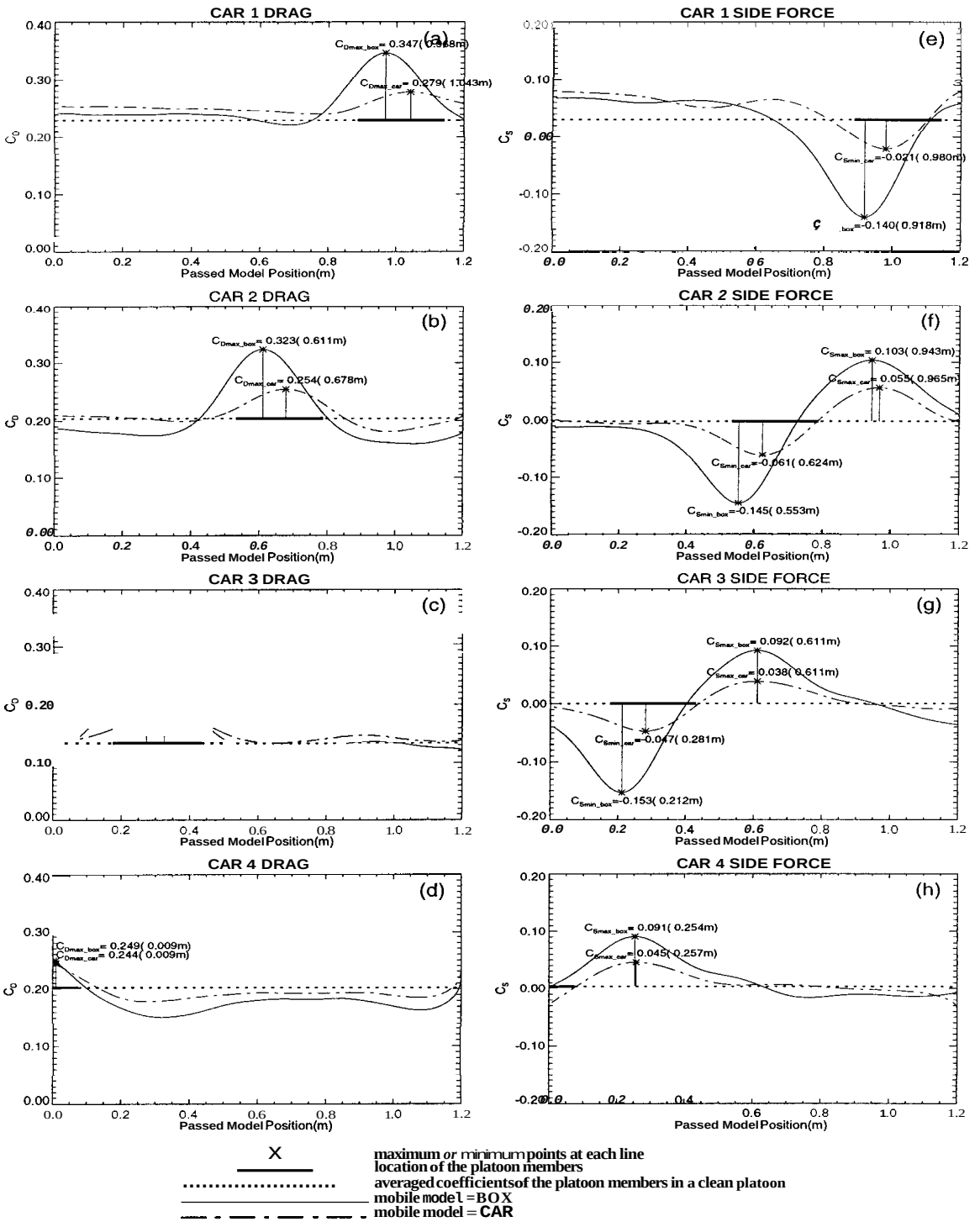

Figure **6.24:** Comparison of mobile model $(d = \frac{1}{2}W, v = -1.25m/s)$.
The drag [frames (a)-(d)] and side force [frames (e)-(h)] coefficients on each car in the platoon are shown with respect to the position of mobile model.

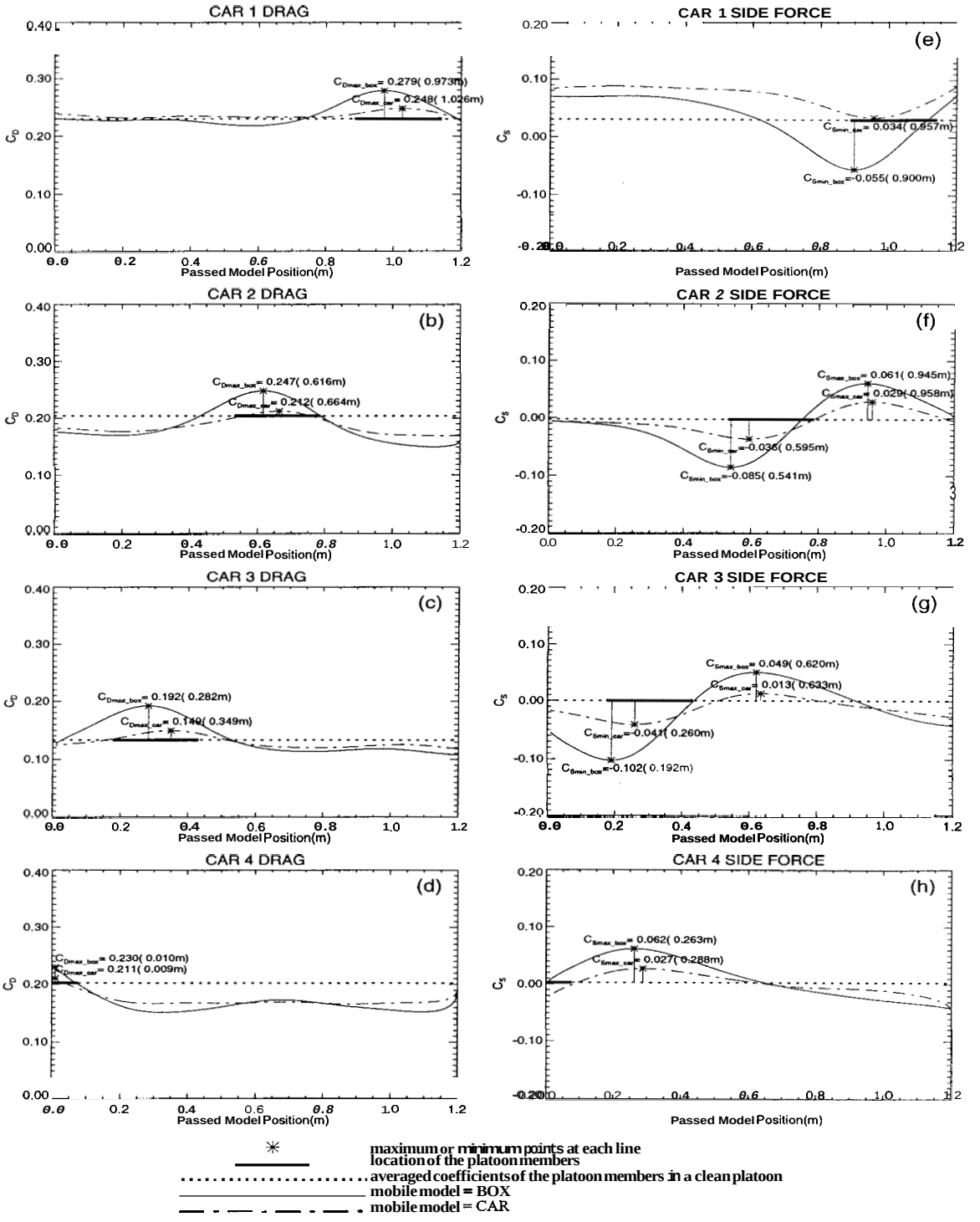

Figure 6.25: Comparison of mobile model ($d = \frac{1}{2}W, v = -2.50m/s$).
The drag [frames (a)-(d)] and side force [frames (e)-(h)] coefficients on each car in the platoon are shown with respect to the position of mobile model.

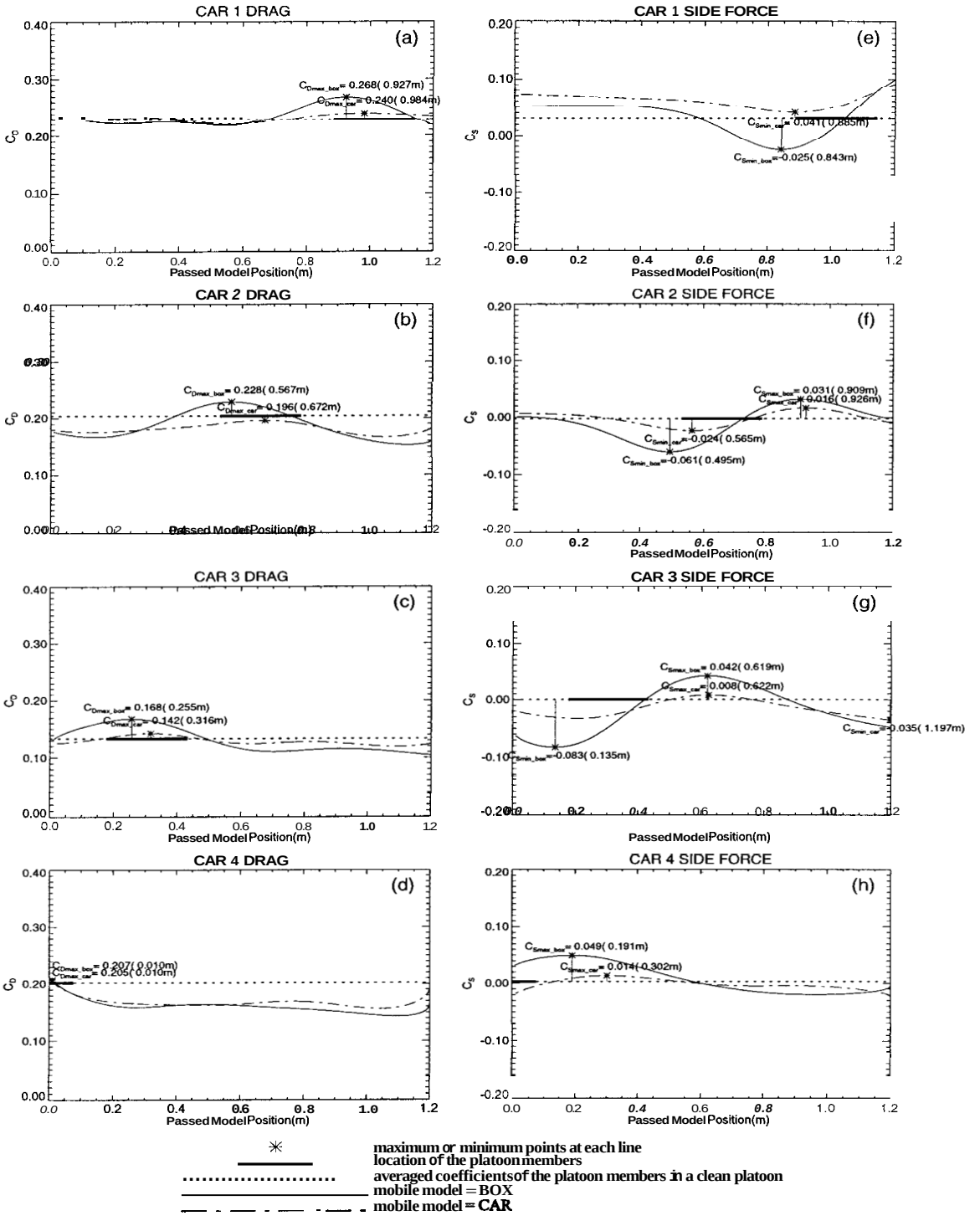

Figure 6.26: Comparison of mobile model ($d = \frac{1}{2}W, v = -3.75m/s$).
The drag [frames (a)-(d)] and side force [frames (e)-(h)] coefficients on each car in the platoon are shown with respect to the position of mobile model.

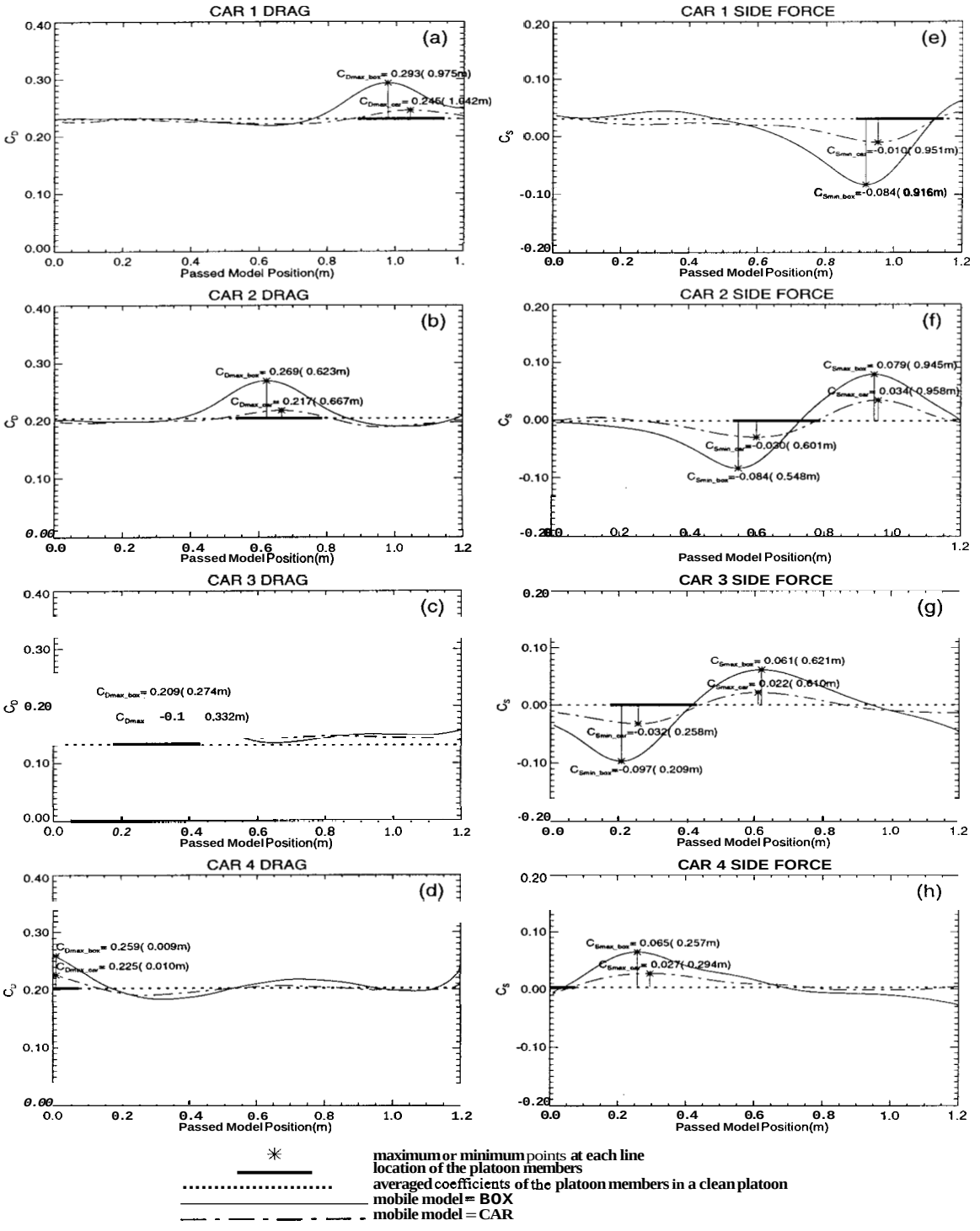

Figure 6.27: Comparison of mobile model $(d = 1W, v = -1.25m/s)$.
The drag [frames (a)-(d)] and side force [frames (e)-(h)] coefficients on each car in the platoon are shown with respect to the position of mobile model.

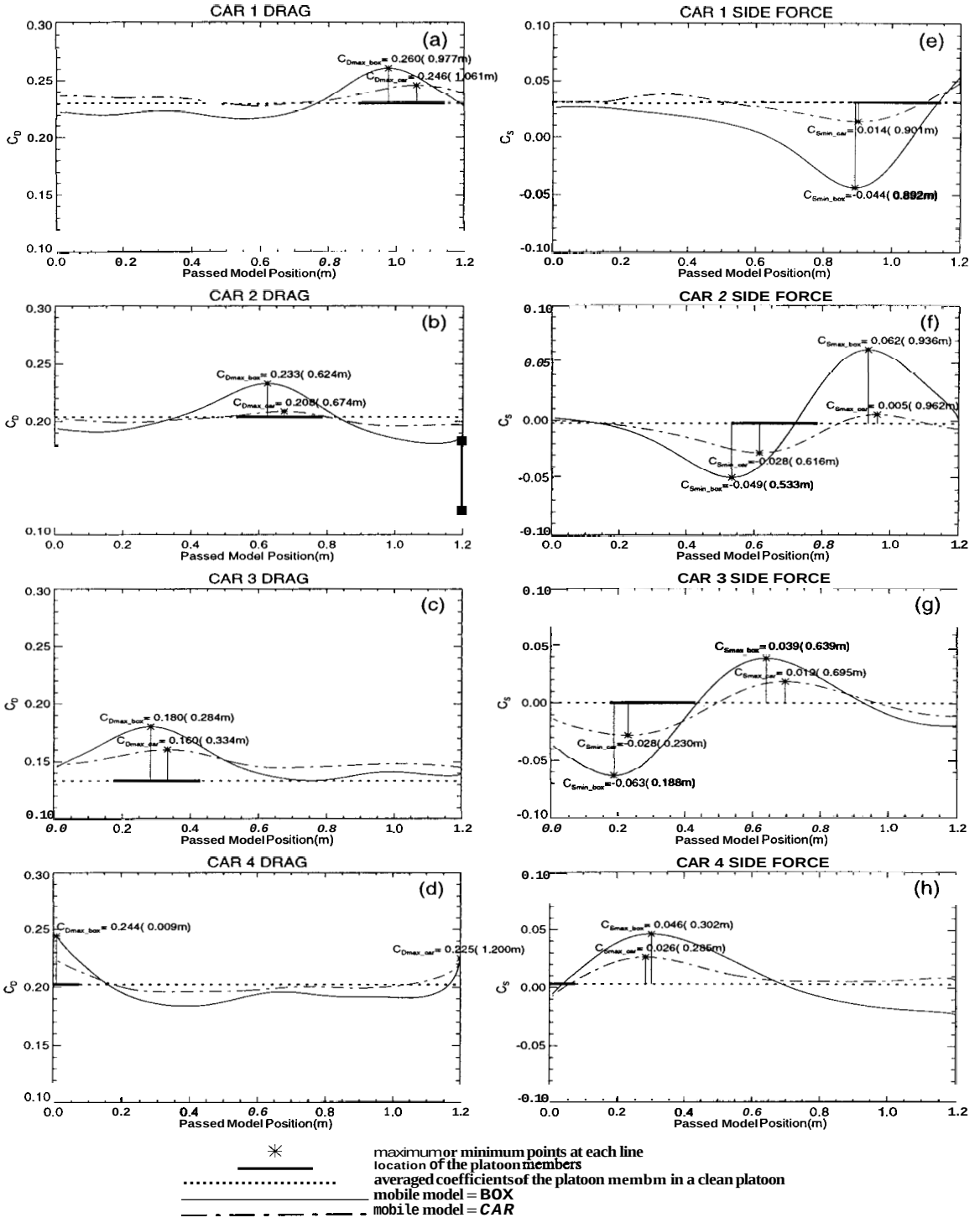

Figure 6.28: Comparison of mobile model $(d = 1W, _{71} = -2.50m/s)$.
The drag [frames (a)-(d)] and side force [frames (e)-(h)] coefficients on each car in the platoon are shown with respect to the position of mobile model.

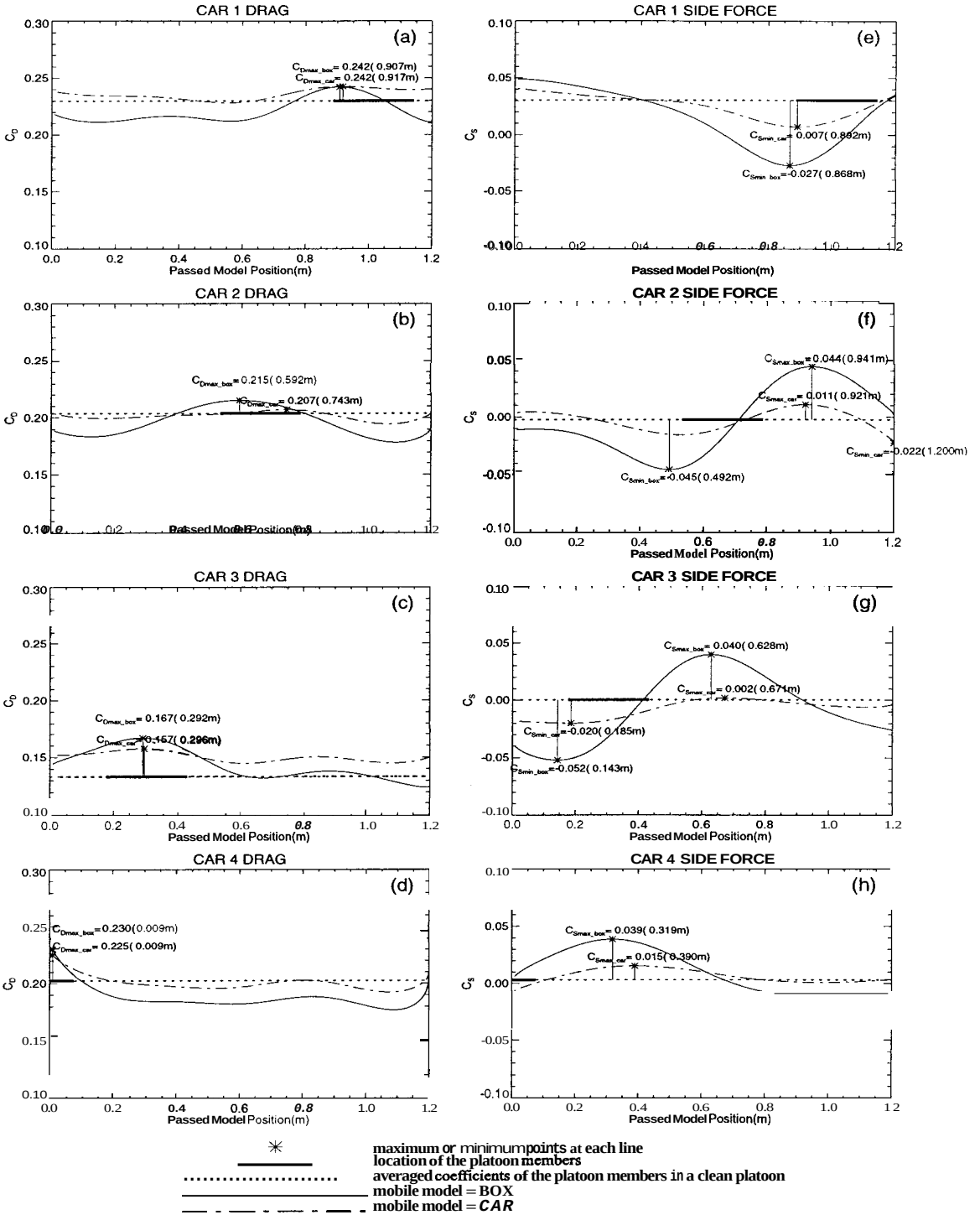

Figure 6.29: Comparison of mobile model $(d = 1W, v = -3.75m/s)$.
The drag [frames (a)-(d)] and side force [frames (e)-(h)] coefficients on each car in the platoon are shown with respect to the position of mobile model.

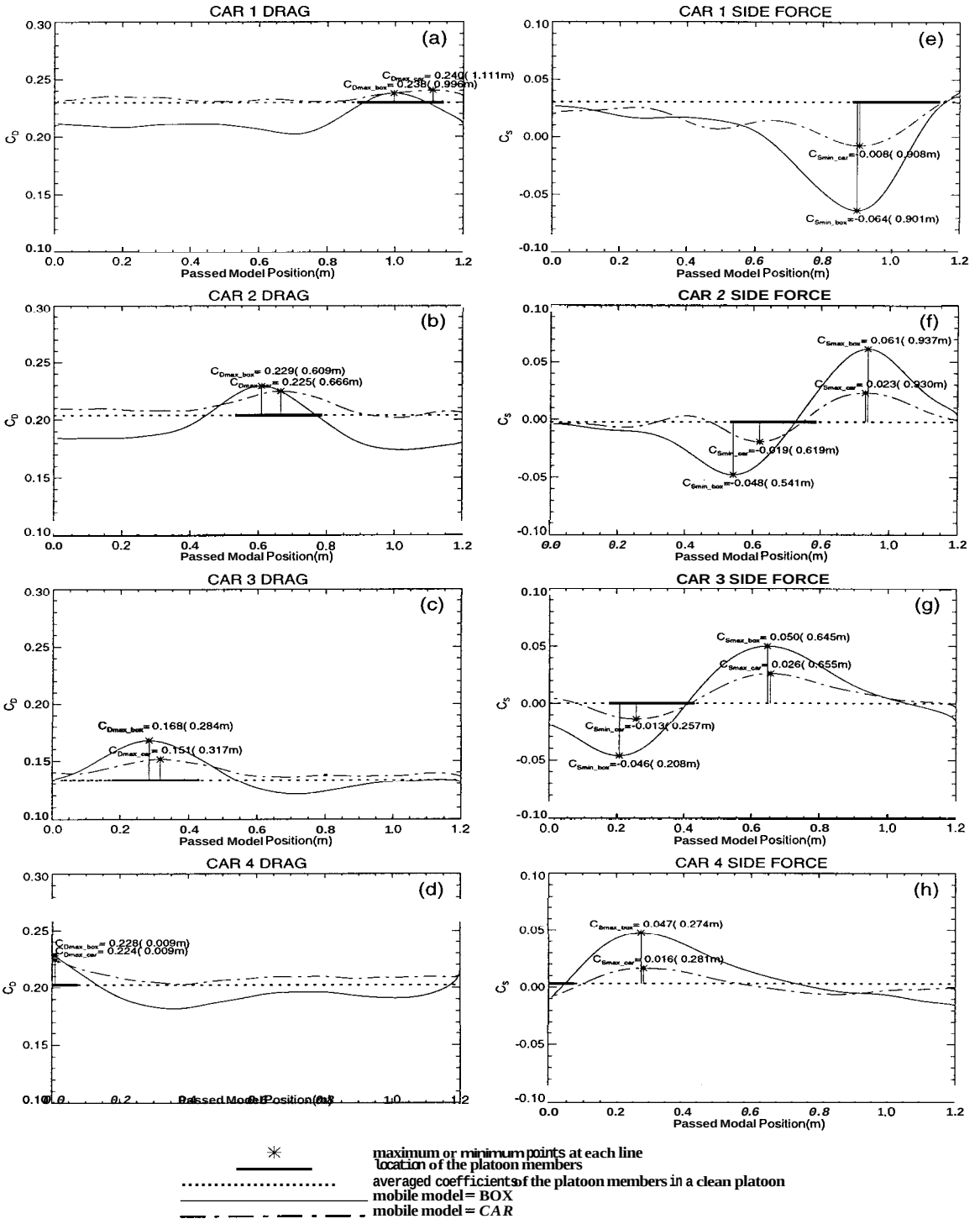

Figure 6.30: Comparison of mobile model ($d = \frac{3}{2}W, v = -1.25m/s$).
The drag [frames (a)-(d)] and side force [frames (e)-(h)] coefficients on each car in the platoon are shown with respect to the position of mobile model.

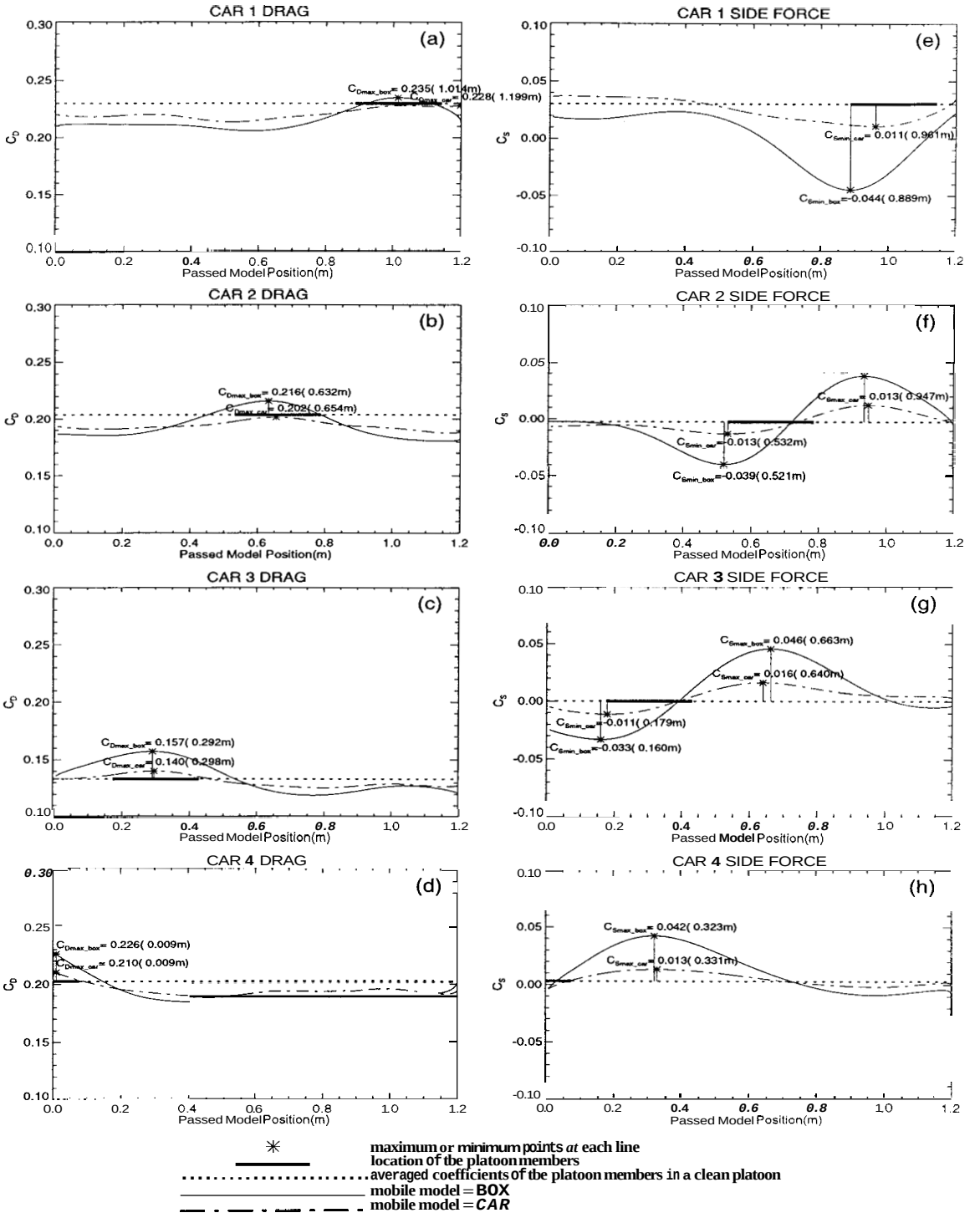

Figure **6.31:** Comparison of mobile model ($d = \frac{3}{2}W, v = -2.50m/s$).
The drag [frames (a)-(d)] and side force [frames (e)-(h)] coefficients on each car in the platoon are shown with respect to the position of mobile model.

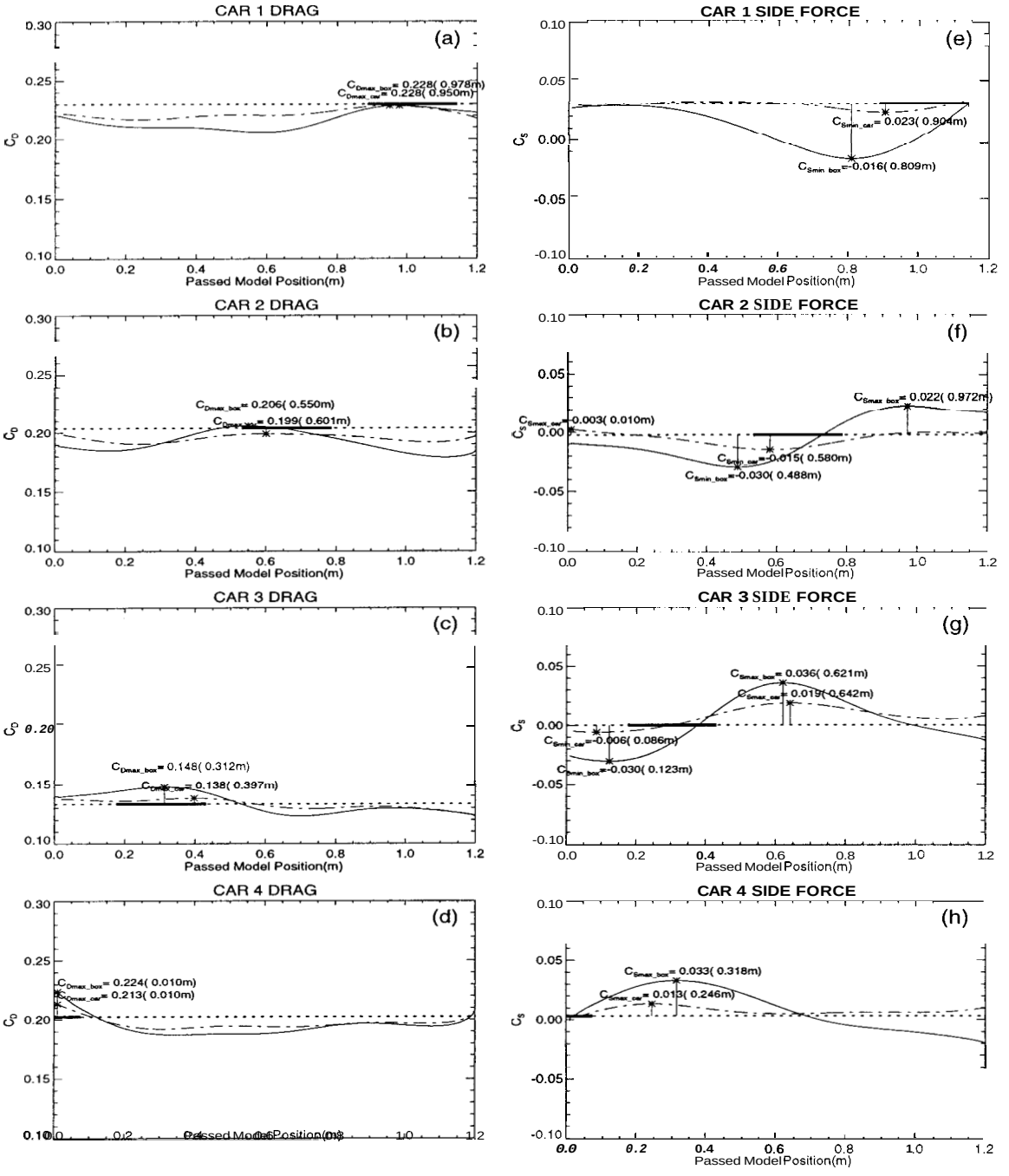

Figure **6.32:** Comparison of mobile model $(d = \frac{3}{2}W, v = -3.75m/s)$.
The drag [frames (a)-(d)] and side force [frames (e)-(h)] coefficients on each car in the platoon are shown with respect to the position of mobile model.

Chapter 7

Position, Velocity, and Acceleration

The position of the mobile model is determined by a resolver which is integrated on the servo motor as shown in figure **2.1.** The resolver, which provides positional feedback to the motor controller, has a resolution of **1024** counts/revolution. After obtaining the information from the resolver about the time history of model's position, we take first derivative to obtain the velocity and second derivative to get the acceleration. Details about the function of motor resolver can be found in Chen [1] and Snyder [4].

In figures **7.1-4,** the first column shows the position profile with respect to time for the five assigned velocities. The second and third columns show the real velocity and acceleration profiles and they are plotted with respect to position. Due to the mobile model's acceleration and deceleration in the beginning and at the end of the testing period, not necessarily all the platoon members are passing (passed by) a constant-speed vehicle. The mobile model's accelerating and decelerating period are expected to affect the results somewhat. Their magnitudes, however, are not controlled factors in this study.

Four pieces of line segment shown on the bottom of each frame in the centered column represent the positions of the four platoon members. Aerodynamic data taken when the mobile model moves backward in velocities $v = -5.00$ and $-6.25 m/s$ are not used in this report, because the cable that drives the mobile model slips on the motor wheel such that the position of the model cannot be accurately determined.

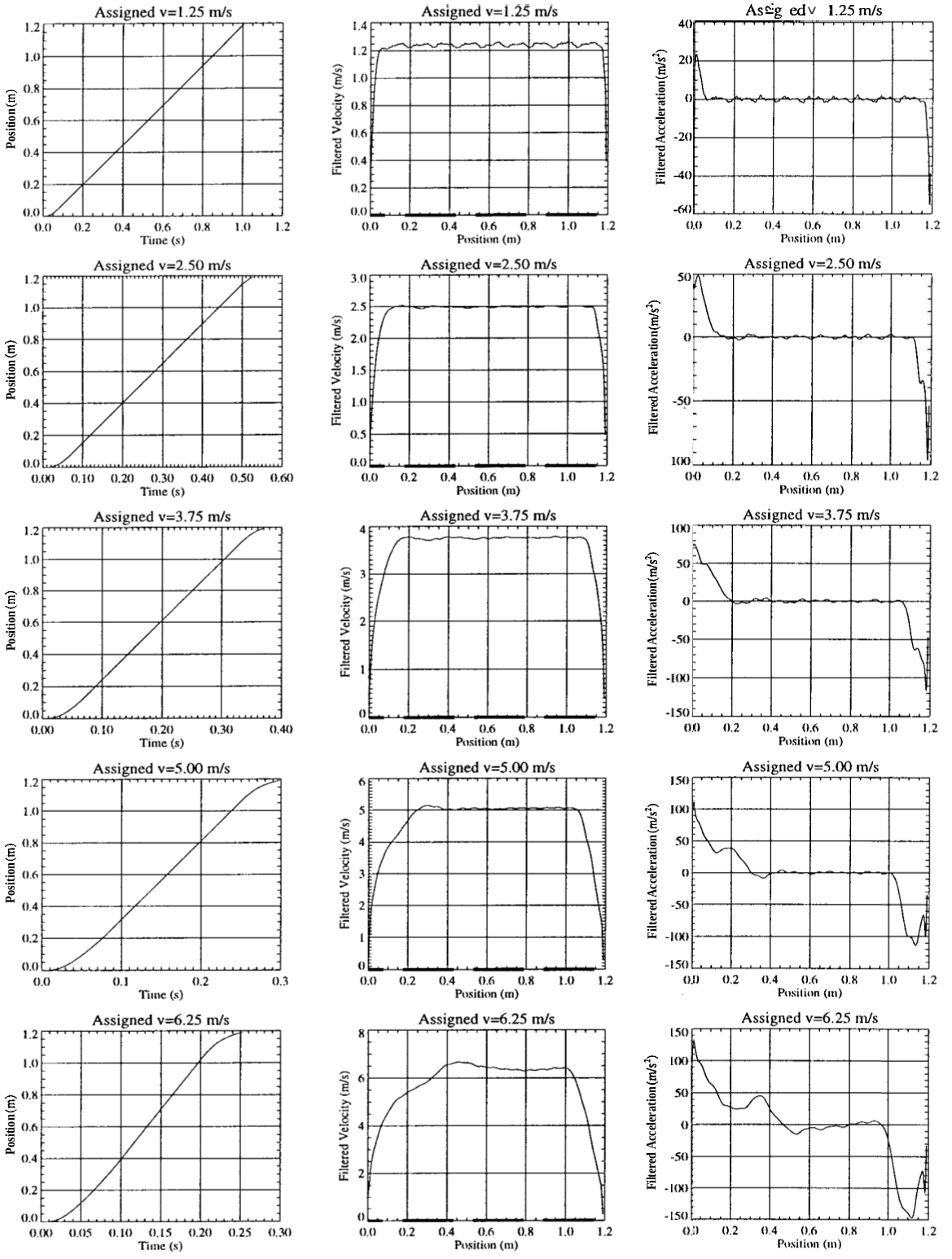

Figure 7.1: Position, velocity and acceleration - a box model in forward motion Frames in the first column show the position vs. time profiles obtained in 5 different velocities. Frames in the second and third columns show velocity nd acceleration information, respectively.

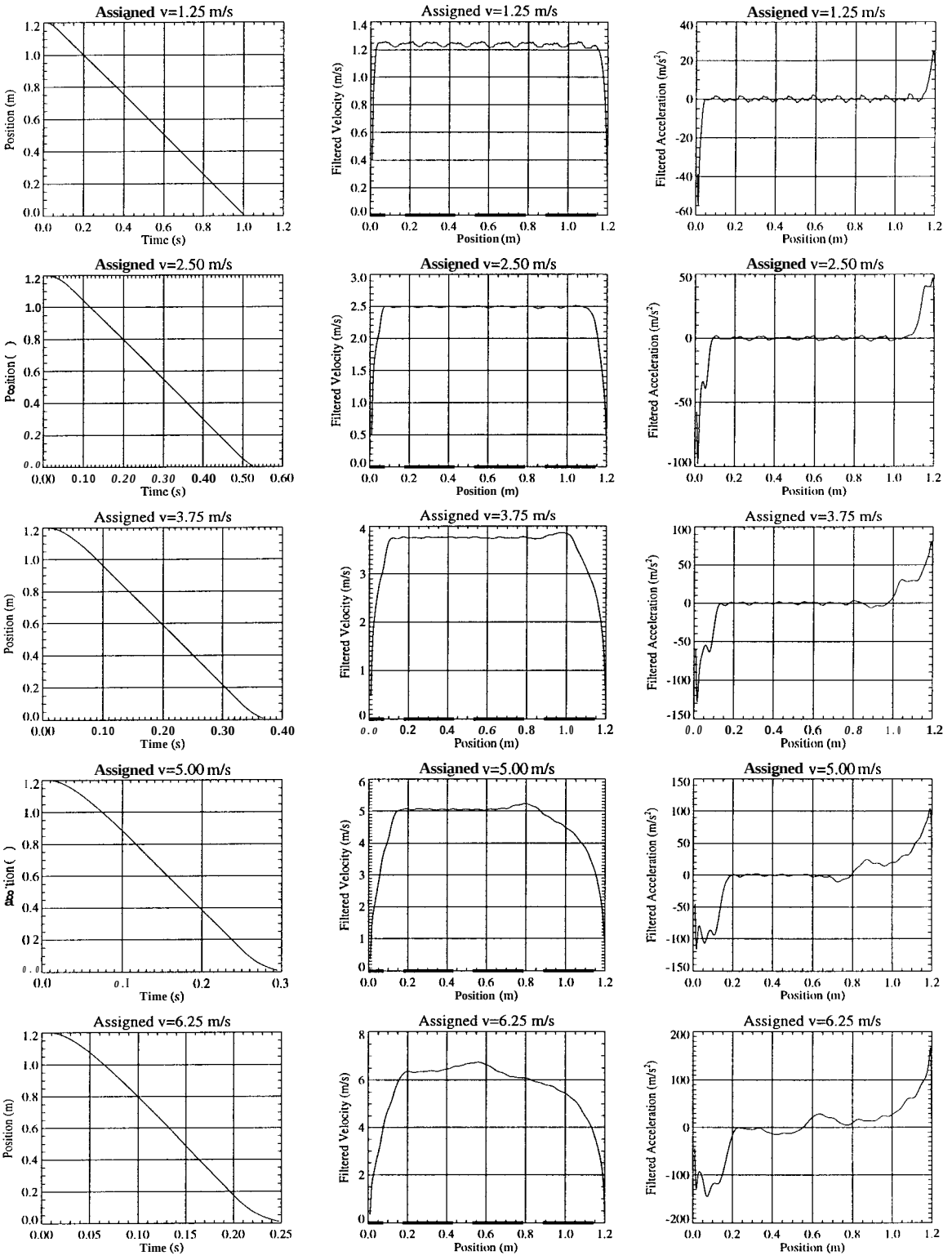

Figure 7.2: Position, velocity and acceleration - a box model in backward motion Frames in the first column show the position vs. time profiles obtained in 5 different velocities. Frames in the second and third columns show velocity nd acceleration information, respectively.

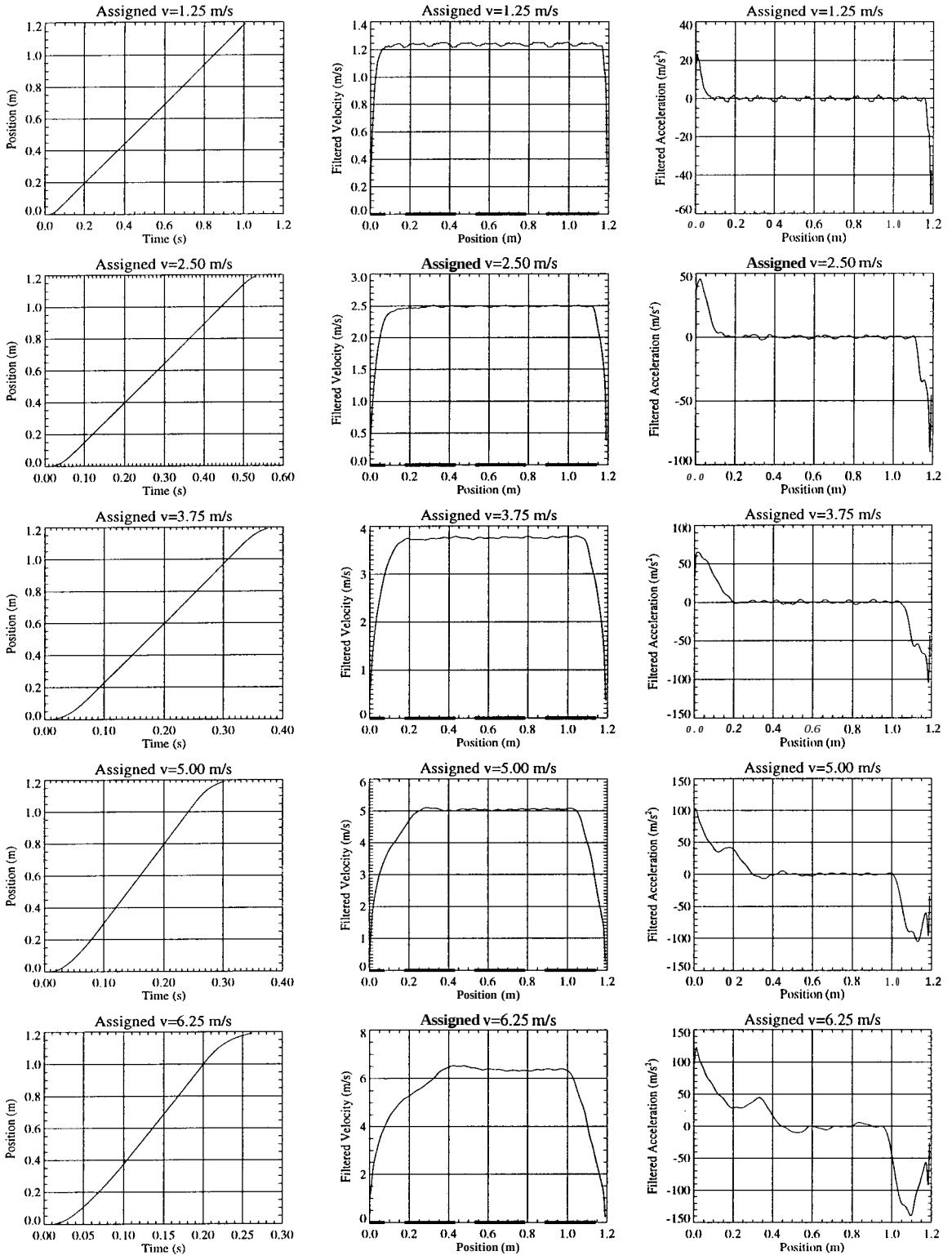

Figure **7.3:** Position, velocity and acceleration - a car model in forward motion Frames in the first column show the position vs. time profiles obtained in 5 different velocities. Frames in the second and third columns show velocity nd acceleration information, respectively.

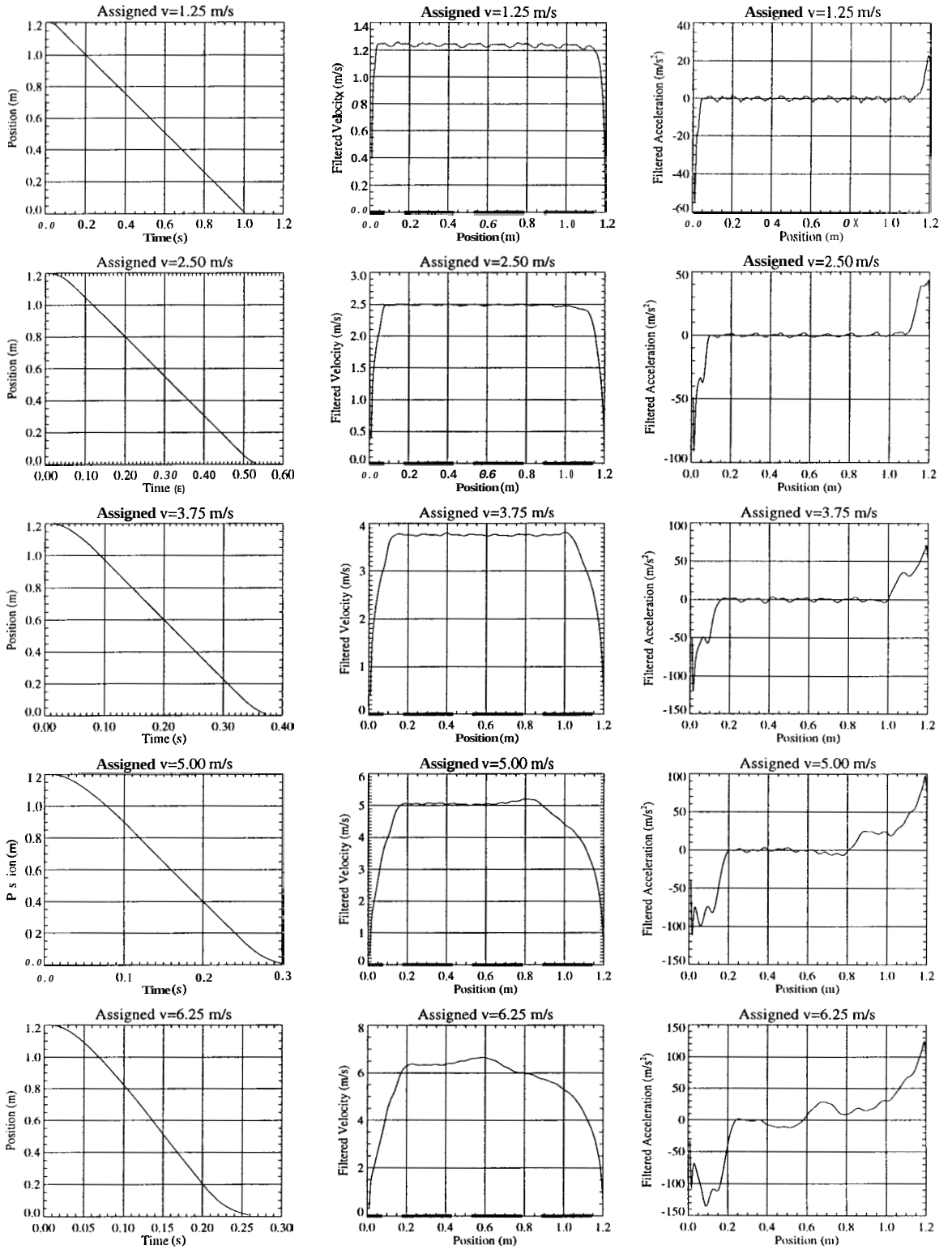

Figure 7.4: Position, velocity and acceleration - **a** car model in backward motion Frames in the first column show the position vs. time profiles obtained in 5 different velocities. Frames in the second and third columns show velocity nd acceleration information, respectively.

Chapter 8

Summary

Wind tunnel experiments are conducted to study transient aerodynamics experienced by a four-car platoon during a passing maneuver. Specifically, four factors have been investigated throughout the study. They are:

- mobile model's direction,
- relative velocities between the mobile model and the platoon,
- lateral spacings between the mobile model and the platoon, and
- the shapes of the mobile model.

The major observations and discoveries are the following:

1. Each platoon member experiences significantly increased drag when the mobile model moves to the proximity of it. The platoon member experiences a repellent force when the mobile vehicle is in the neighborhood of its rear half. The side force reverses its direction and points toward the mobile model when it is in the proximity of the front half of the platoon member.

2. The trends of force change are similar for all the four cars in the platoon, in terms of the relative position of the platoon member and the mobile model.

3. The mobile directions does not affect the force and moments experienced by the platoon members significantly. Similar trends of forces and moment change are observed in both cases of a car passing a platoon and a car overtaken by a platoon.

4. The lower relative velocity between the platoon and the mobile model is, the greater impacts are experienced by the platoon members. The transient data agree with steady state measurements (zero relative velocity) very well.

5. The closer the mobile model to the platoon is, the greater forces are experienced by the cars in the platoon.

6. The box model with sharp corners generates much more impact to the platoon than the streamlined passenger vehicle model. The platoon members experience much greater forces when a rectangular box is used as the mobile model.

7. The measured yaw moments are negligible compared with the magnitude of drag and side force.

8. Although this study is designed to investigate aerodynamic effects on a platoon during constant-speed passing maneuvers, the acceleration and deceleration are inevitable because of the length of the wind tunnel test section. The acceleration and deceleration, which are unknown factors for the aerodynamic force changes on the platoon during passing maneuvers, need further study to quantify their effects. However, according to the data collected in this report, the force coefficients have not shown significant dependence on acceleration/deceleration during passing maneuvers.

This report summarizes the data collected during the investigation of platoon aerodynamics during passing maneuvers. Quantitative data analysis and discussion about the results will be provided in the final report.

Bibliography

[1] A. L. Chen, 0 . Savaş, K. Hedrick, "Transient Vehicle Aerodynamics in Four-Car Platoons", *California PATH Research Report,* UCB-ITS-PRR-97-50, 1997.

[2] A. L. Chen, K. Hedrick, 0. Savag, "Transient Aerodynamics in Vehicle Interactions : Data Base Summary", *California PATH Research, Report,* UCB-ITS-PWP-98-3, 1998.

[3] B. Marcu, F. Browand, "The Aerodynamic Forces on Misaligned Platoons", *California PATH Research, Report,* UCB-ITS-PRR-98-4,1998.

[4] P. A. Snyder, "Control Implications of Platoon Aerodynamics", Master's thesis, University of California, Berkeley, 1998.

[5] L. Tsuei, 0. Savag "A Wind Tunnel Investigation of the Transient Aerodynamic Effects on a Four-Car Platoon during Passing Maneuvers", submitted to *SAE 2000, International Congress and Exposition.*